Supplementary Material

Synthesis of New Brassinosteroid Analogs with Androstane Skeleton and Heterocyclic Acyl Side Chains. Preliminary Molecular Docking Studies.

Omara Araya [1], María Núñez [1]*, Marco Mellado [2], Andrés F. Olea [3] and Luis Espinoza-Catalán [1]*

[1] Departamento de Química, Universidad Técnica Federico Santa María, Avenida España 1680, Valparaíso 2340000, Chile; omara.araya@usm.cl (O.A.); maria.nunezg@usm.cl (M.N.); luis.espinozac@usm.cl. (L.E.-C.)
[2] Centro de Investigación en Ingeniería de Materiales, Universidad Central de Chile, Santiago 8330507, Chile; marco.mellado@ucentral.cl (M.M.)
[3] Instituto de Ciencias Aplicadas, Facultad de Ingeniería, Universidad Autónoma de Chile, Av. del Valle Sur 534, Santiago, Chile and CP 8580640; andres.olea@uautonoma.cl (A.F.O)
* Correspondence: maria.nunezg@usm.cl (M.N.); luis.espinozac@usm.cl (L.E.-C)

Index **pag.**

Figure S1. ^{1}H NMR spectrum of 6-Oxo-23,24-dinor-5α-Cholan-2-en-22-yl-1*H*-pyrrole-2-carboxylate (**33a**)……. **6**

Figure S2. ^{13}C{^{1}H} NMR spectrum of 6-Oxo-23,24-dinor-5α-Cholan-2-en-22-yl-1*H*-pyrrole-2-carboxylate (**33a**). ……. **6**

Figure S3. ^{13}C{^{1}H} DEPT-135 NMR spectrum of 6-Oxo-23,24-dinor-5α-Cholan-2-en-22-yl-1H-pyrrole-2-carboxylate (**33a**). …….. **7**

Figure S4. 2D ^{1}H-^{13}C HSQC spectrum of 6-Oxo-23,24-dinor-5α-Cholan-2-en-22-yl-1H-pyrrole-2-carboxylate (**33a**). ……. **7**

Figure S5. 2D ^{1}H-^{13}C HMBC spectrum of 6-Oxo-23,24-dinor-5α-Cholan-2-en-22-yl-1H-pyrrole-2-carboxylate (**33a**). …….. **8**

Figure S6. ^{1}H NMR spectrum of 6-Oxo-23,24-dinor-5α-Cholan-2-en-22-yl-1H-indole-2-carboxylate (**36a**). …… **8**

Figure S7. ^{13}C{^{1}H} NMR spectrum of 6-Oxo-23,24-dinor-5α-Cholan-2-en-22-yl-1H-indole-2-carboxylate (**36a**). …….. **9**

Figure S8. ^{13}C{^{1}H} DEPT-135 NMR spectrum of 6-Oxo-23,24-dinor-5α-Cholan-2-en-22-yl-1H-indole-2-carboxylate (**36a**). ……. **9**

Figure S9. 2D ^{1}H-^{13}C HSQC spectrum of 6-Oxo-23,24-dinor-5α-Cholan-2-en-22-yl-1H-indole-2-carboxylate (**36a**). ……. **10**

Figure S10. 2D ^{1}H-^{13}C HMBC spectrum of 6-Oxo-23,24-dinor-5α-Cholan-2-en-22-yl-1H-indole-2-carboxylate (**36a**). …… **10**

Figure S11. ^{1}H NMR spectrum of 6-Oxo-23,24-dinor-5α-Cholan-2-en-22-yl-furan-2-carboxylate (**34a**). ……. **11**

Figure S12. ^{13}C{^{1}H} NMR spectrum of 6-Oxo-23,24-dinor-5α-Cholan-2-en-22-yl-furan-2-carboxylate (**34a**). …….. **11**

Figure S13. ^{13}C{^{1}H} DEPT-135 NMR spectrum of 6-Oxo-23,24-dinor-5α-Cholan-2-en-22-yl-furan-2-carboxylate (**34a**). …….. **12**

Figure S14. 2D ^{1}H-^{13}C HSQC spectrum of 6-Oxo-23,24-dinor-5α-Cholan-2-en-22-yl-furan-2-carboxylate (**34a**). ……. **12**

Figure S15. 2D ^{1}H-^{13}C HMBC spectrum of 6-Oxo-23,24-dinor-5α-Cholan-2-en-22-yl-furan-2-carboxylate (**34a**). ……. **13**

Figure S16. ^{1}H NMR spectrum of 6-Oxo-23,24-dinor-5α-Cholan-2-en-22-yl-thiophene-2-carboxylate (**35a**). ……. **13**

Figure S17. ^{13}C{^{1}H} NMR spectrum of 6-Oxo-23,24-dinor-5α-Cholan-2-en-22-yl-thiophene-2-carboxylate (**35a**). …….. **14**

Figure S18. ^{13}C{^{1}H} DEPT-135 NMR spectrum of 6-Oxo-23,24-dinor-5α-Cholan-2-en-22-yl-thiophene-2-carboxylate (**35a**). …….. **14**

Figure S19. 2D ^{1}H-^{13}C HSQC spectrum of 6-Oxo-23,24-dinor-5α-Cholan-2-en-22-yl-thiophene-2-carboxylate (**35a**). …… **15**

Figure S20. 2D ^{1}H-^{13}C HMBC spectrum of 6-Oxo-23,24-dinor-5α-Cholan-2-en-22-yl-thiophene-2-carboxylate (**35a**). …… **15**

Figure S21. ^{1}H NMR spectrum of 6-Oxo-23,24-dinor-5α-Cholan-2-en-22-yl-tetrahydro-2H-pyran-4-carbocarboxylate (**37a**). …… **16**

Figure S22. ^{13}C{^{1}H} NMR spectrum of 6-Oxo-23,24-dinor-5α-Cholan-2-en-22-yl-tetrahydro-2H-pyran-4-carbocarboxylate (**37a**). ……... **16**

Figure S23. ^{13}C{^{1}H} DEPT-135 NMR spectrum of 6-Oxo-23,24-dinor-5α-Cholan-2-en-22-yl-tetrahydro-2H-pyran-4-carbocarboxylate (**37a**). …….. **17**

Figure S24. 2D HSQC ^{1}H-^{13}C spectrum of 6-Oxo-5α-androst-2-en-23,24-dinor-22-tetrahydro-2*H*-pyran-4-carbocarboxylate-22-yl (**37a**). ……. **17**

Figure S25. 2D ^{1}H-^{13}C HMBC spectrum of 6-Oxo-23,24-dinor-5α-Cholan-2-en-22-yl-tetrahydro-2H-pyran-4-carbocarboxylate (**37a**). ……... **18**

Figure S26. 1D selective NOESY NMR spectrum of 6-Oxo-23,24-dinor-5α-Cholan-2-en-22-yl-tetrahydro-2H-pyran-4-carbocarboxylate (**37a**). …….. **18**

Figure S27. ^{1}H NMR spectrum of 2α,3α-Dihydroxy-6-oxo-23,24-dinor-5α-cholan-22-yl-1H-pyrrole-2-carboxylate (**33**). …… **19**

Figure S28. ^{13}C{^{1}H} NMR spectrum of 2α,3α-Dihydroxy-6-oxo-23,24-dinor-5α-cholan-22-yl-1H-pyrrole-2-carboxylate (**33**). ……. **19**

Figure S29. $^{13}C\{^{1}H\}$ DEPT-135 NMR spectrum of 2*α*,3*α*-Dihydroxy-6-oxo-23,24-dinor-5*α*-cholan-22-yl-1H-pyrrole-2-carboxylate (**33**). …….. **20**

Figure S30. 2D ^{1}H-^{13}C HSQC spectrum of 2*α*,3*α*-Dihydroxy-6-oxo-23,24-dinor-5*α*-cholan-22-yl-1H-pyrrole-2-carboxylate (**33**). …….. **20**

Figure S31. 2D ^{1}H-^{13}C HMBC spectrum of 2*α*,3*α*-Dihydroxy-6-oxo-23,24-dinor-5*α*-cholan-22-yl-1H-pyrrole-2-carboxylate (**33**). ……. **21**

Figure S32. HRMS spectrum of 2*α*,3*α*-Dihydroxy-6-oxo-23,24-dinor-5*α*-cholan-22-yl-1H-pyrrole-2-carboxylate (**33**). ……. **21**

Figure S33. ^{1}H NMR spectrum of 2*α*,3*α*-Dihydroxy-6-oxo-23,24-dinor-5*α*-cholan-22-yl-furan-2-carboxylate (**34**). ……. **22**

Figure S34. $^{13}C\{^{1}H\}$ NMR spectrum of 2*α*,3*α*-Dihydroxy-6-oxo-23,24-dinor-5*α*-cholan-22-yl-furan-2-carboxylate (**34**). …… **22**

Figure S35. $^{13}C\{^{1}H\}$ DEPT-135 NMR spectrum of 2*α*,3*α*-Dihydroxy-6-oxo-23,24-dinor-5*α*-cholan-22-yl-furan-2-carboxylate (**34**). …….. **23**

Figure S36. 2D ^{1}H-^{13}C HSQC spectrum of 2*α*,3*α*-Dihydroxy-6-oxo-23,24-dinor-5*α*-cholan-22-yl-furan-2-carboxylate (**34**). …….. **23**

Figure S37. 2D ^{1}H-^{13}C HMBC spectrum of 2*α*,3*α*-Dihydroxy-6-oxo-23,24-dinor-5*α*-cholan-22-yl-furan-2-carboxylate (**34**). …… **24**

Figure S38. HRMS spectrum of 2*α*,3*α*-Dihydroxy-6-oxo-23,24-dinor-5*α*-cholan-22-yl-furan-2-carboxylate (**34**). …….. **24**

Figure S39. ^{1}H NMR spectrum of 2*α*,3*α*-Dihydroxy-6-oxo-23,24-dinor-5*α*-cholan-22-yl-thiophene-2-carboxylate (**35**). …….. **25**

Figure S40. $^{13}C\{^{1}H\}$ NMR spectrum of 2*α*,3*α*-Dihydroxy-6-oxo-23,24-dinor-5*α*-cholan-22-yl-thiophene-2-carboxylate (**35**). …… **25**

Figure S41. $^{13}C\{^{1}H\}$ DEPT-135 NMR spectrum of 2*α*,3*α*-Dihydroxy-6-oxo-23,24-dinor-5*α*-cholan-22-yl-thiophene-2-carboxylate (**35**). …….. **26**

Figure S42. 2D ^{1}H-^{13}C HSQC spectrum of 2*α*,3*α*-Dihydroxy-6-oxo-23,24-dinor-5*α*-cholan-22-yl-thiophene-2-carboxylate (**35**). . ……. **26**

Figure S43. 2D ^{1}H-^{13}C HMBC spectrum of 2*α*,3*α*-Dihydroxy-6-oxo-23,24-dinor-5*α*-cholan-22-yl-thiophene-2-carboxylate (**35**). …… **27**

Figure S44. HRMS spectrum of 2*α*,3*α*-Dihydroxy-6-oxo-23,24-dinor-5*α*-cholan-22-yl-thiophene-2-carboxylate (**35**). ……... **27**

Figure S45. ^{1}H NMR spectrum of 2*α*,3*α*-Dihydroxy-6-oxo-23,24-dinor-5*α*-cholan-22-yl-1H-indole-2-carboxylate (**36**). ……... **28**

Figure S46. $^{13}C\{^{1}H\}$ NMR spectrum of 2*α*,3*α*-Dihydroxy-6-oxo-23,24-dinor-5*α*-cholan-22-yl-1H-indole-2-carboxylate (**36**). ……. **28**

Figure S47. $^{13}C\{^{1}H\}$ DEPT-135 NMR spectrum of 2*α*,3*α*-Dihydroxy-6-oxo-23,24-dinor-5*α*-cholan-22-yl-1H-indole-2-carboxylate (**36**). …….. **29**

Figure S48. 2D ^{1}H-^{13}C HSQC spectrum of 2*α*,3*α*-Dihydroxy-6-oxo-23,24-dinor-5*α*-cholan-22-yl-1H-indole-2-carboxylate (**36**). …… **29**

Figure S49. 2D ^{1}H-^{13}C HMBC spectrum of 2*α*,3*α*-Dihydroxy-6-oxo-23,24-dinor-5*α*-cholan-22-yl-1H-indole-2-carboxylate (**36**). …… **30**

Figure S50. HRMS spectrum of 2*α*,3*α*-Dihydroxy-6-oxo-23,24-dinor-5*α*-cholan-22-yl-1H-indole-2-carboxylate (**36**). …….. **30**

Figure S51. ^{1}H NMR spectrum of 2*α*,3*α*-Dihydroxy-6-oxo-23,24-dinor-5*α*-cholan-22-yl-2H-pyran-4-carbocarboxylate (**37**). ……. **31**

Figure S52. $^{13}C\{^{1}H\}$ NMR spectrum of 2*α*,3*α*-Dihydroxy-6-oxo-23,24-dinor-5*α*-cholan-22-yl-2H-pyran-4-carbocarboxylate (**37**). …….. **31**

Figure S53. $^{13}C\{^{1}H\}$ DEPT-135 NMR spectrum of 2*α*,3*α*-Dihydroxy-6-oxo-23,24-dinor-5*α*-cholan-22-yl-2H-pyran-4-carbocarboxylate (**37**). ……. **32**

Figure S54. 2D ^{1}H-^{13}C HSQC spectrum of 2*α*,3*α*-Dihydroxy-6-oxo-23,24-dinor-5*α*-cholan-22-yl-2H-pyran-4-carbocarboxylate (**37**). …….. **32**

Figure S55. 2D ^{1}H-^{13}C HMBC spectrum of 2*α*,3*α*-Dihydroxy-6-oxo-23,24-dinor-5*α*-cholan-22-yl-2H-pyran-4-carbocarboxylate (**37**). …….. **33**

Figure S56. HRMS spectrum of 2*α*,3*α*-Dihydroxy-6-oxo-23,24-dinor-5*α*-cholan-22-yl-2H-pyran-4-carbocarboxylate (**37**). ……. **33**

Figure S57. Redocking of brassinolide into the active site of the BRI1–BAK1. BRI1–BAK1 in cartoon mode and ligands in stick mode…….. **34**

Figure S58. Results of molecular docking for new BRs analogs. BRI1–BAK1 in cartoon mode and ligands in stick mode…… **34**

Figure S59 Results of molecular docking of compound **33** in the active site of BRI1–BAK1. A. 3D visualization and B. 2D representations of the most important interactions. …… **34**

Figure S60. Results of molecular docking of compound **34** in the active site of BRI1–BAK1. A. 3D visualization and B. 2D representations of the most important interactions. …… **35**

Figure S61. Results of molecular docking of compound **35** in the active site of BRI1–BAK1. A. 3D visualization and B. 2D representations of the most important interactions. …… **35**

Figure S62. Results of molecular docking of compound **36** in the active site of BRI1–BAK1. A. 3D visualization and B. 2D representations of the most important interactions. …… **35**

Figure S63. Results of molecular docking of compound **37** in the active site of BRI1–BAK1. A. 3D visualization and B. 2D representations of the most important interactions. …… **36**

Figure S64 Results of molecular docking for compound **36** and brassinolide within the active site of BRI1–BAK1. A. 3D visualization of compound **36**; B. 2D representation of interactions of **36** with residues in BRI1–BAK1; C. 3D visualization of brassinolide docked to the active site; D. 2D representation of interactions of brassinolide with residues in BRI1–BAK1……. **36**

Figure S65 Molecular docking results for **33** and **36** in the active site of BRI1–BAK1, showing the aminoacids and distance for potential hydrogen bonding. Color code: Blue: C atoms of **33**; White: C atoms compound **33**; Green: C atomos of BRI1–BAK1…… **37**

Table S1 Binding energies and interactions obtained for BRs analogs (**33-37**) and brassinolide……. **38**

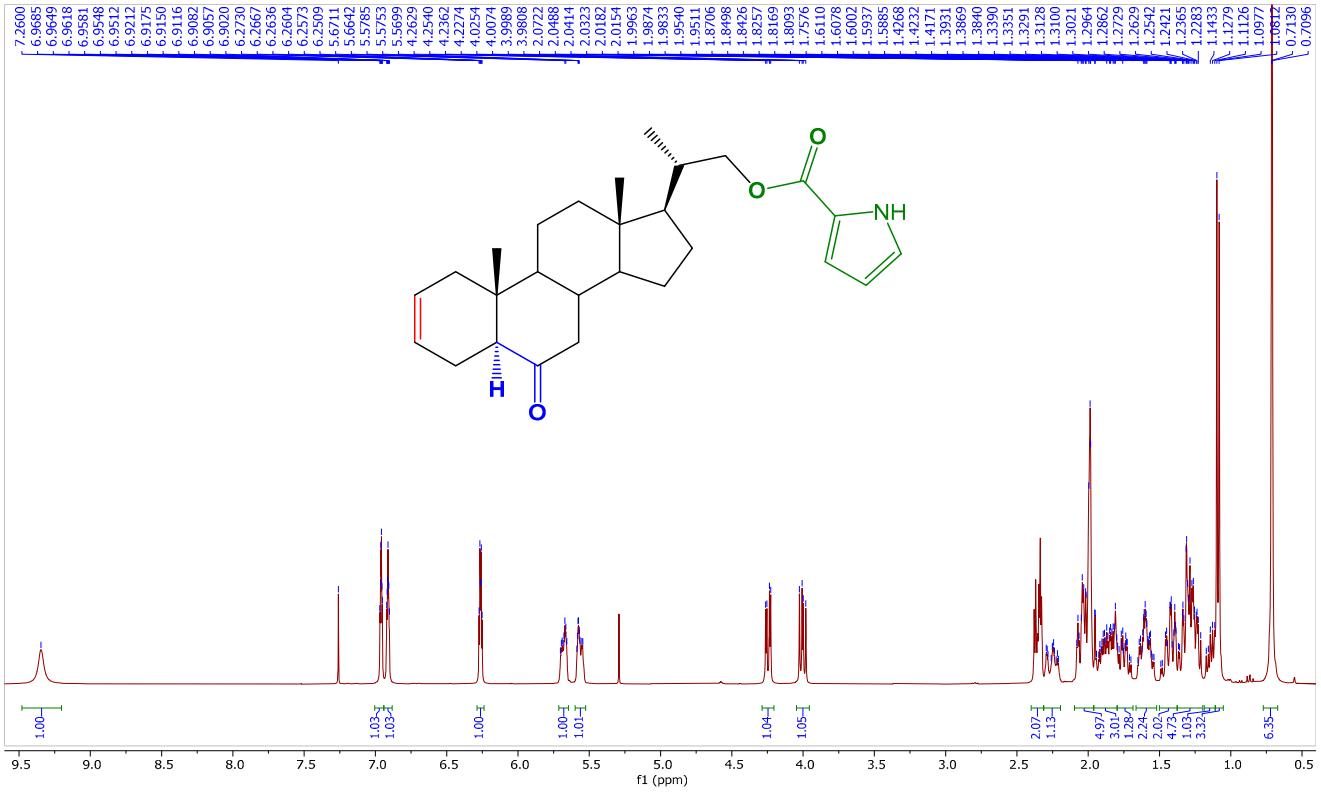


Figure S1. ^{1}H NMR spectrum of 6-Oxo-23,24-dinor-5*α*-Cholan-2-en-22-yl-1*H*-pyrrole-2-carboxylate (**33a**).

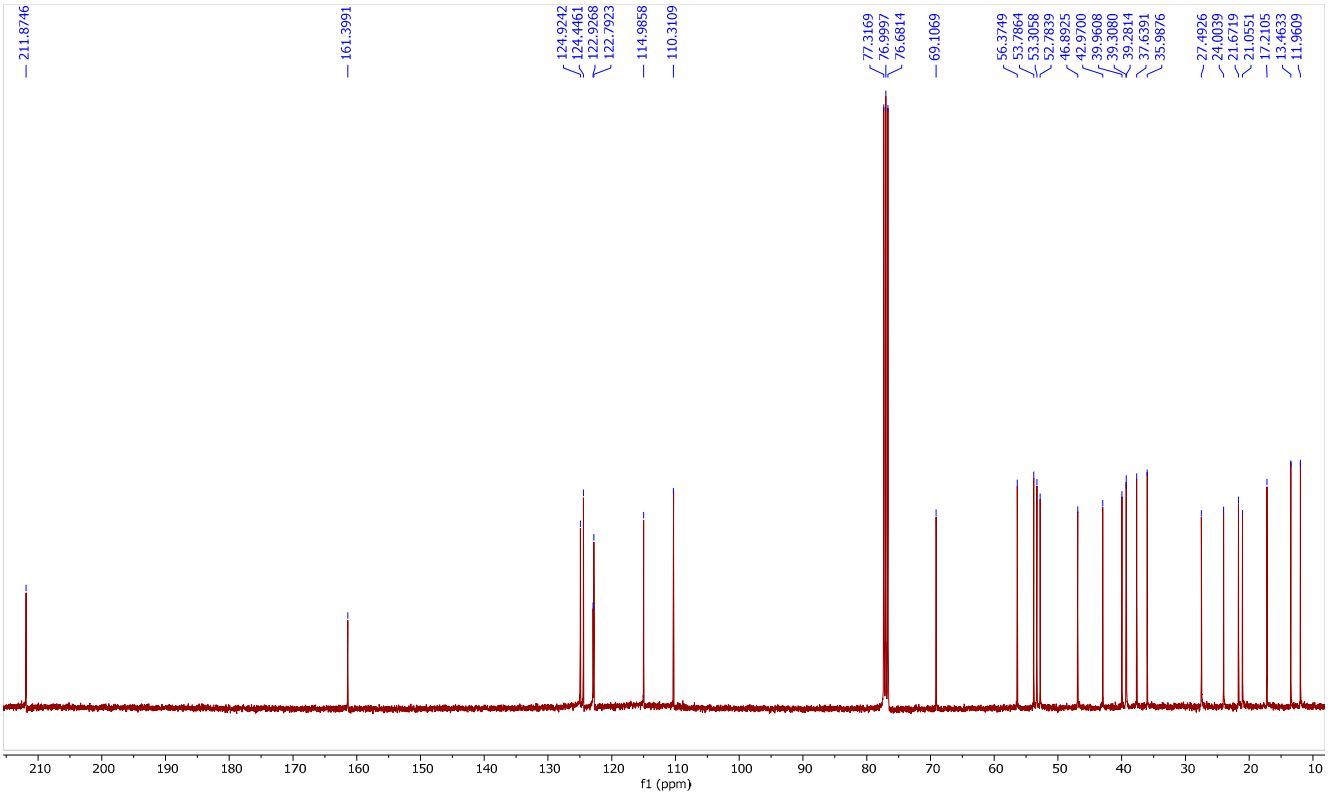


Figure S2. ^{13}C{^{1}H} NMR spectrum of 6-Oxo-23,24-dinor-5*α*-Cholan-2-en-22-yl-1*H*-pyrrole-2-carboxylate (**33a**).

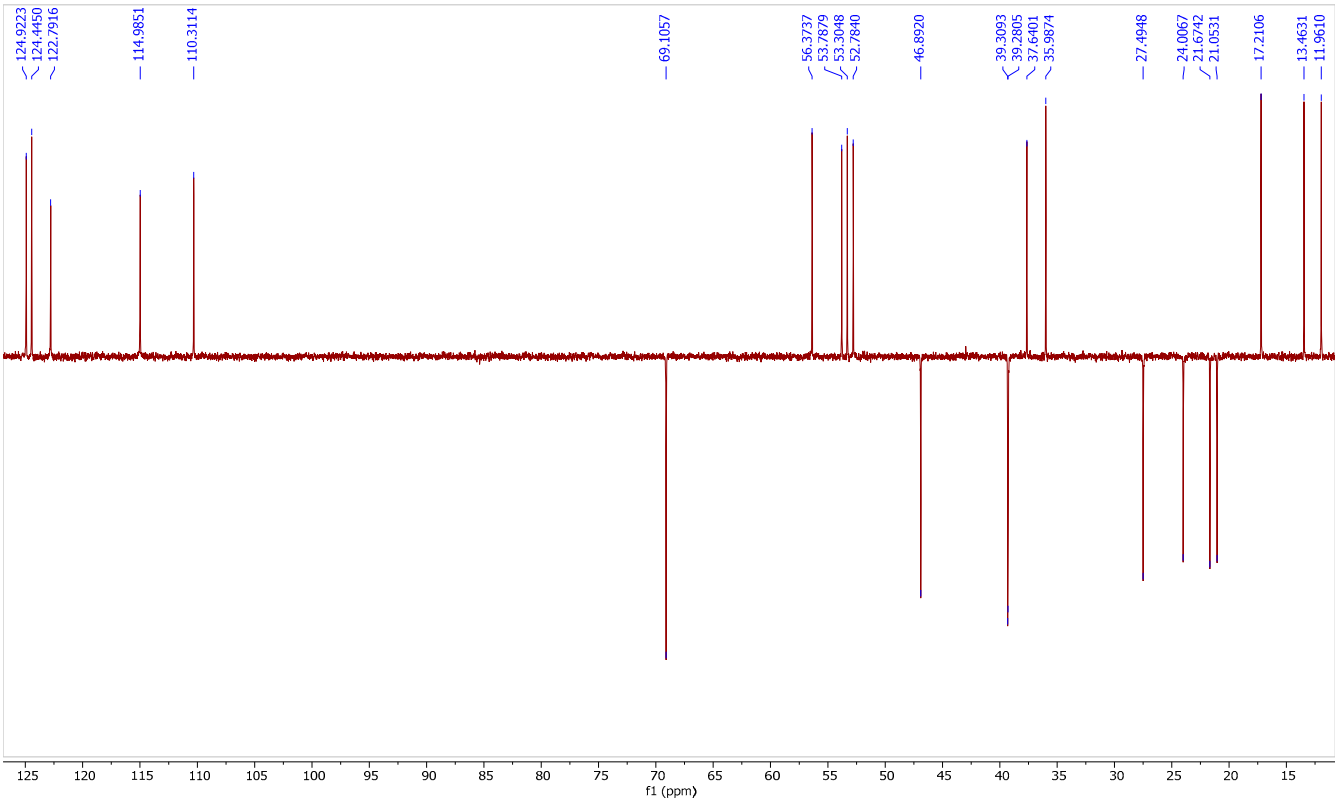


Figure S3. $^{13}C\{^{1}H\}$ DEPT-135 NMR spectrum of 6-Oxo-23,24-dinor-5α-Cholan-2-en-22-yl-1*H*-pyrrole-2-carboxylate (**33a**).

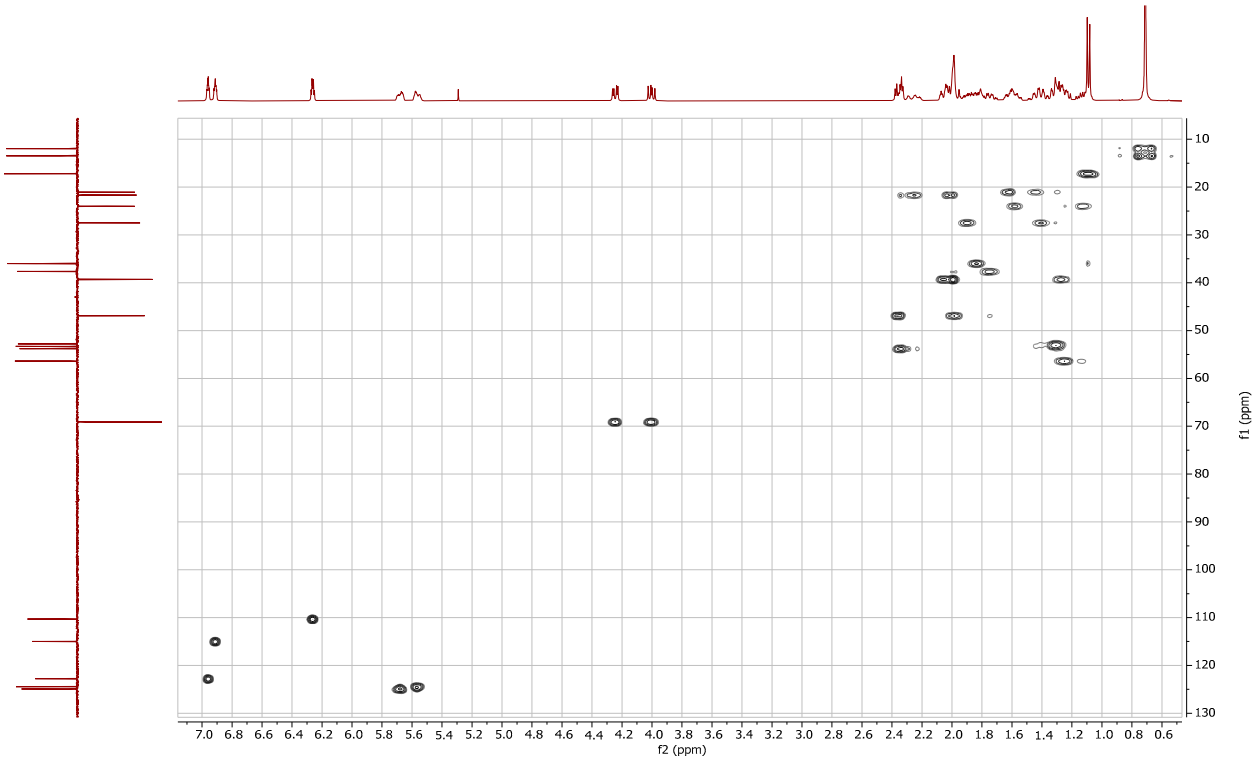


Figure S4. 2D ^{1}H-^{13}C HSQC spectrum of 6-Oxo-23,24-dinor-5α-Cholan-2-en-22-yl-1*H*-pyrrole-2-carboxylate (**33a**).

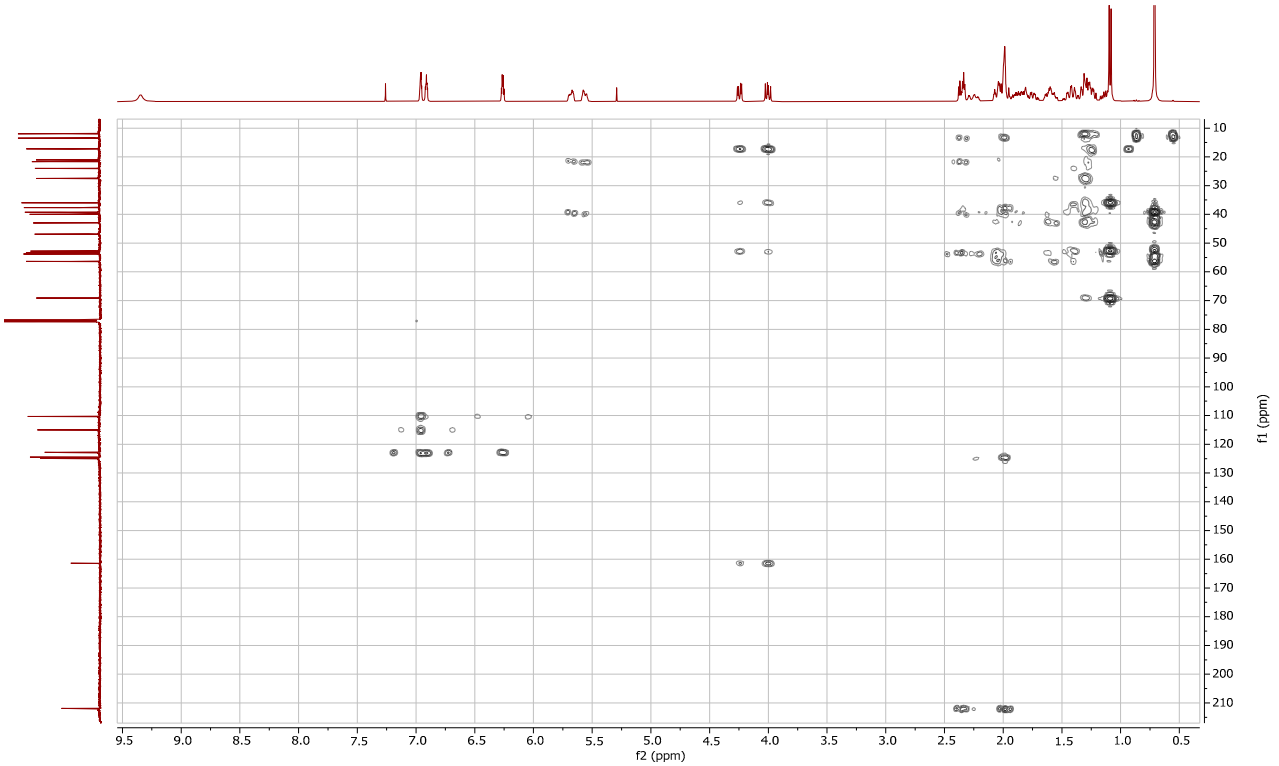


Figure S5. 2D ^{1}H-^{13}C HMBC spectrum of 6-Oxo-23,24-dinor-5α-Cholan-2-en-22-yl-1*H*-pyrrole-2-carboxylate (**33a**).

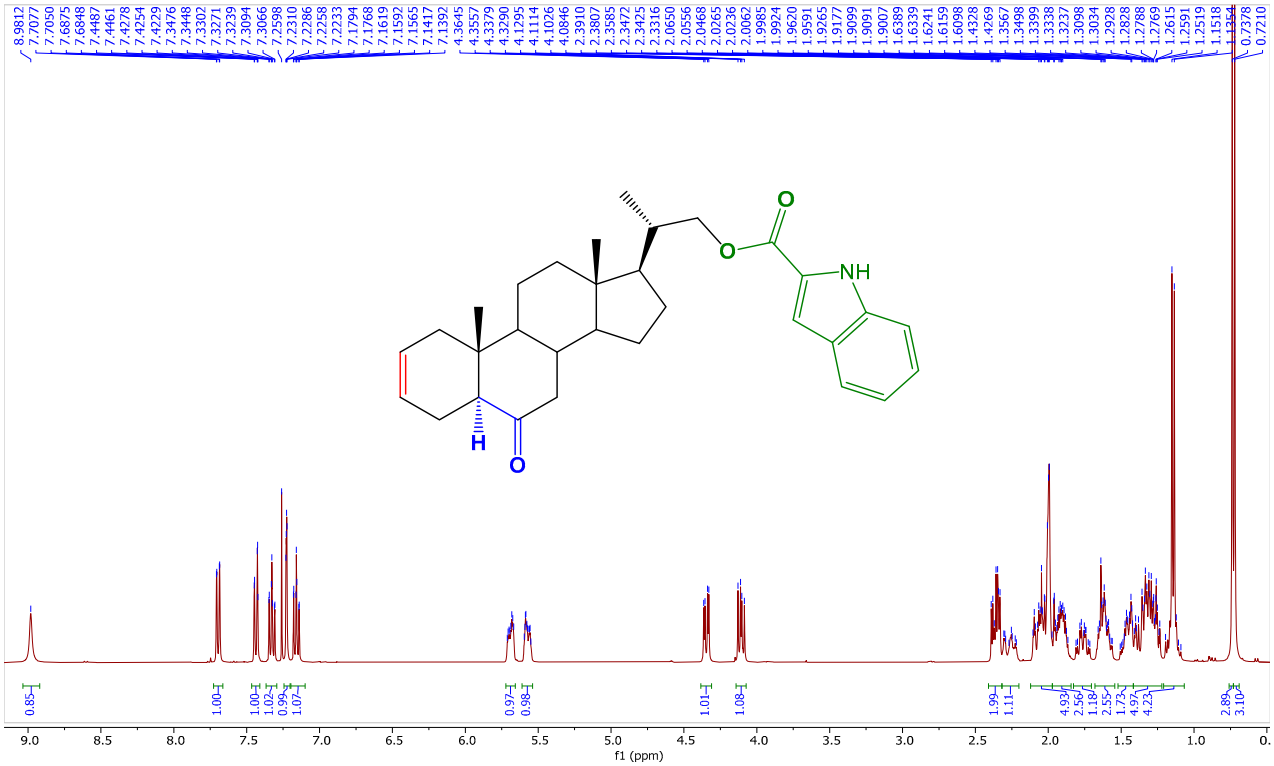


Figure S6. ^{1}H NMR spectrum of 6-Oxo-23,24-dinor-5α-Cholan-2-en-22-yl-1*H*-indole-2-carboxylate (**36a**)

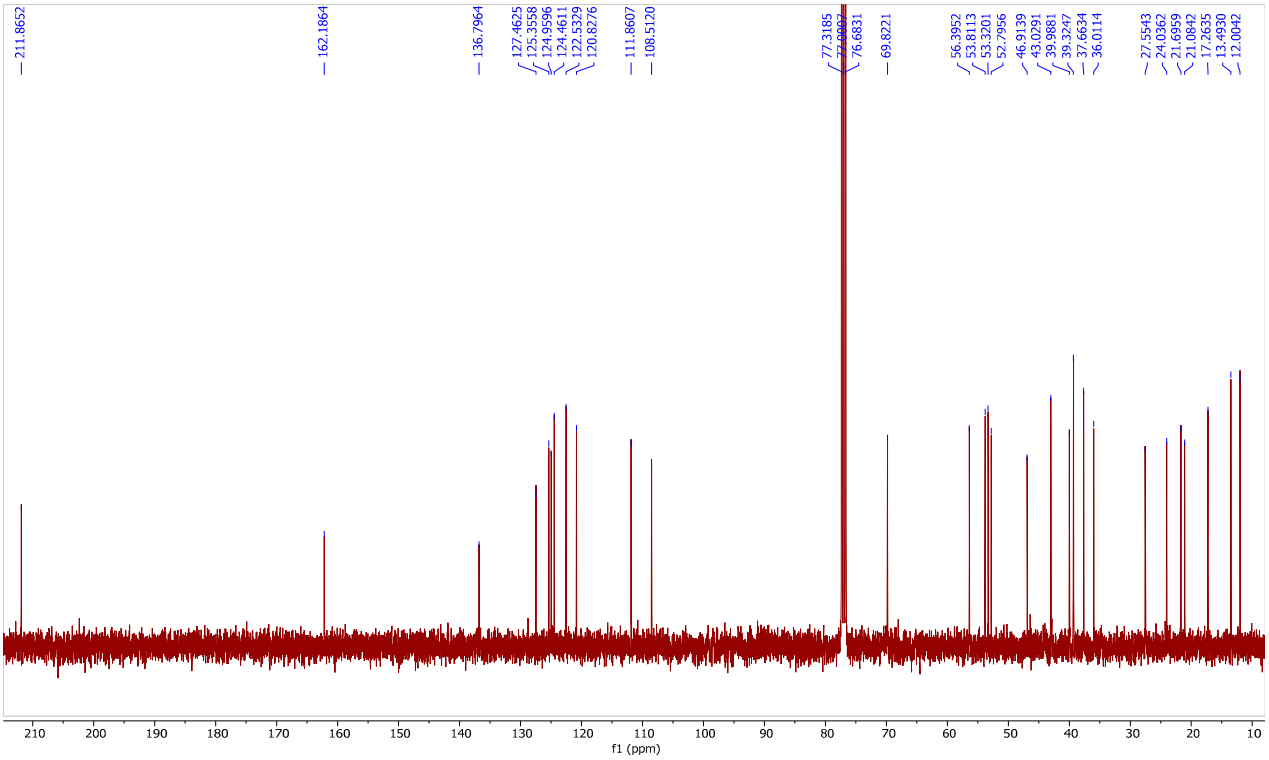


Figure S7. $^{13}C\{^{1}H\}$ NMR spectrum of 6-Oxo-23,24-dinor-5α-Cholan-2-en-22-yl-1*H*-indole-2-carboxylate (**36a**)

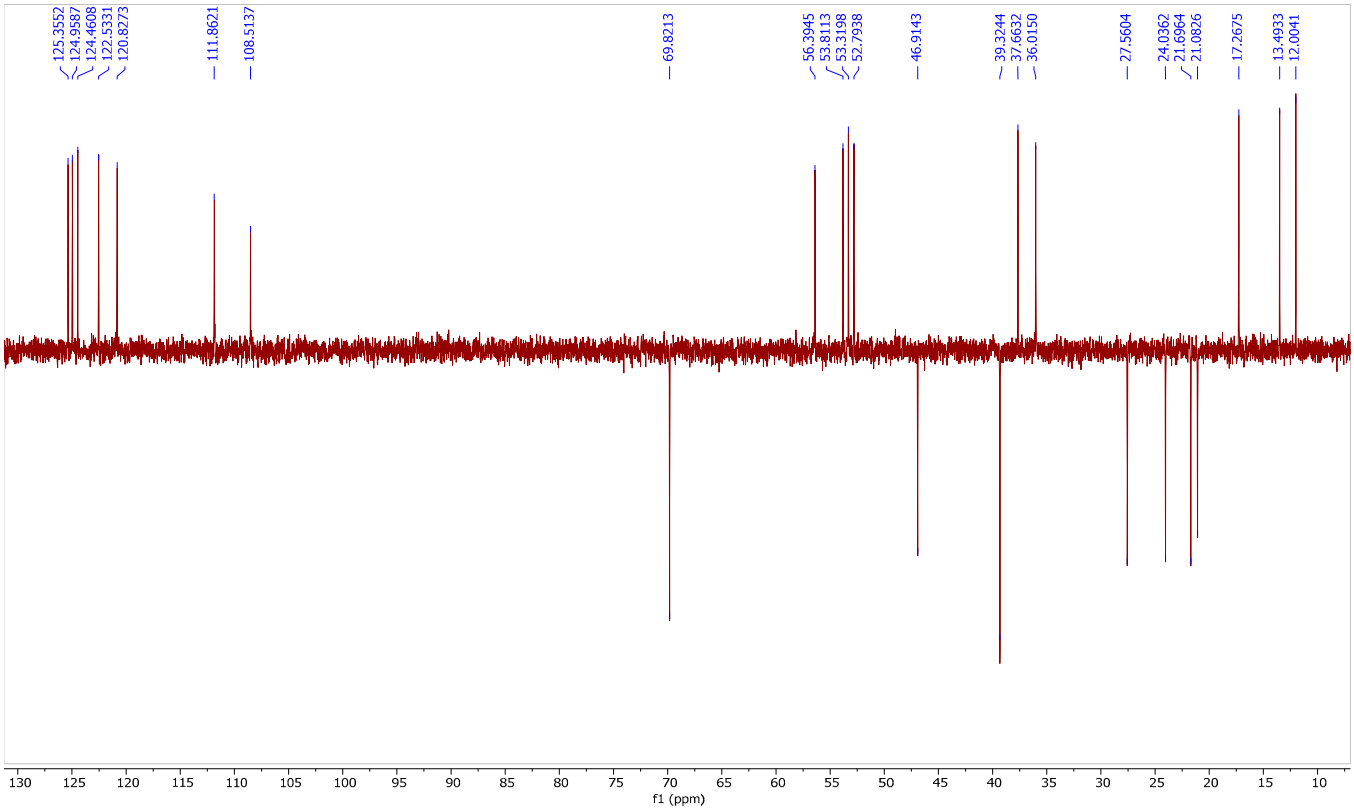


Figure S8. $^{13}C\{^{1}H\}$ DEPT-135 NMR spectrum of 6-Oxo-23,24-dinor-5α-Cholan-2-en-22-yl-1*H*-indole-2-carboxylate (**36a**)

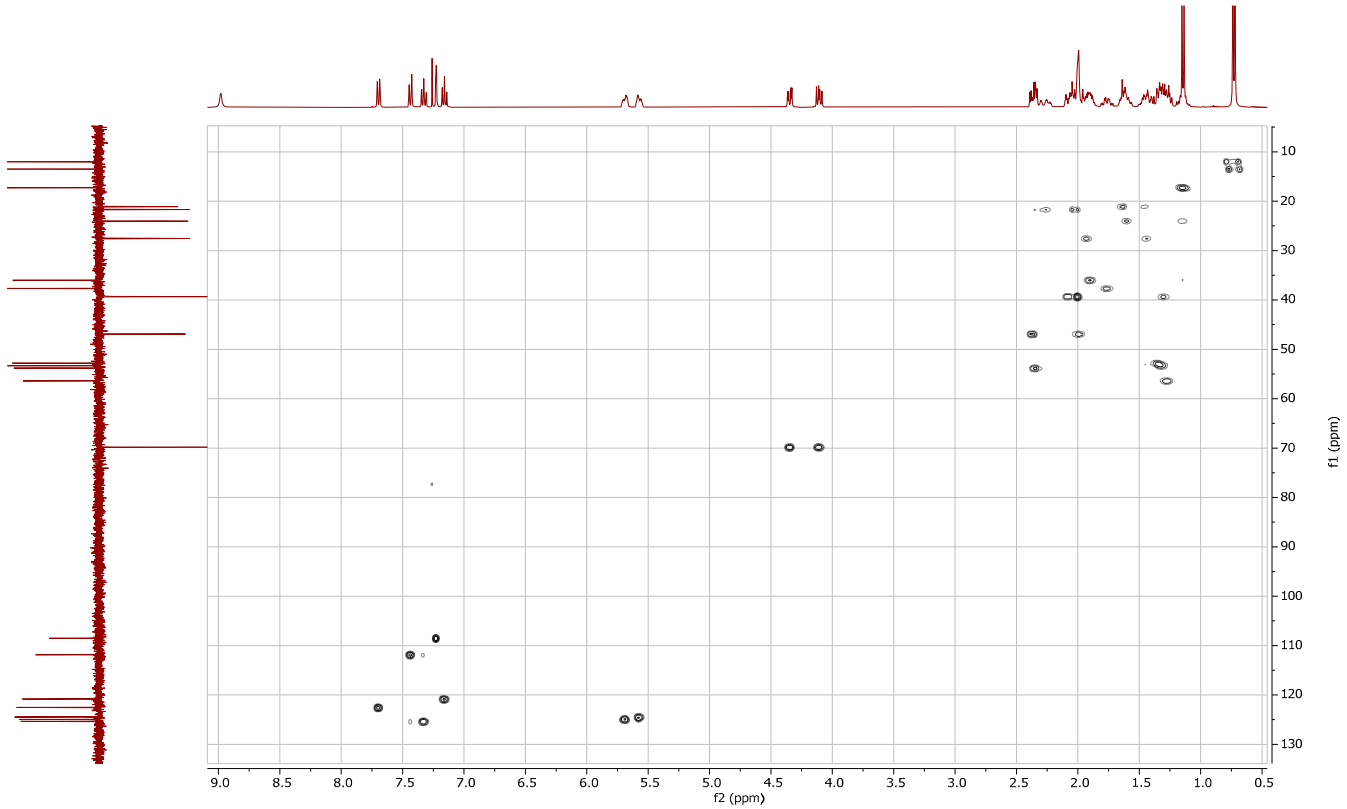


Figure S9. 2D ^{1}H-^{13}C HSQC spectrum of 6-Oxo-23,24-dinor-5α-Cholan-2-en-22-yl-1*H*-indole-2-carboxylate (**36a**)

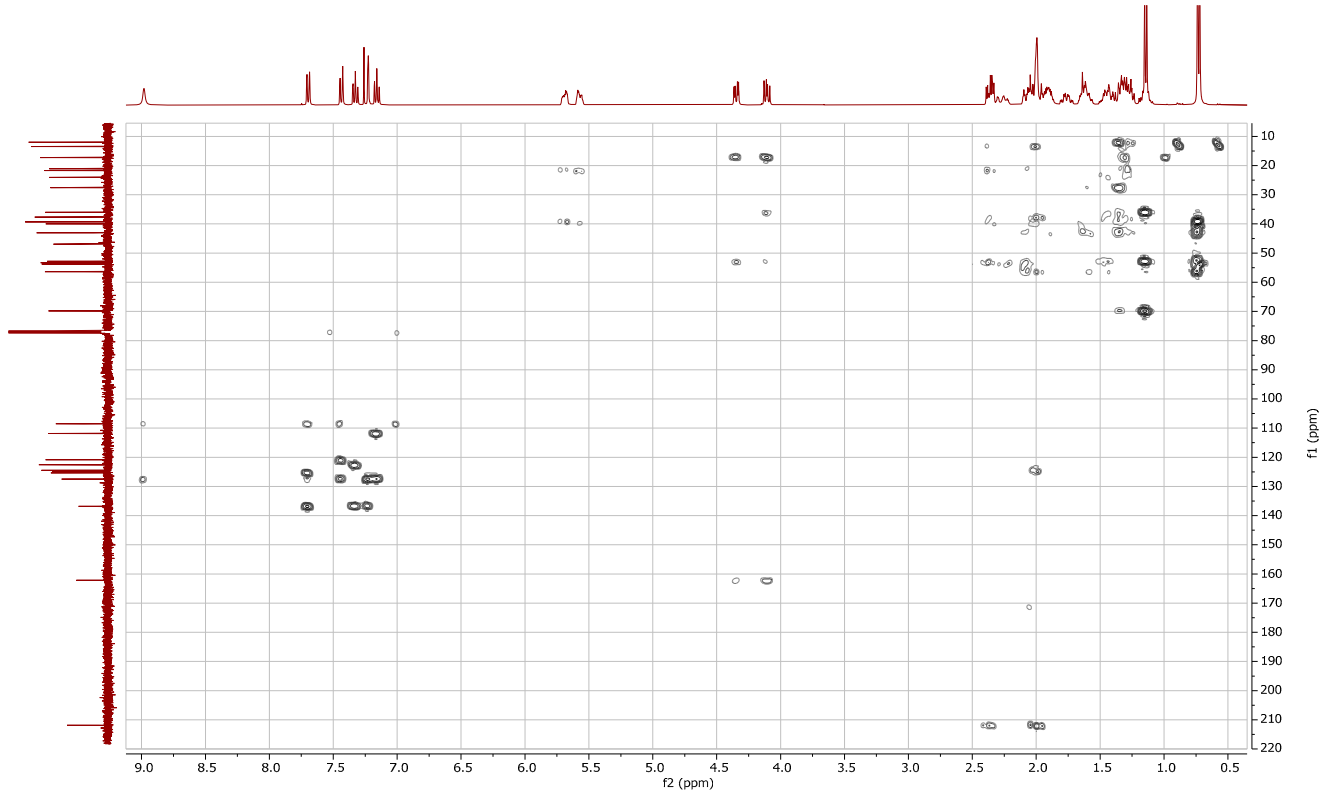


Figure S10. 2D ^{1}H-^{13}C HMBC spectrum of 6-Oxo-23,24-dinor-5α-Cholan-2-en-22-yl-1*H*-indole-2-carboxylate (**36a**)

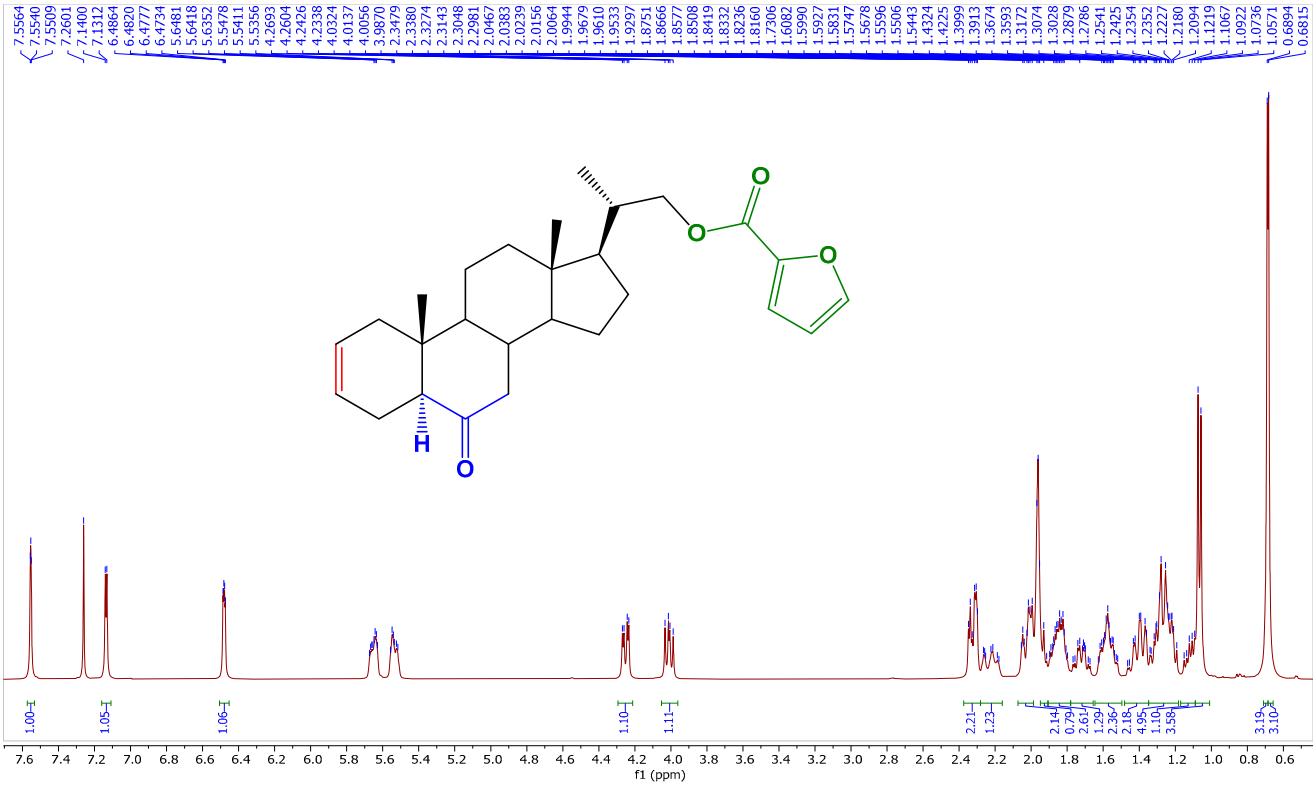


Figure S11. ^{1}H NMR spectrum of 6-Oxo-23,24-dinor-5α-Cholan-2-en-22-yl-furan-2-carboxylate (**34a**)

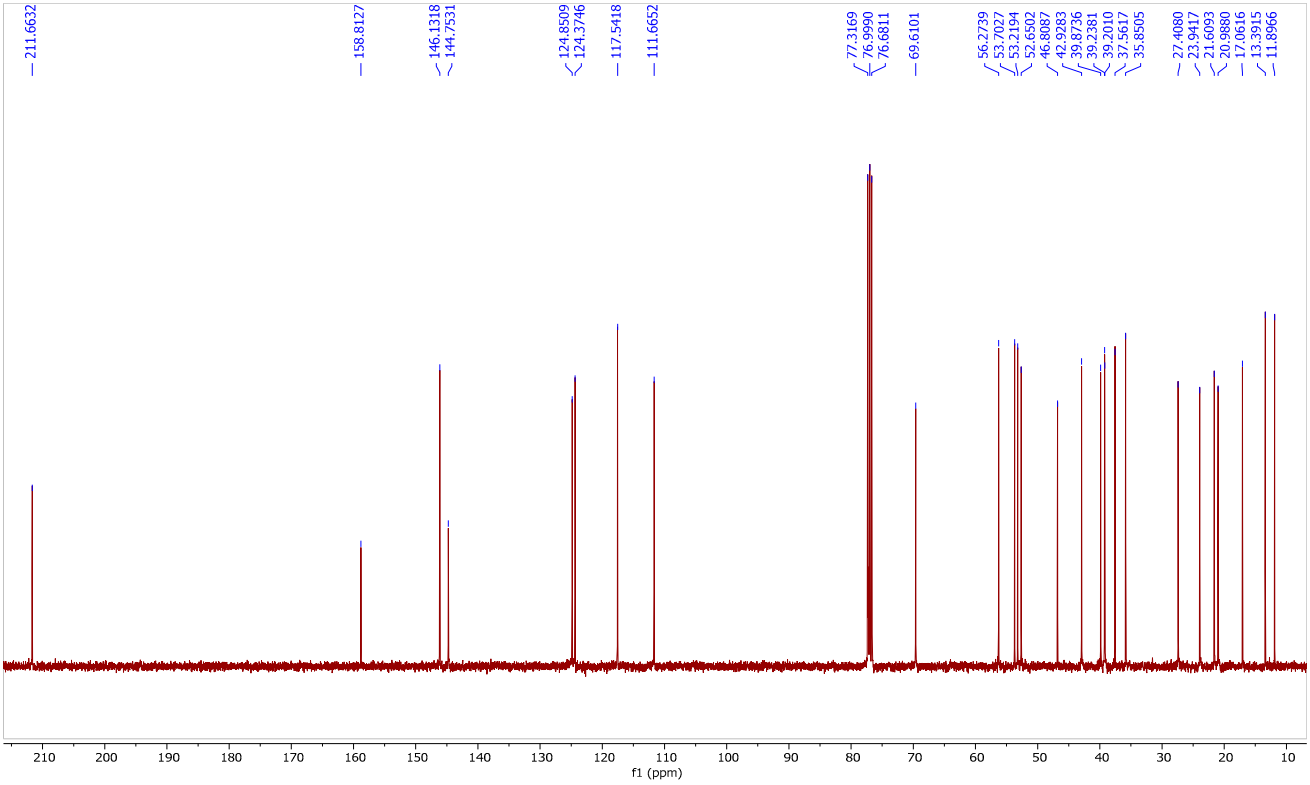


Figure S12. ^{13}C{^{1}H} NMR spectrum of 6-Oxo-23,24-dinor-5α-Cholan-2-en-22-yl-furan-2-carboxylate (**34a**)

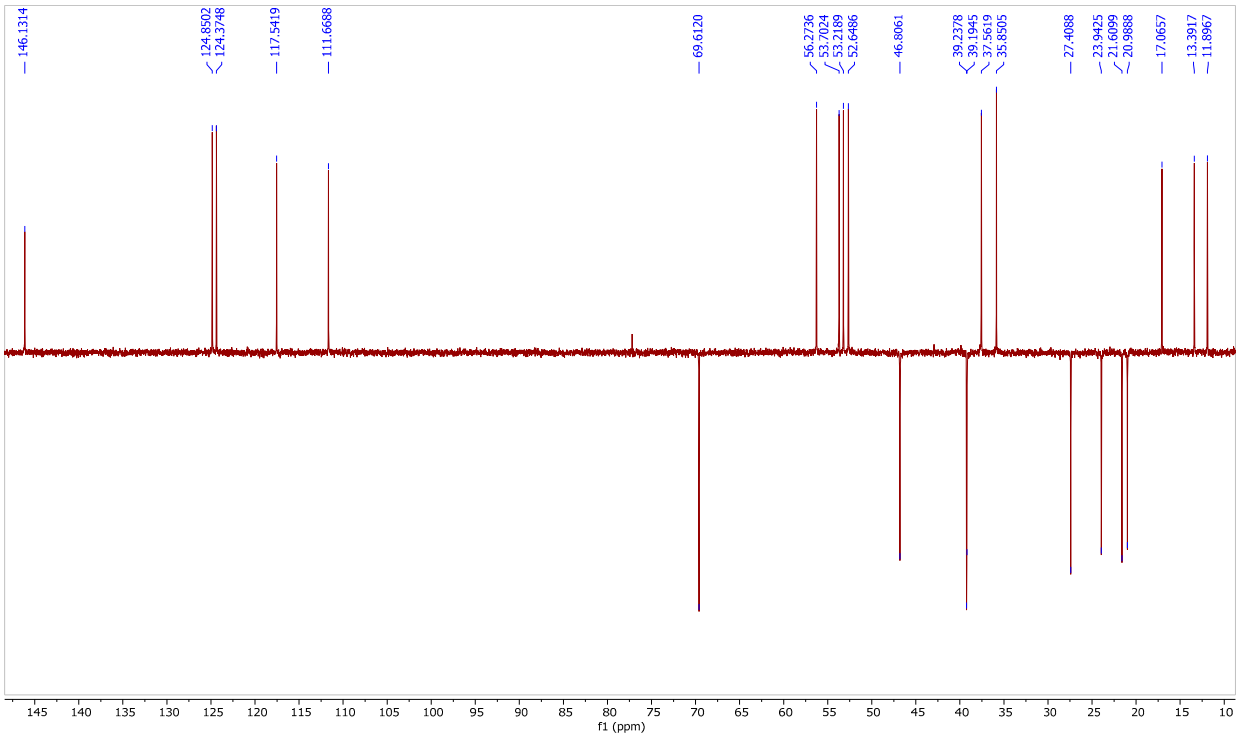


Figure S13. $^{13}C\{^{1}H\}$ DEPT-135 NMR spectrum of 6-Oxo-23,24-dinor-5α-Cholan-2-en-22-yl-furan-2-carboxylate (**34a**)

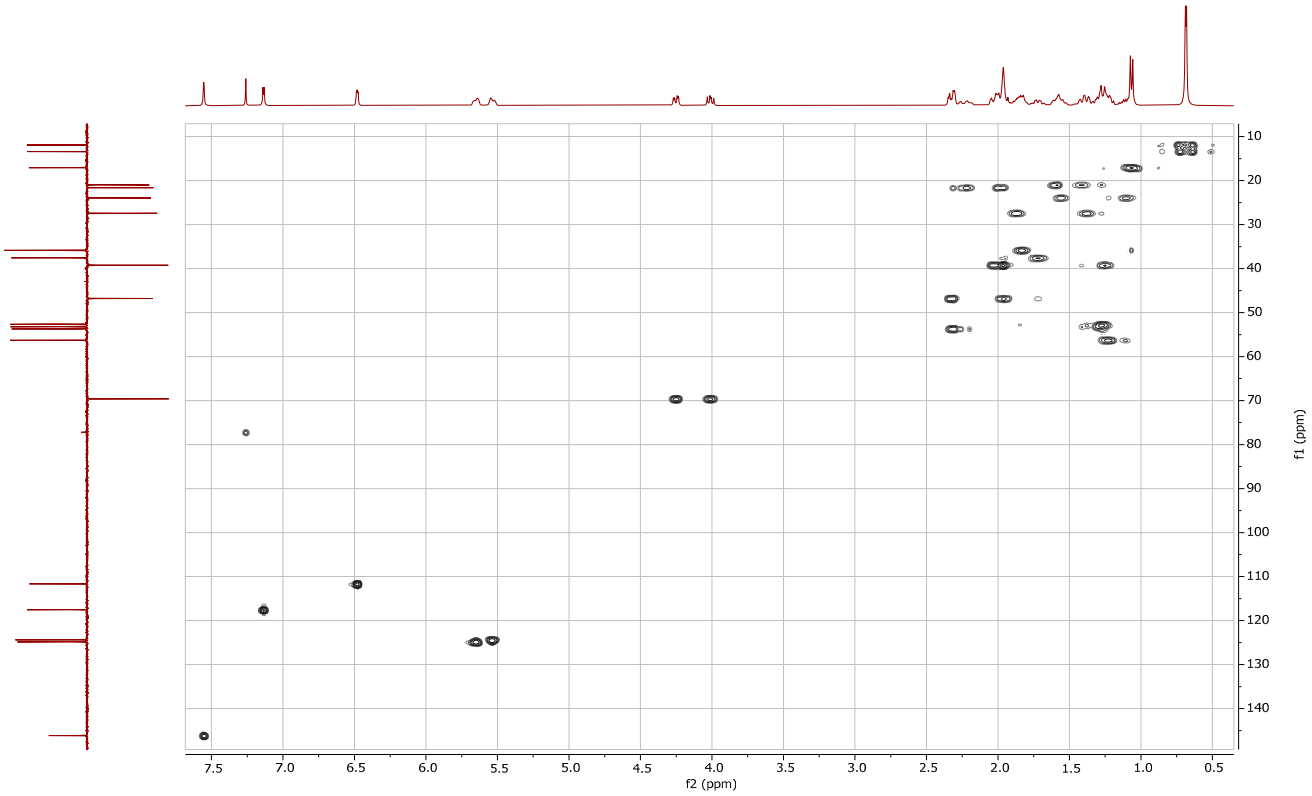


Figure S14. 2D ^{1}H-^{13}C HSQC spectrum of 6-Oxo-23,24-dinor-5α-Cholan-2-en-22-yl-furan-2-carboxylate (**34a**)

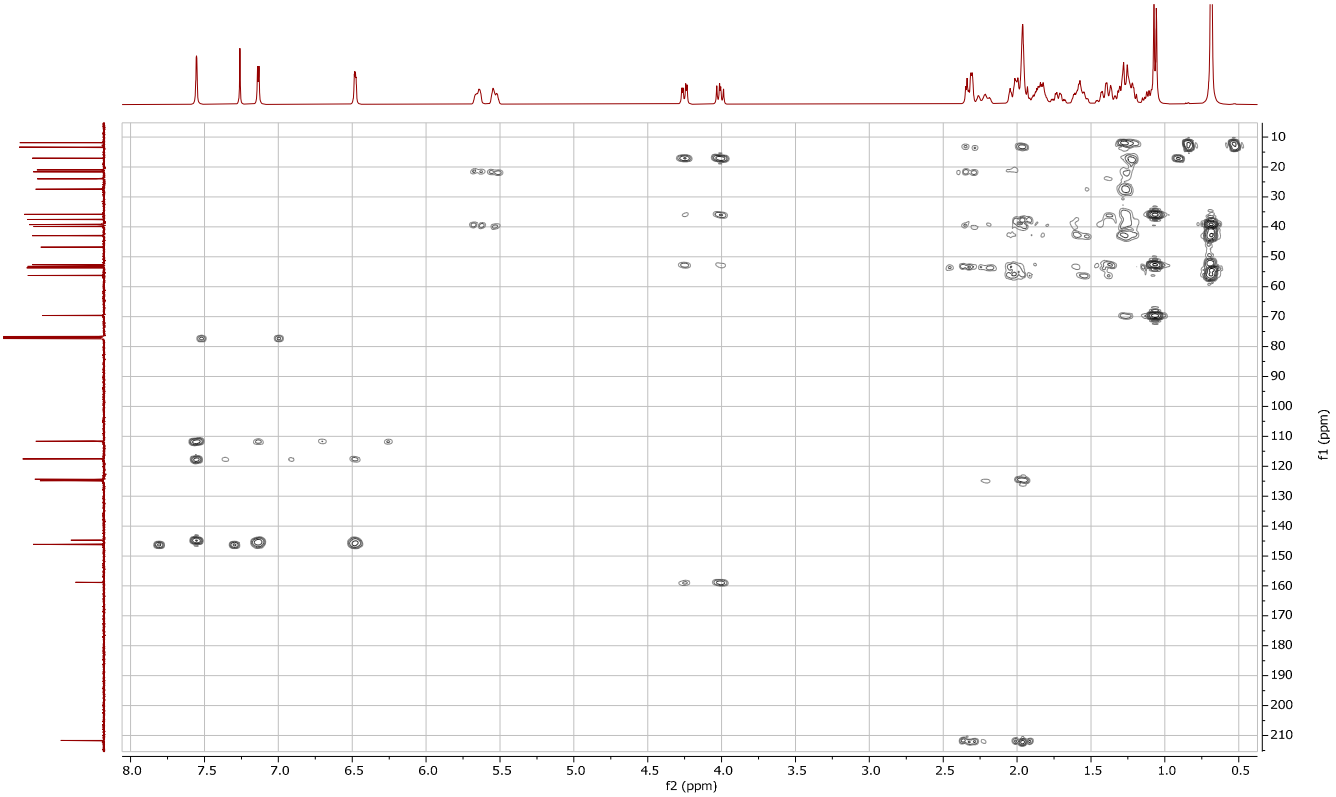


Figure S15. 2D ^{1}H-^{13}C HMBC spectrum of 6-Oxo-23,24-dinor-5α-Cholan-2-en-22-yl-furan-2-carboxylate (**34a**)

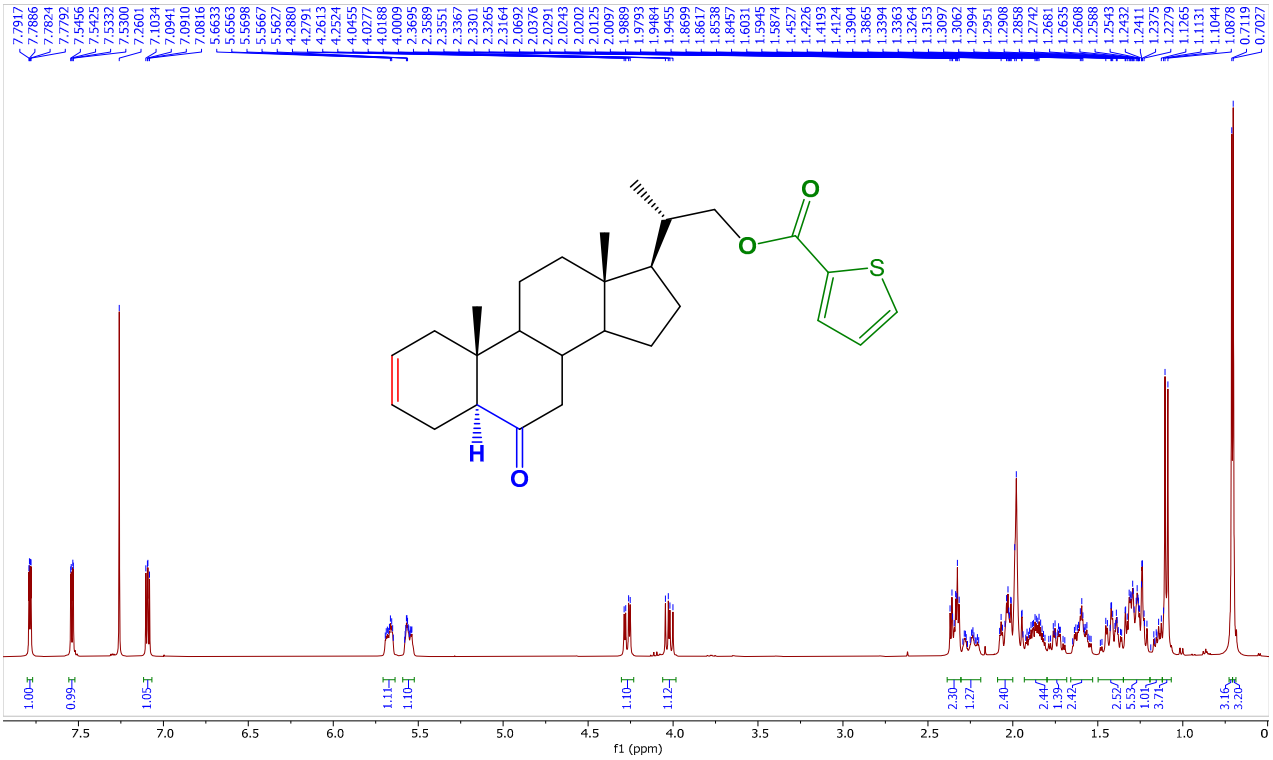


Figure S16. ^{1}H NMR spectrum of 6-Oxo-23,24-dinor-5α-Cholan-2-en-22-yl-thiophene-2-carboxylate (**35a**)

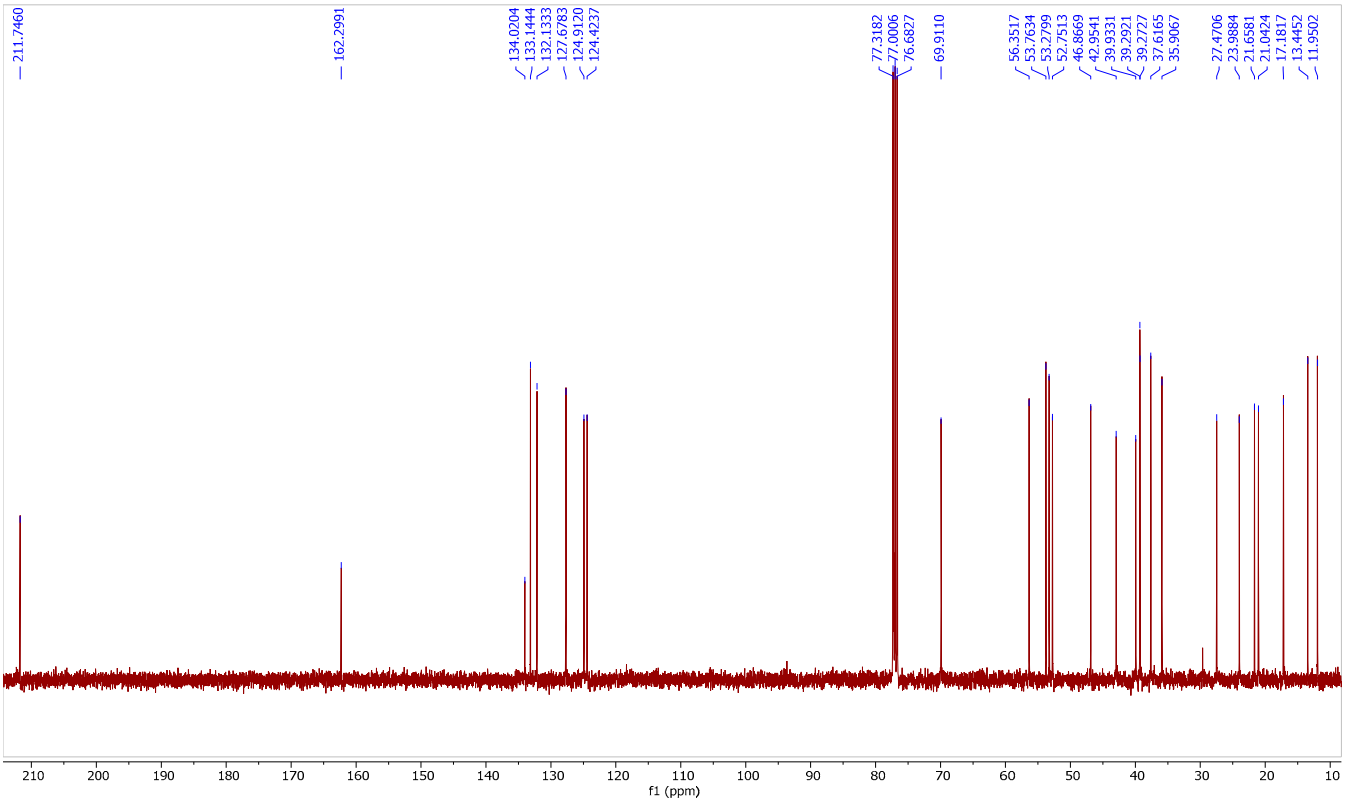


Figure S17. $^{13}C\{^{1}H\}$ NMR spectrum of 6-Oxo-23,24-dinor-5*α*-Cholan-2-en-22-yl-thiophene-2-carboxylate (**35a**)

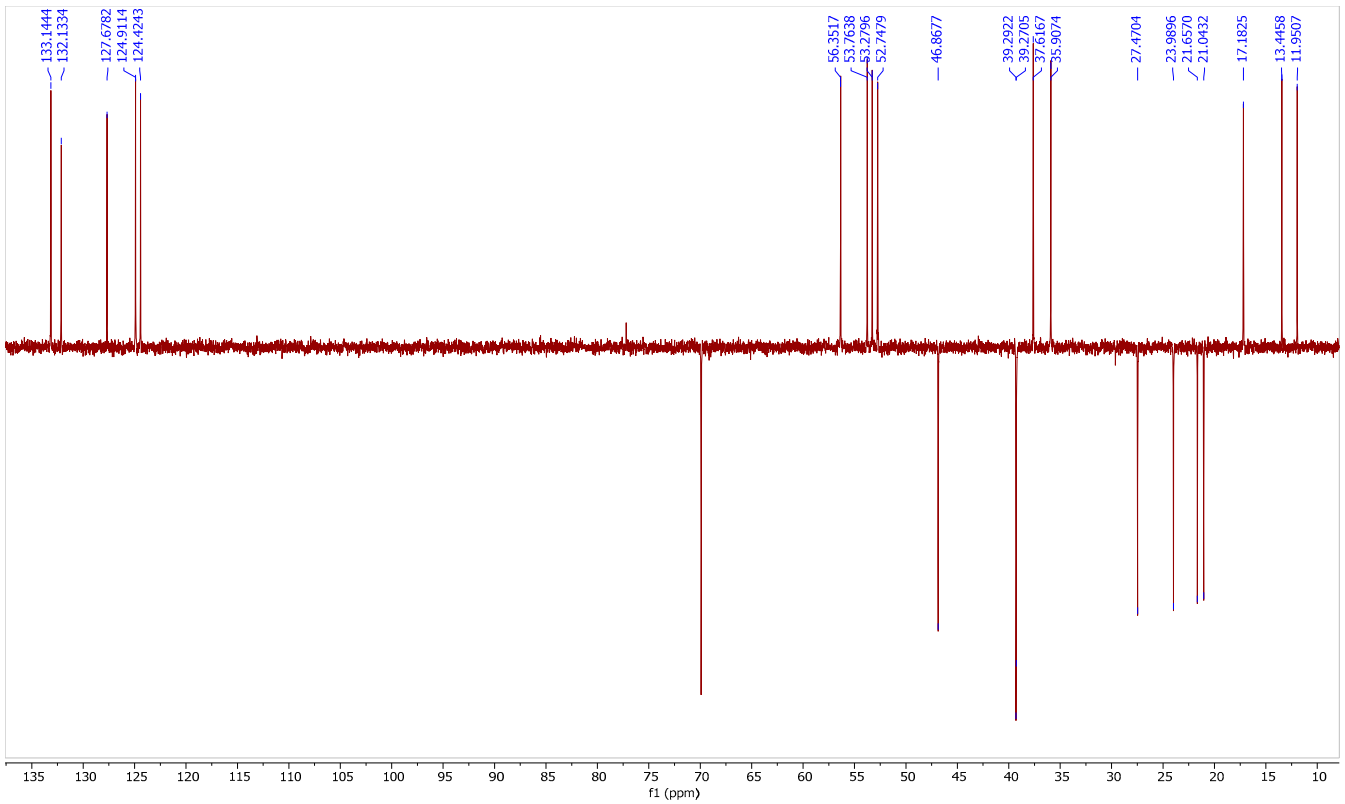


Figure S18. $^{13}C\{^{1}H\}$ DEPT-135 NMR spectrum of 6-Oxo-23,24-dinor-5*α*-Cholan-2-en-22-yl-thiophene-2-carboxylate (**35a**)

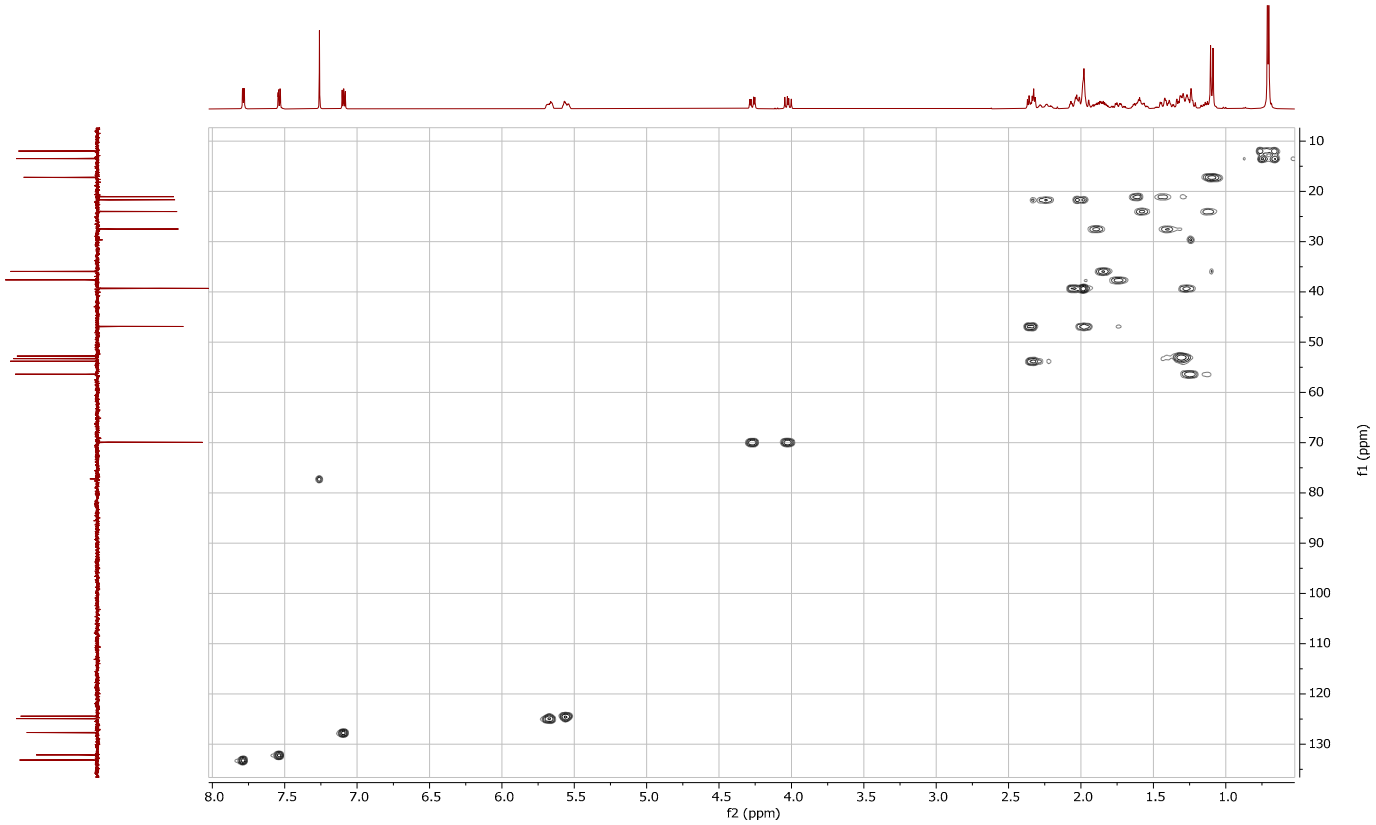


Figure S19. 2D ^{1}H-^{13}C HSQC spectrum of 6-Oxo-23,24-dinor-5α-Cholan-2-en-22-yl-thiophene-2-carboxylate (**35a**)

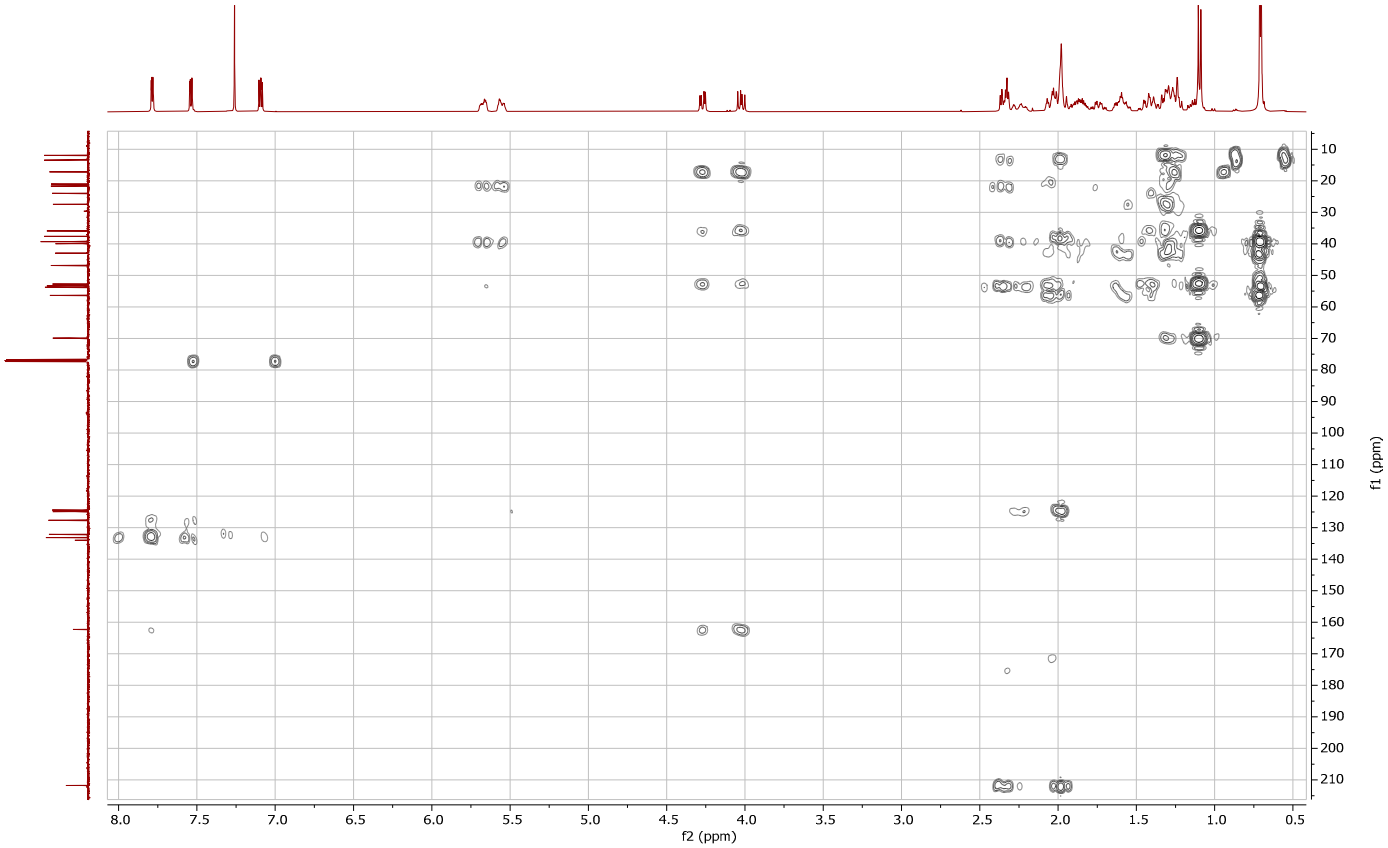


Figure S20. 2D ^{1}H-^{13}C HMBC spectrum of 6-Oxo-23,24-dinor-5α-Cholan-2-en-22-yl-thiophene-2-carboxylate (**35a**)

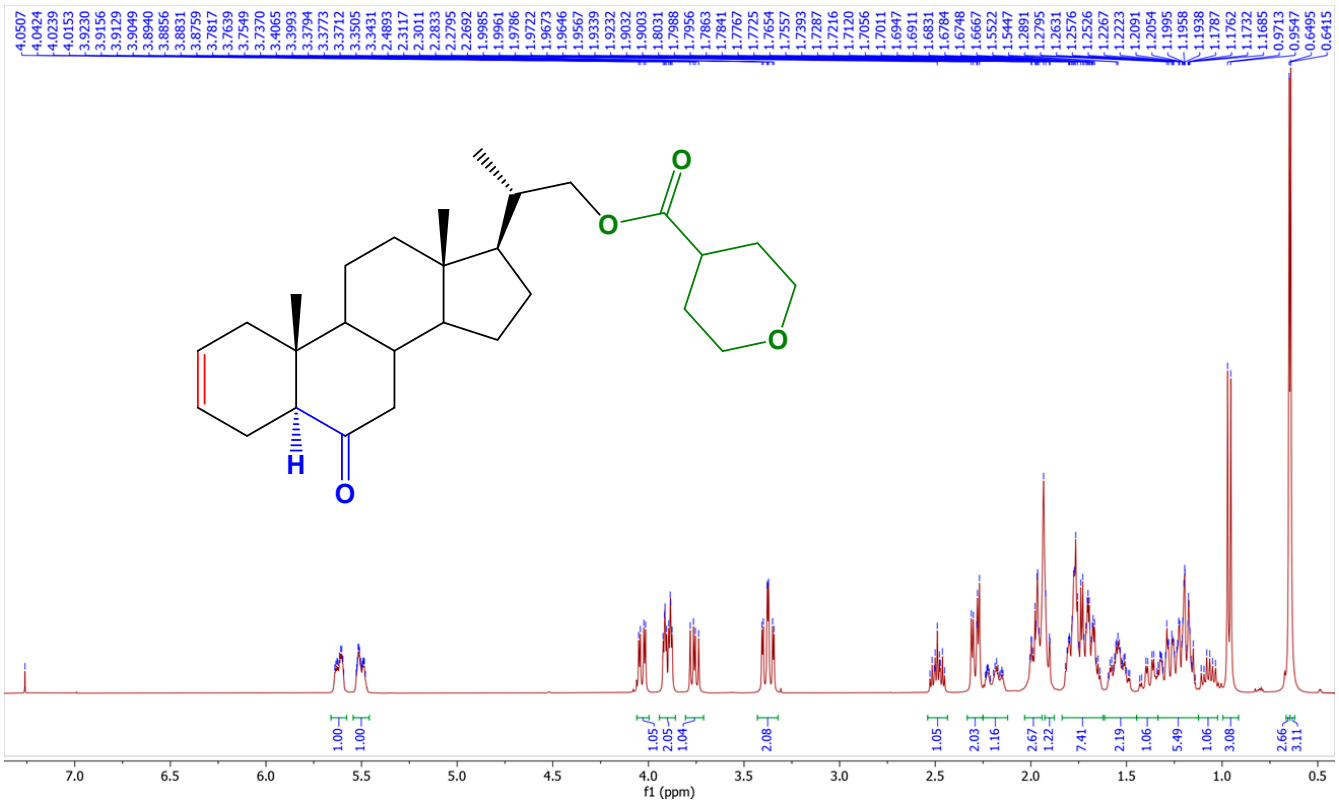


Figure S21. ^{1}H NMR spectrum of 6-Oxo-23,24-dinor-5*α*-Cholan-2-en-22-yl-tetrahydro-2*H*-pyran-4-carbocarboxylate (**37a**)

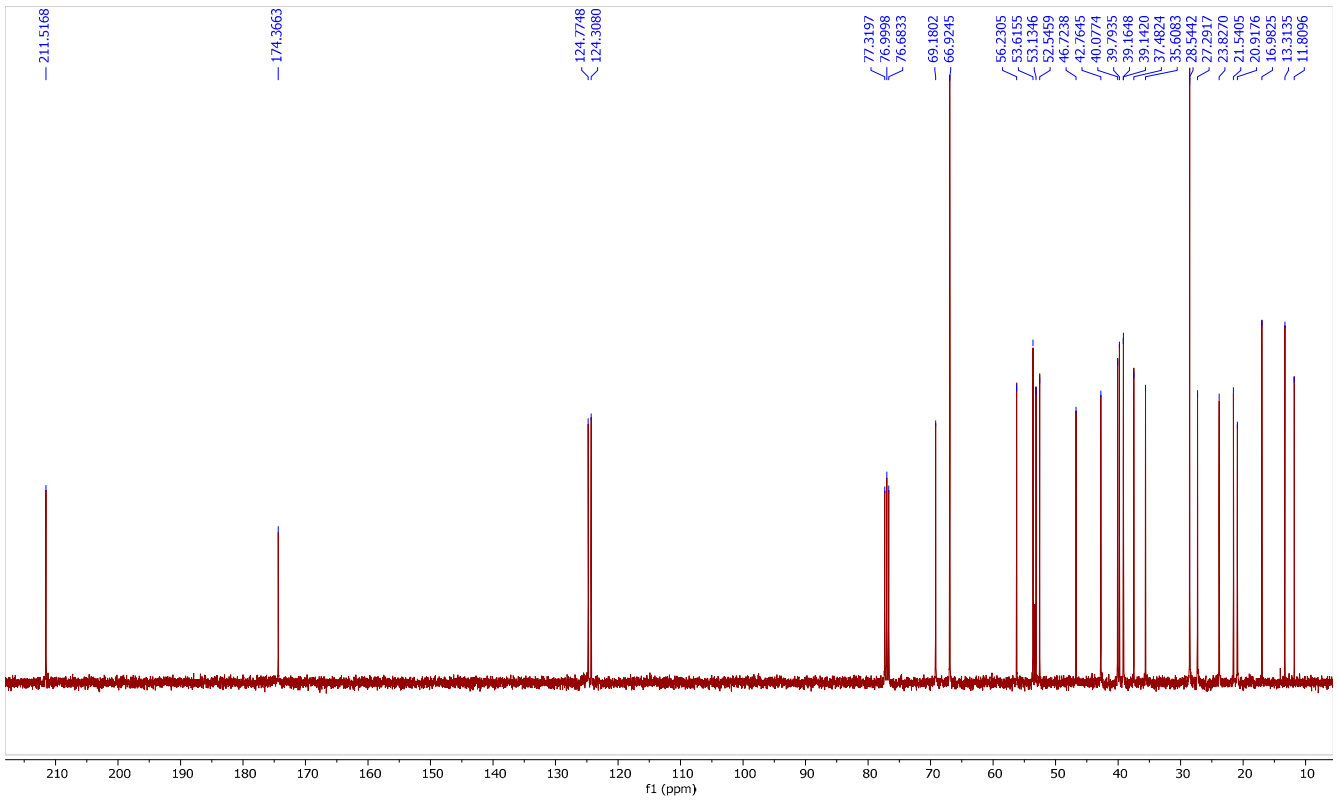


Figure S22. ^{13}C{^{1}H} NMR spectrum of 6-Oxo-23,24-dinor-5*α*-Cholan-2-en-22-yl-tetrahydro-2*H*-pyran-4-carbocarboxylate (**37a**)

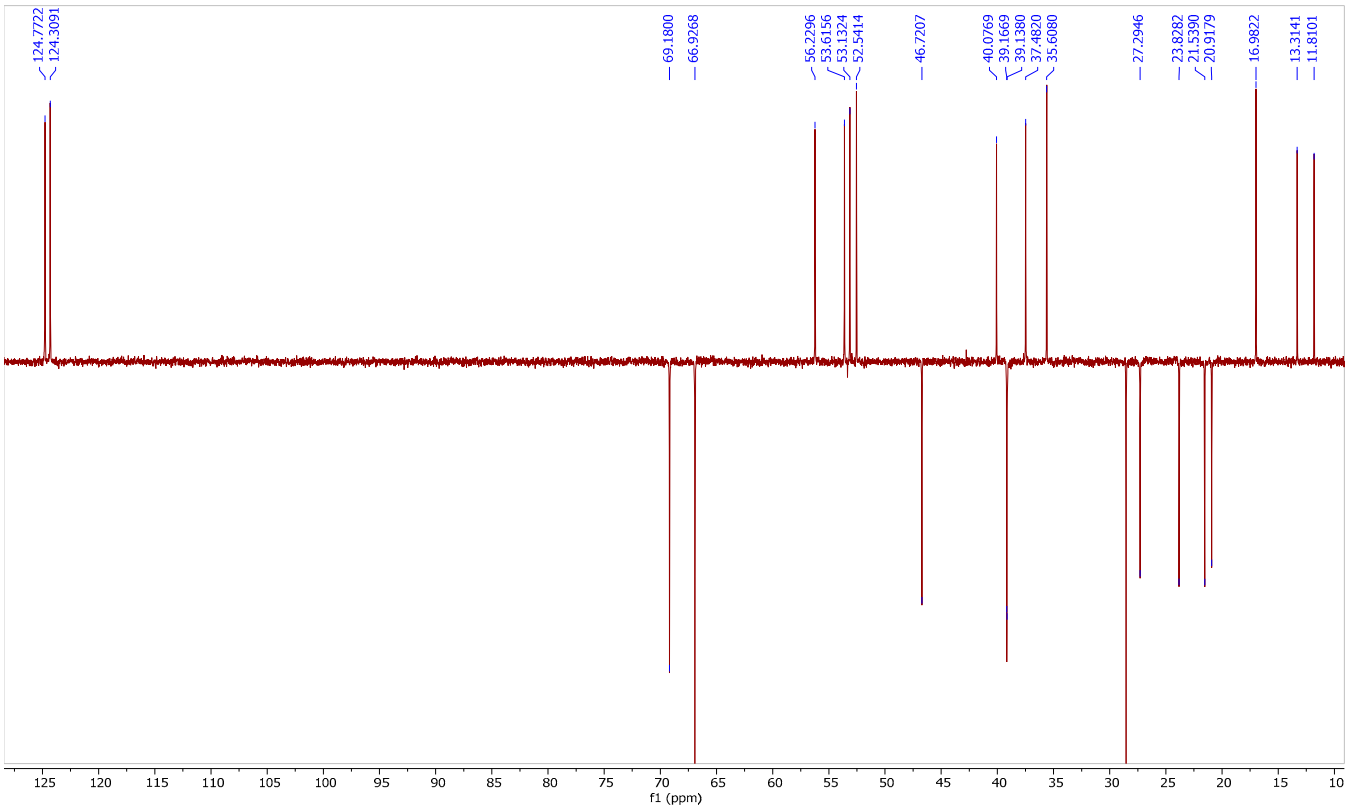


Figure S23. $^{13}C\{^{1}H\}$ DEPT-135 NMR spectrum of 6-Oxo-23,24-dinor-5*α*-Cholan-2-en-22-yl-tetrahydro-2*H*-pyran-4-carbocarboxylate (**37a**)

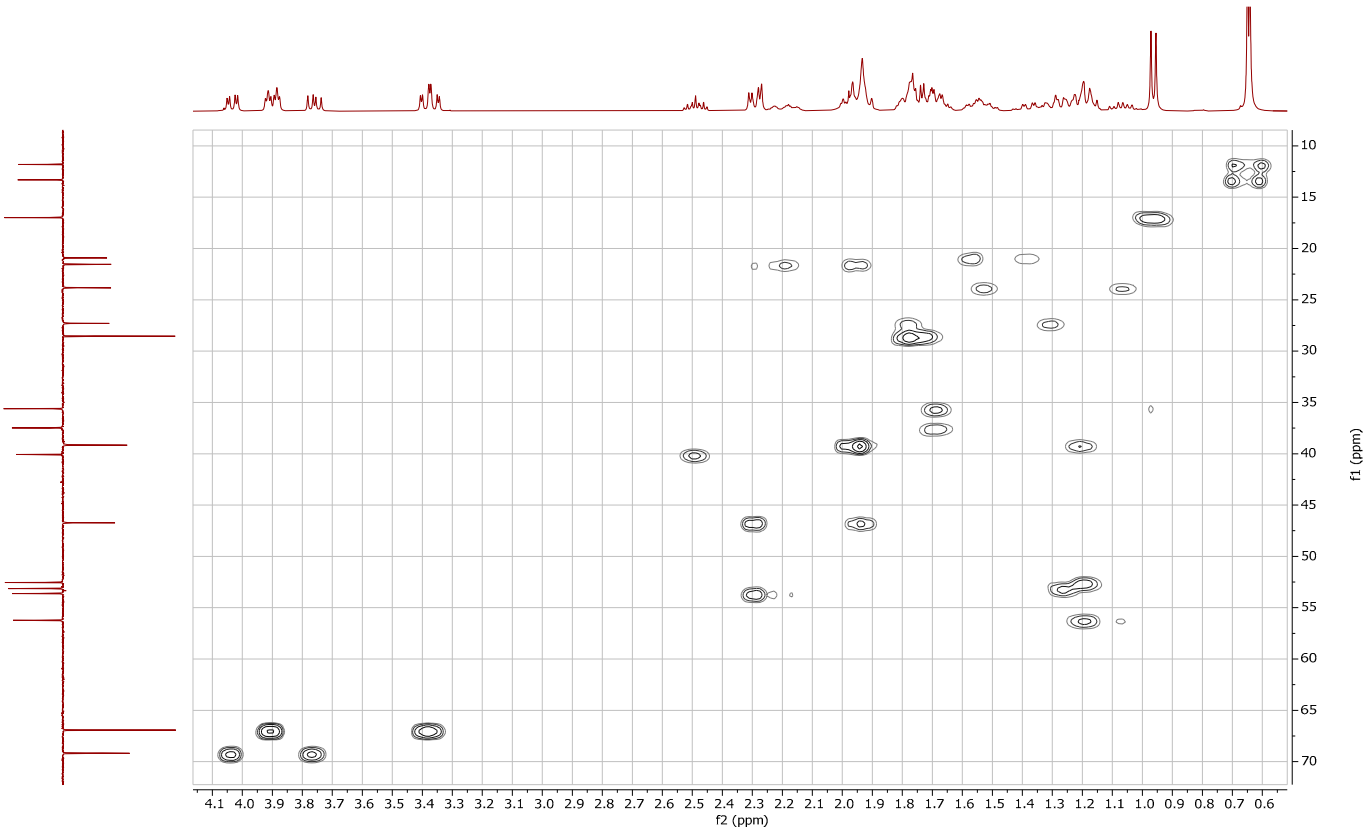


Figure S24. 2D ^{1}H-^{13}C HSQC spectrum of 6-Oxo-23,24-dinor-5*α*-Cholan-2-en-22-yl-tetrahydro-2*H*-pyran-4-carbocarboxylate (**37a**)

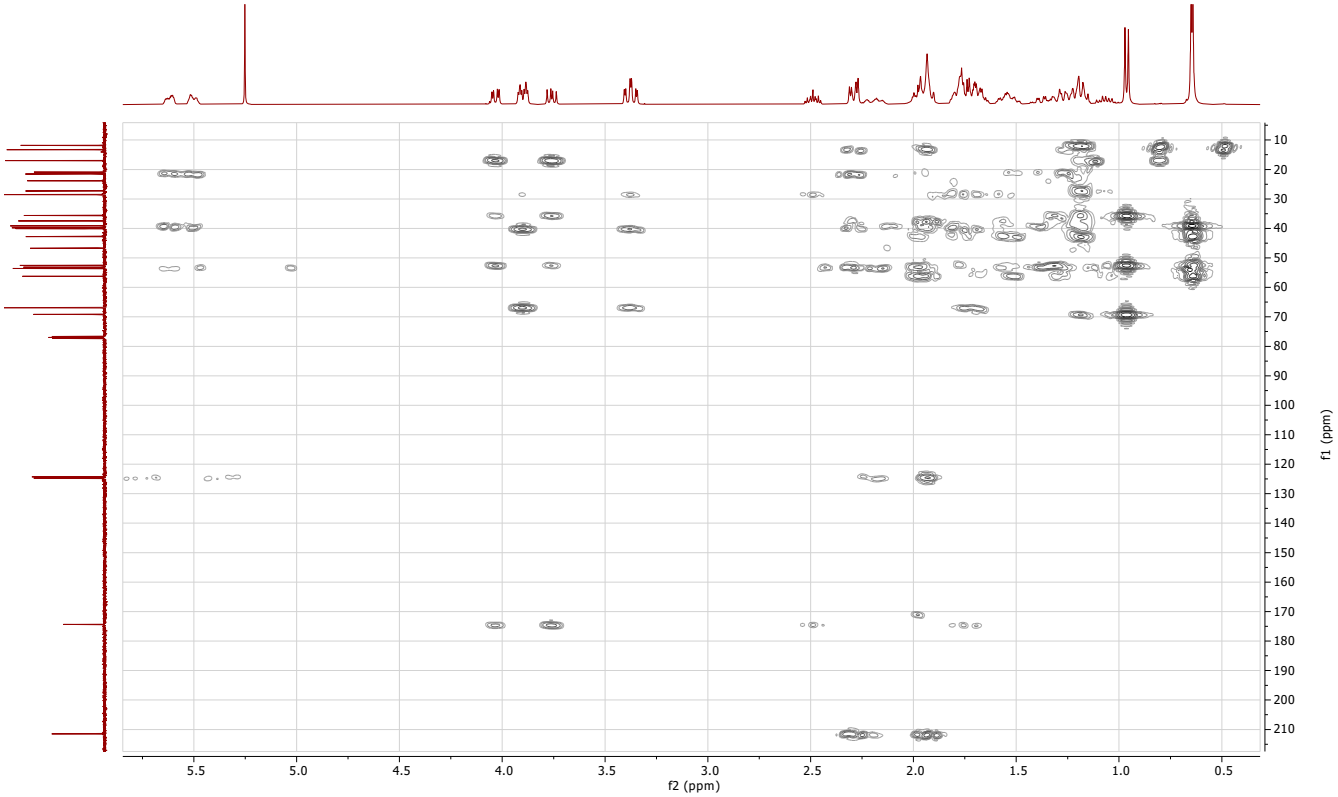


Figure S25. 2D ^{1}H-^{13}C HMBC spectrum of 6-Oxo-23,24-dinor-5α-Cholan-2-en-22-yl-tetrahydro-2*H*-pyran-4-carbocarboxylate (**37a**)

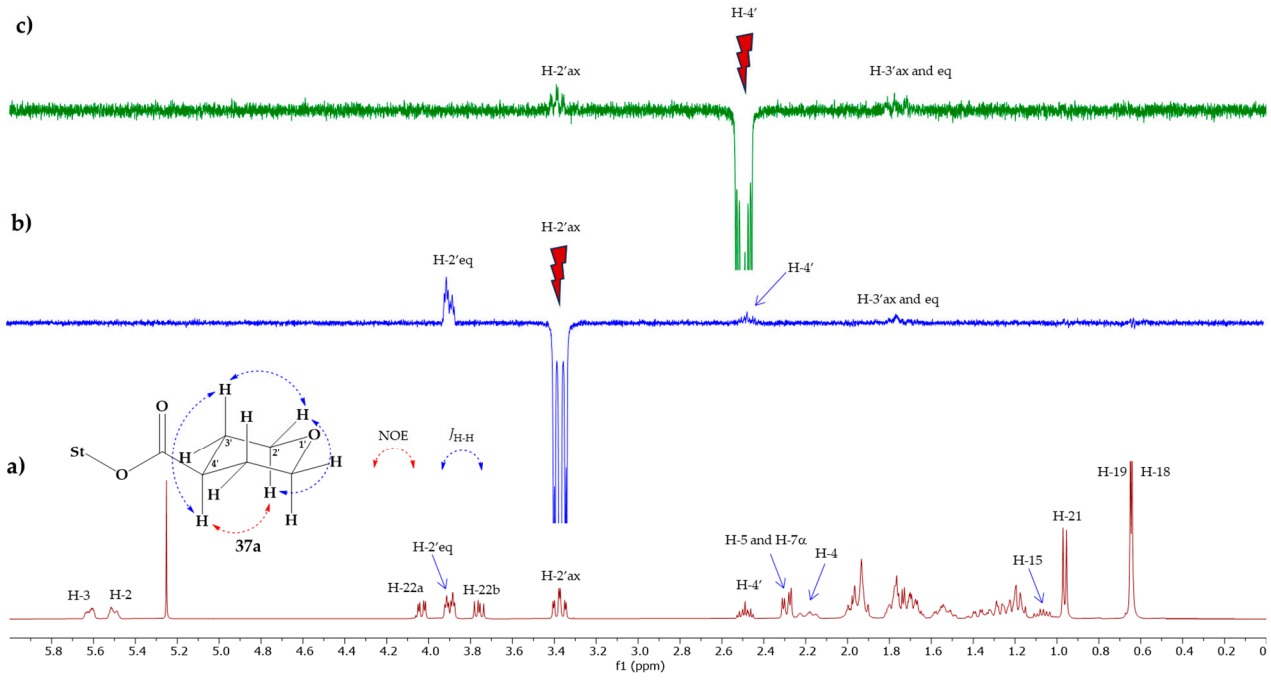


Figure S26. 1D selective NOESY NMR spectrum 6-Oxo-23,24-dinor-5α-Cholan-2-en-22-yl-tetrahydro-2*H*-pyran-4-carbocarboxylate (**37a**)

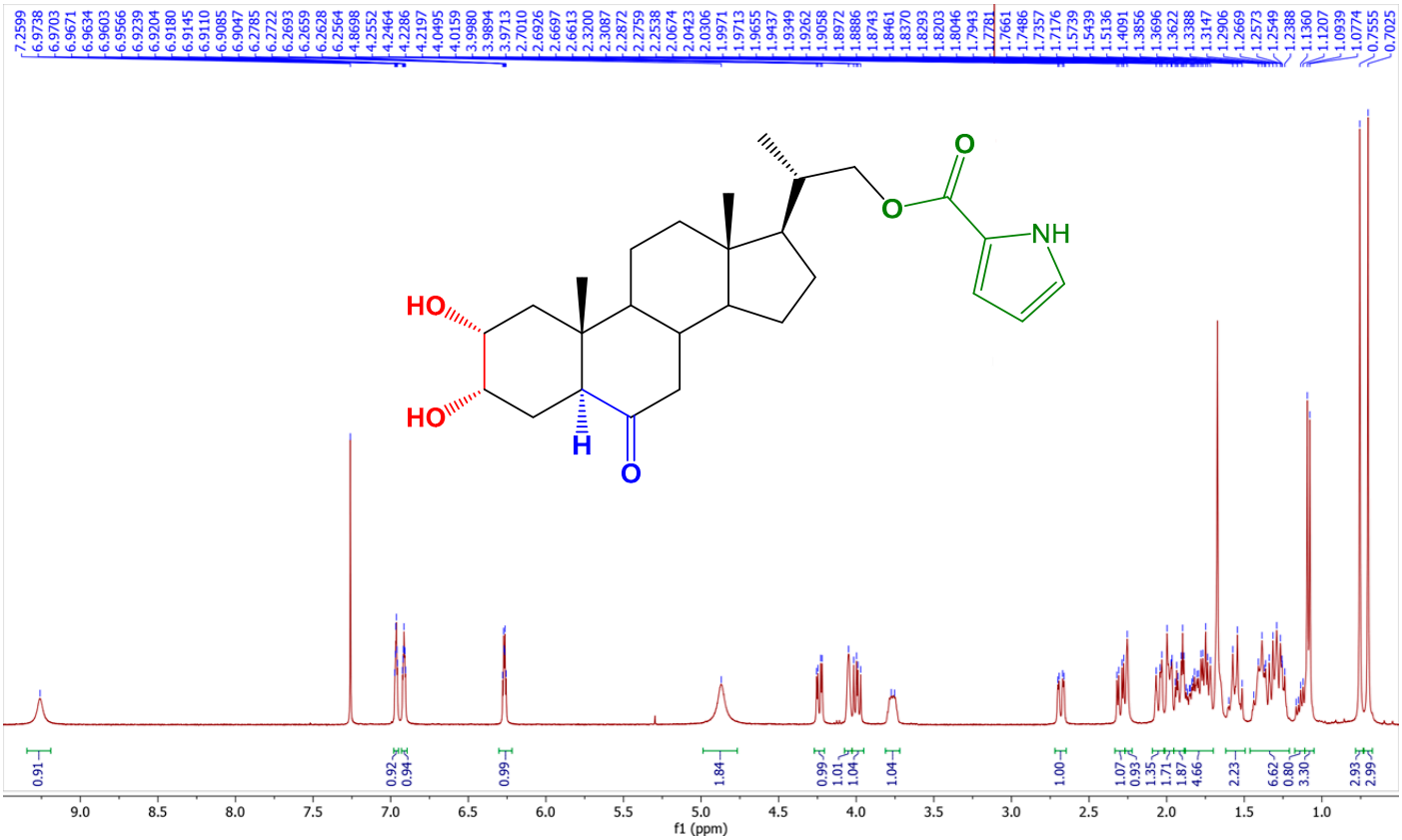


Figure S27. ^{1}H NMR spectrum of 2α,3α-Dihydroxy-6-oxo-23,24-dinor-5α-cholan-22-yl-1*H*-pyrrole-2-carboxylate (**33**)

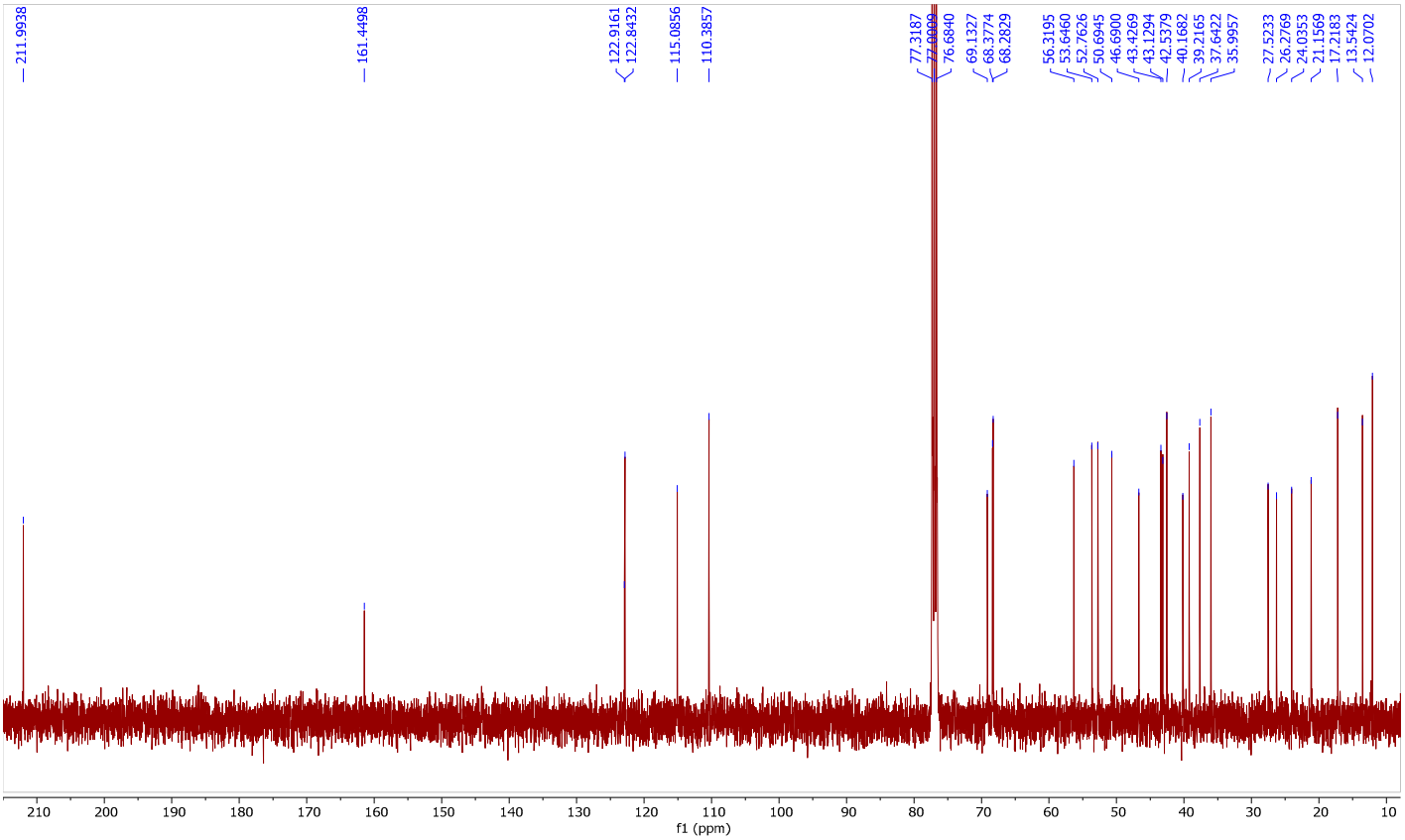


Figure S28. ^{13}C{^{1}H} NMR spectrum of 2α,3α-Dihydroxy-6-oxo-23,24-dinor-5α-cholan-22-yl-1*H*-pyrrole-2-carboxylate (**33**)

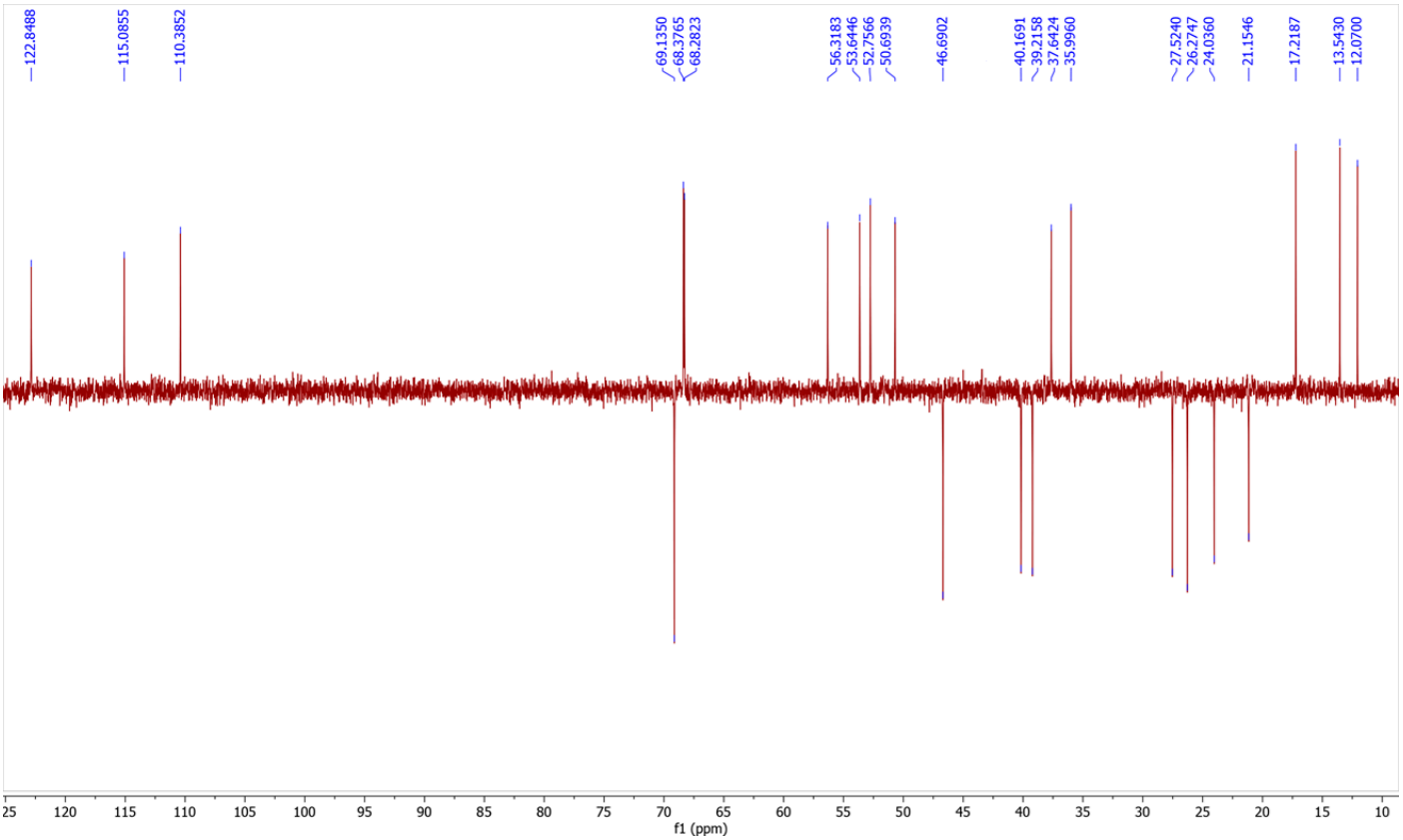


Figure S29. $^{13}C\{^{1}H\}$ DEPT-135 NMR spectrum of 2*α*,3*α*-Dihydroxy-6-oxo-23,24-dinor-5*α*-cholan-22-yl-1*H*-pyrrole-2-carboxylate (**33**)

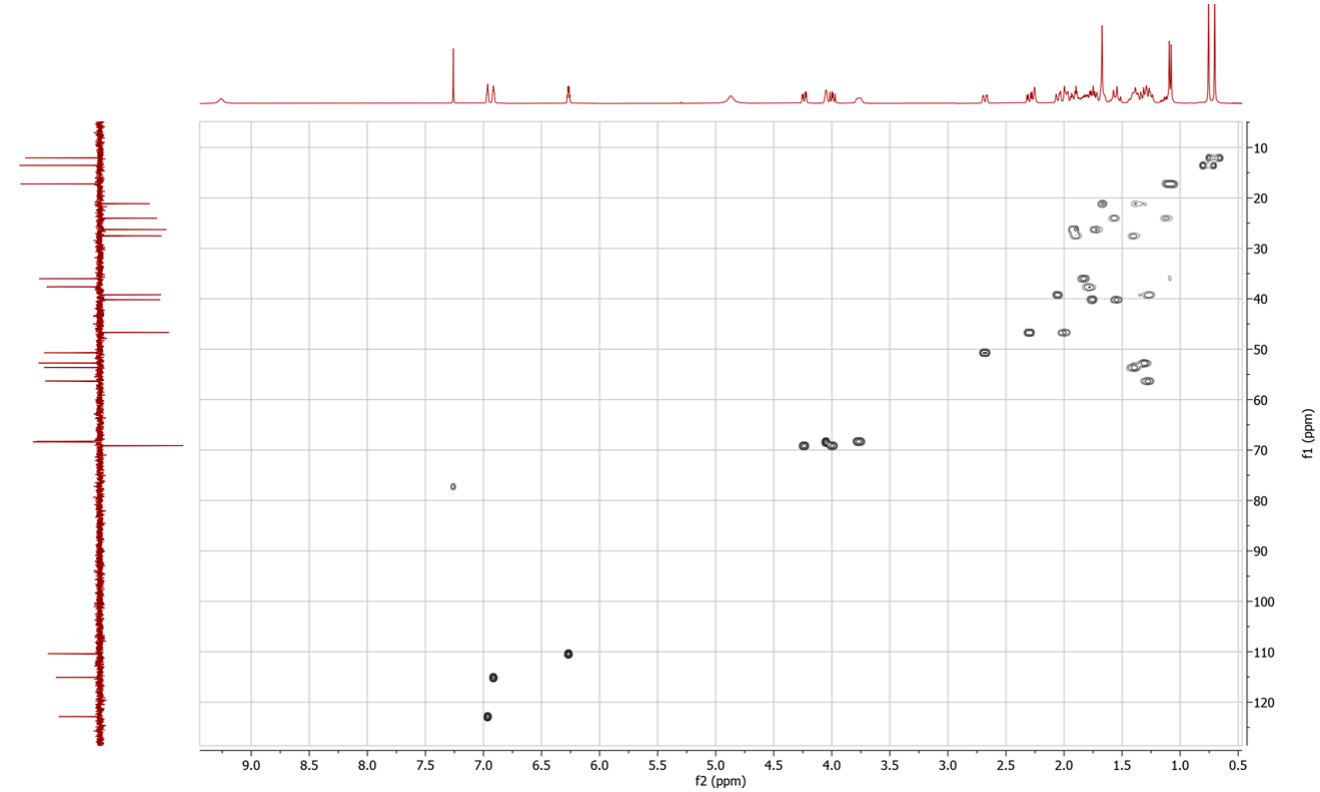


Figure S30. 2D ^{1}H-^{13}C HSQC spectrum of 2*α*,3*α*-Dihydroxy-6-oxo-23,24-dinor-5*α*-cholan-22-yl-1*H*-pyrrole-2-carboxylate (**33**)

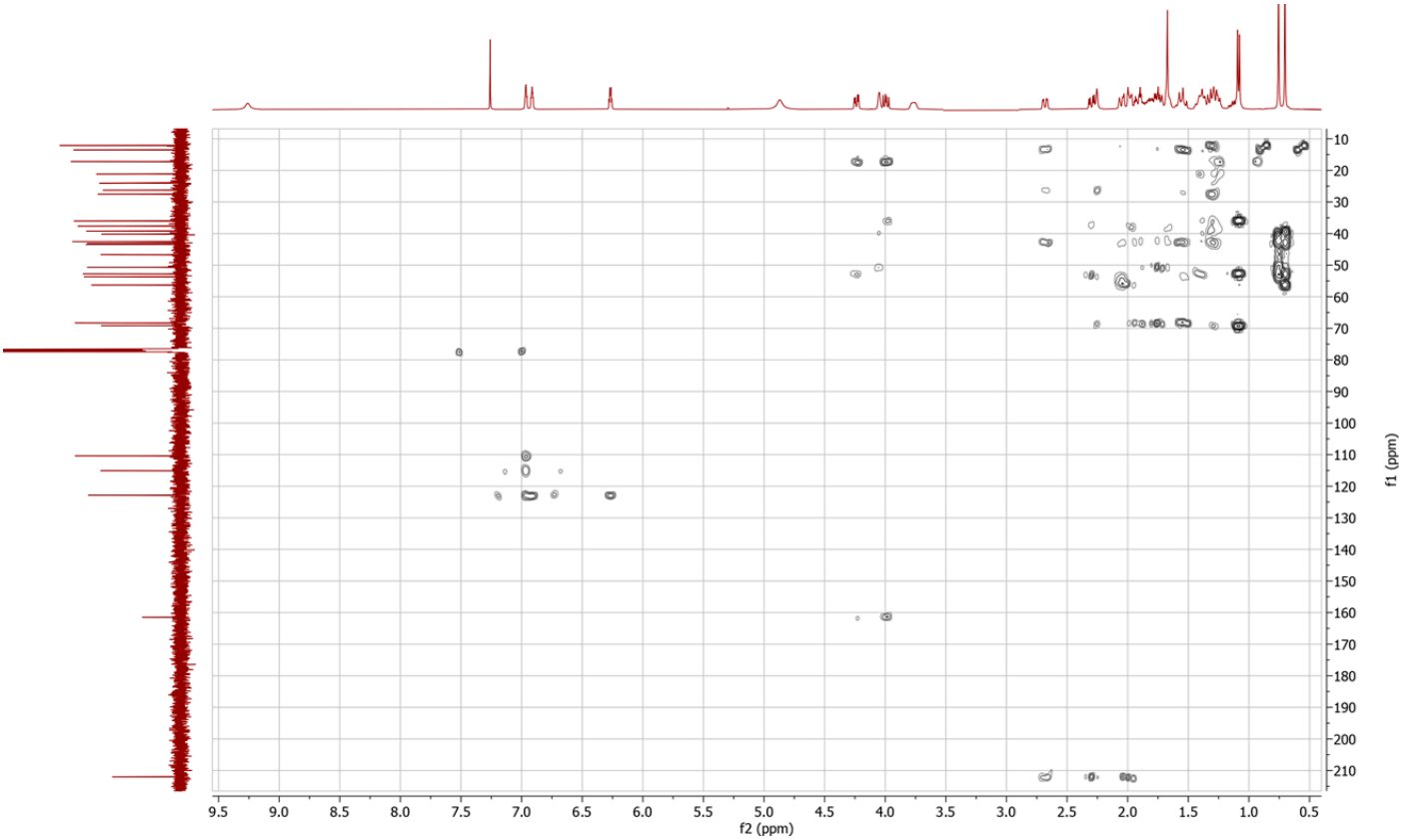


Figure S31. 2D ^{1}H-^{13}C HMBC spectrum of 2*α*,3*α*-Dihydroxy-6-oxo-23,24-dinor-5*α*-cholan-22-yl-1*H*-pyrrole-2-carboxylate (**33**)

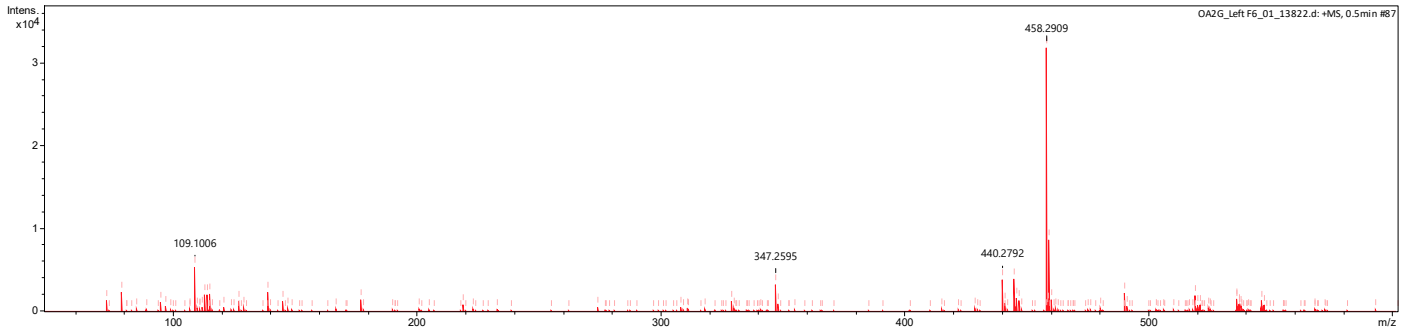


Figure S32. HRMS spectrum of 2*α*,3*α*-Dihydroxy-6-oxo-23,24-dinor-5*α*-cholan-22-yl-1*H*-pyrrole-2-carboxylate (**33**)

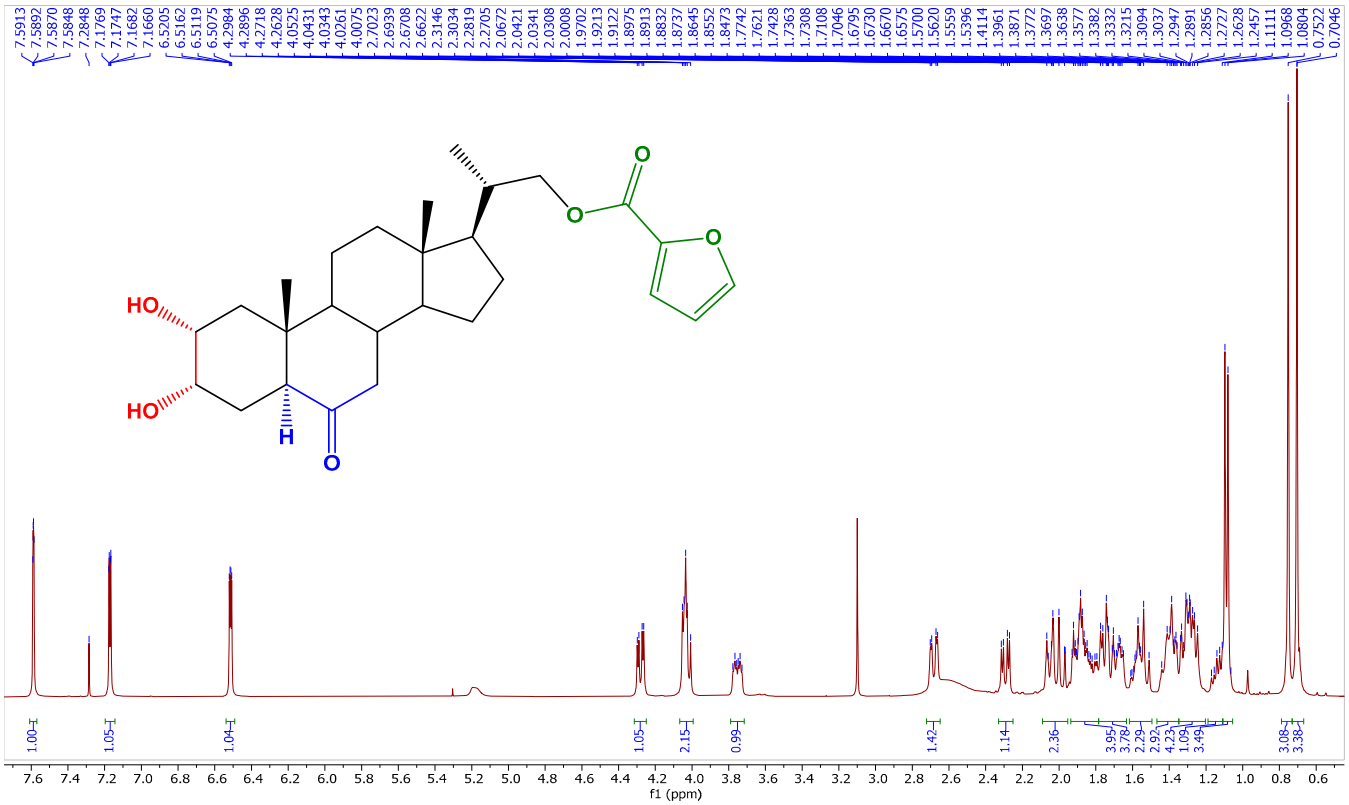


Figure S33. ^{1}H NMR spectrum of 2α,3α-Dihydroxy-6-oxo-23,24-dinor-5α-cholan-22-yl-furan-2-carboxylate (**34**)

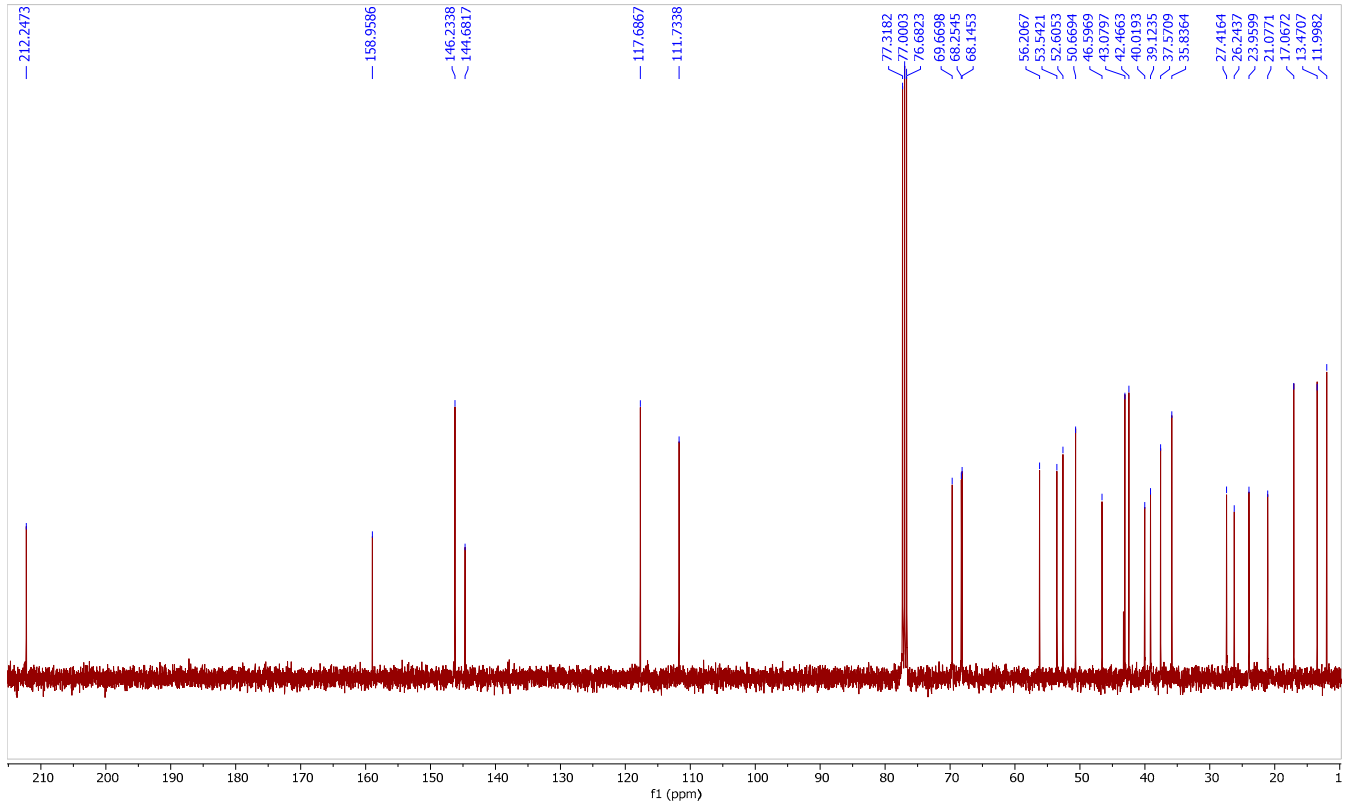


Figure S34. ^{13}C{^{1}H} NMR spectrum of 2α,3α-Dihydroxy-6-oxo-23,24-dinor-5α-cholan-22-yl-furan-2-carboxylate (**34**)

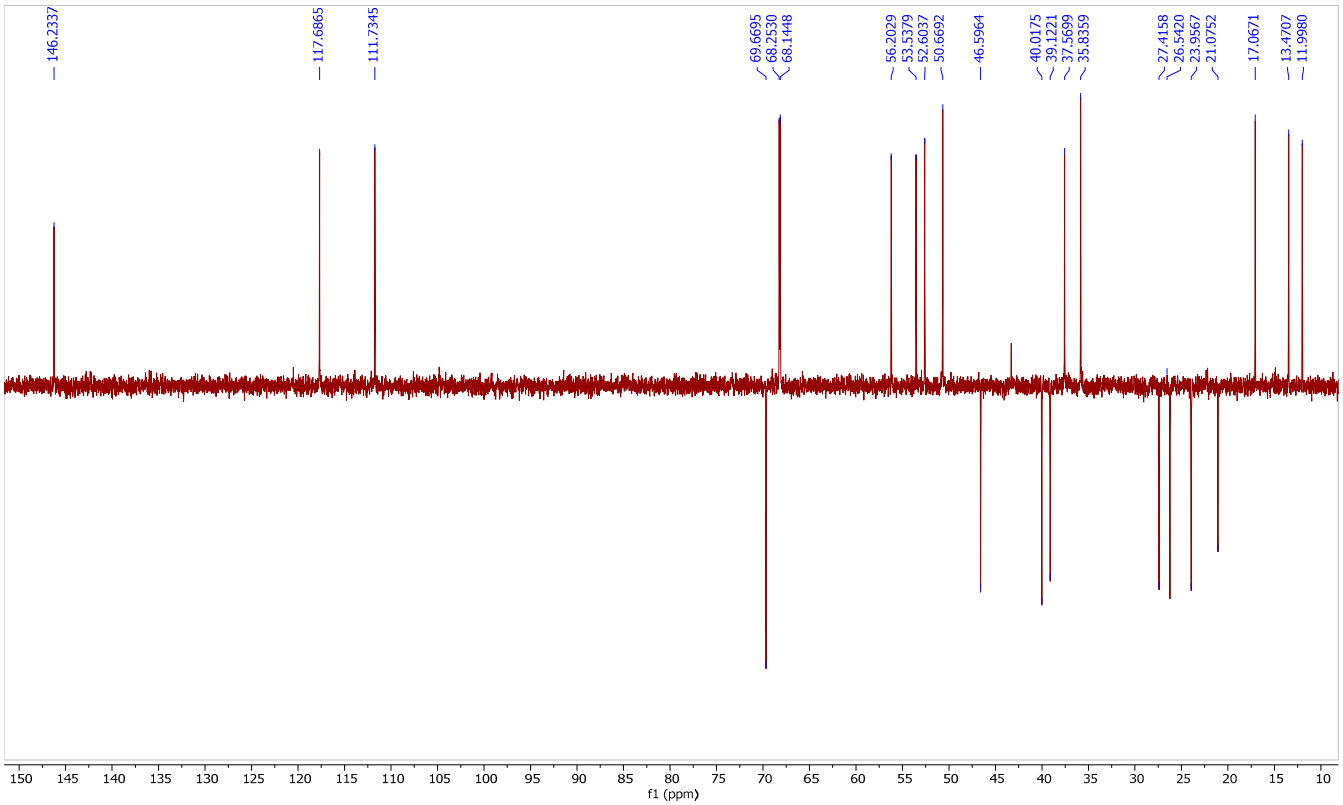


Figure S35. $^{13}C\{^{1}H\}$ DEPT-135 NMR spectrum of 2*α*,3*α*-Dihydroxy-6-oxo-23,24-dinor-5*α*-cholan-22-yl-furan-2-carboxylate (**34**)

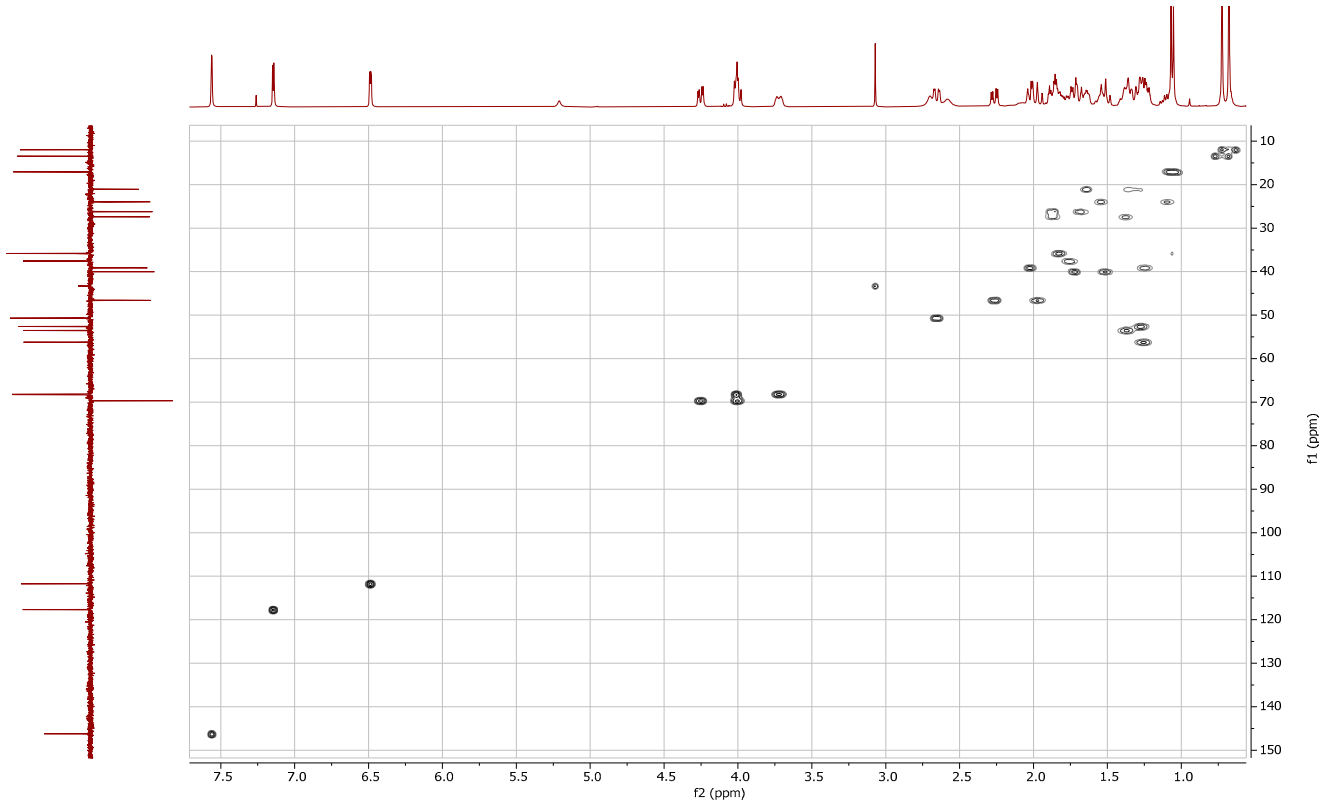


Figure S36. 2D ^{1}H-^{13}C HSQC spectrum of 2*α*,3*α*-Dihydroxy-6-oxo-23,24-dinor-5*α*-cholan-22-yl-furan-2-carboxylate (**34**)

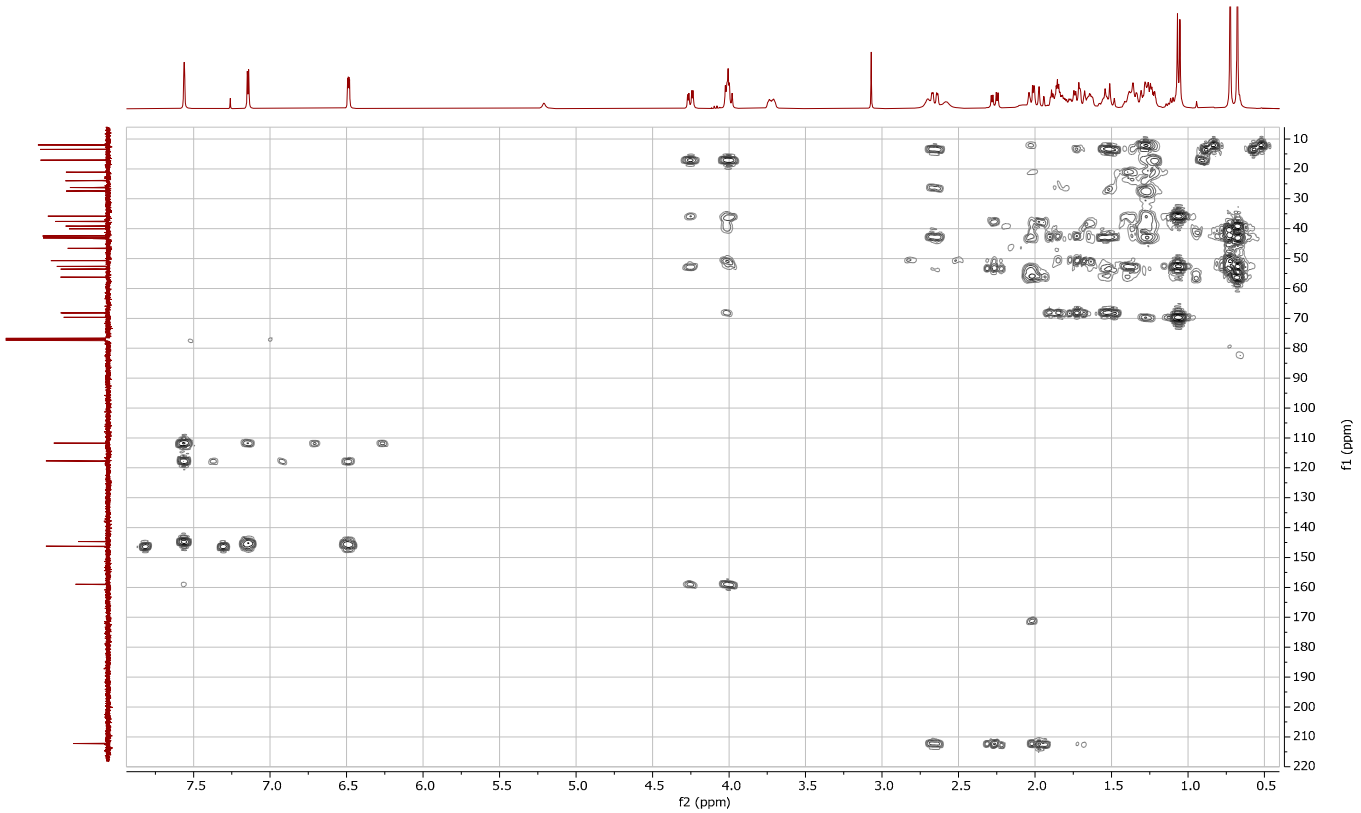


Figure 37. 2D ^{1}H-^{13}C HMBC spectrum of 2α,3α-Dihydroxy-6-oxo-23,24-dinor-5α-cholan-22-yl-furan-2-carboxylate (**34**)

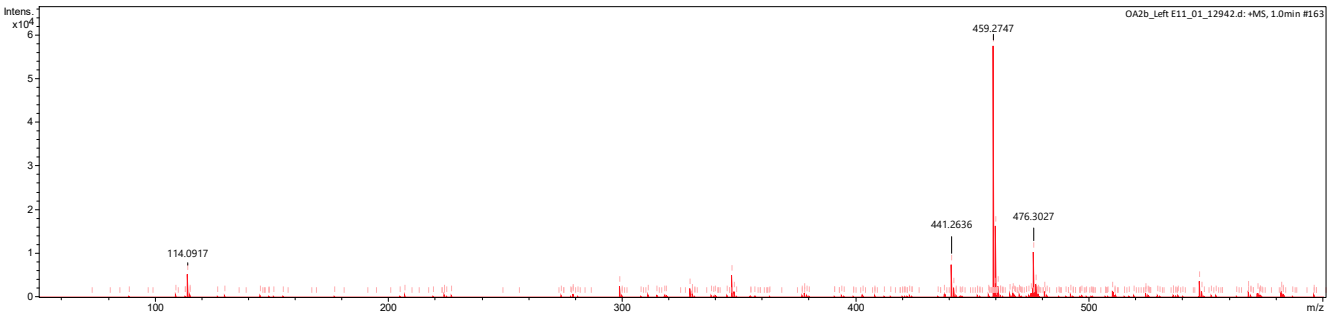


Figure S38. HRMS spectrum of 2α,3α-Dihydroxy-6-oxo-23,24-dinor-5α-cholan-22-yl-furan-2-carboxylate (**34**)

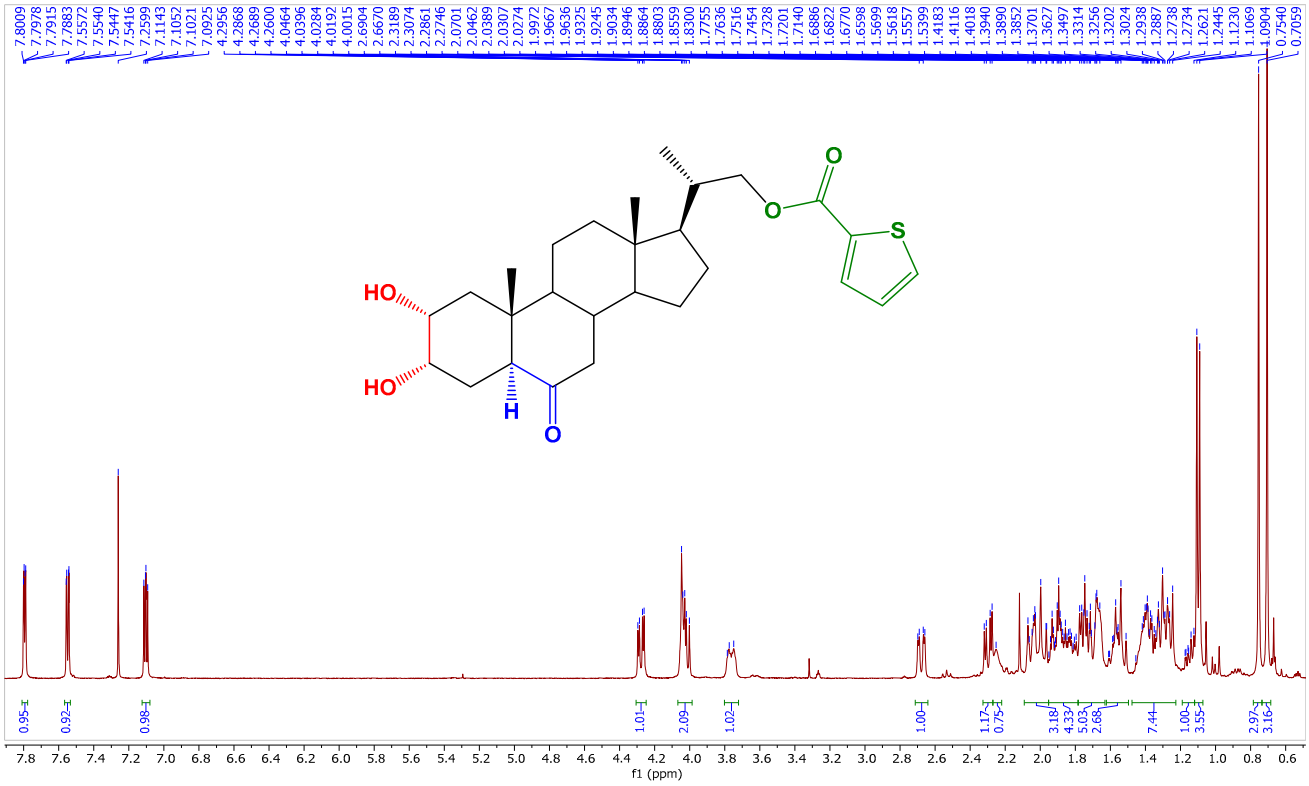


Figure S39. ^{1}H NMR spectrum of 2α,3α-Dihydroxy-6-oxo-23,24-dinor-5α-cholan-22-yl-thiophene-2-carboxylate (**35**)

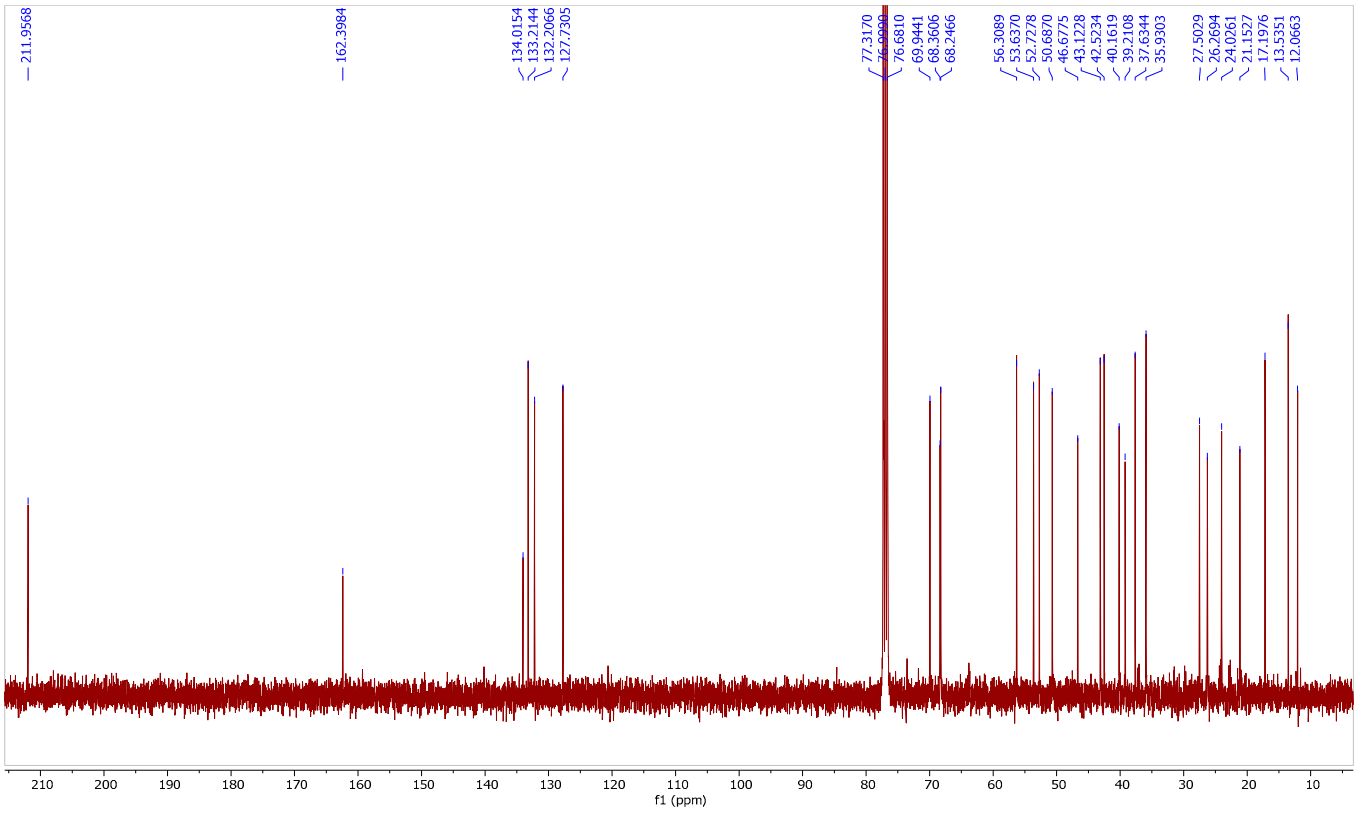


Figure S40. ^{13}C{^{1}H} NMR spectrum of 2α,3α-Dihydroxy-6-oxo-23,24-dinor-5α-cholan-22-yl-thiophene-2-carboxylate (**35**)

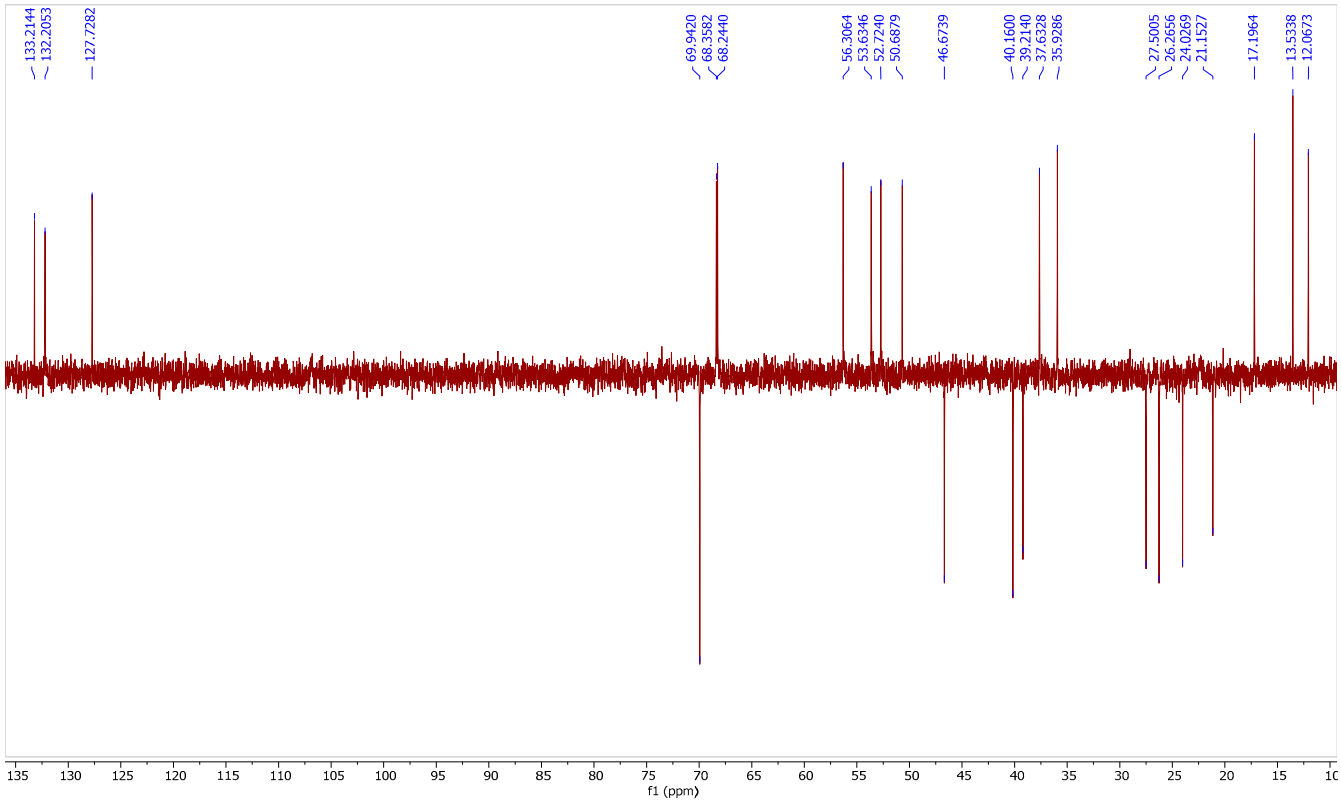


Figure S41. $^{13}C\{^{1}H\}$ DEPT-135 NMR spectrum of 2*α*,3*α*-Dihydroxy-6-oxo-23,24-dinor-5*α*-cholan-22-yl-thiophene-2-carboxylate (**35**)

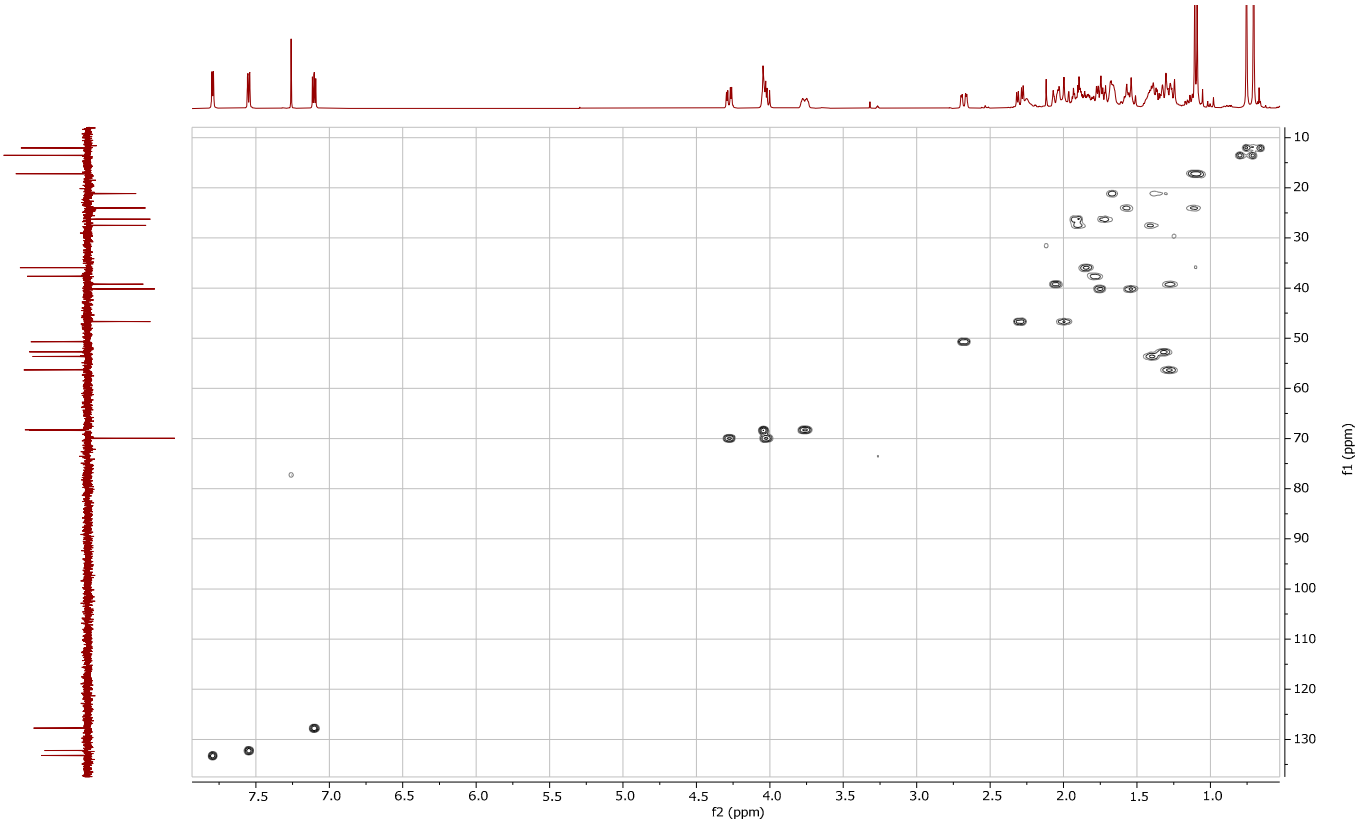


Figure S42. 2D ^{1}H-^{13}C HSQC spectrum of 2*α*,3*α*-Dihydroxy-6-oxo-23,24-dinor-5*α*-cholan-22-yl-thiophene-2-carboxylate (**35**)

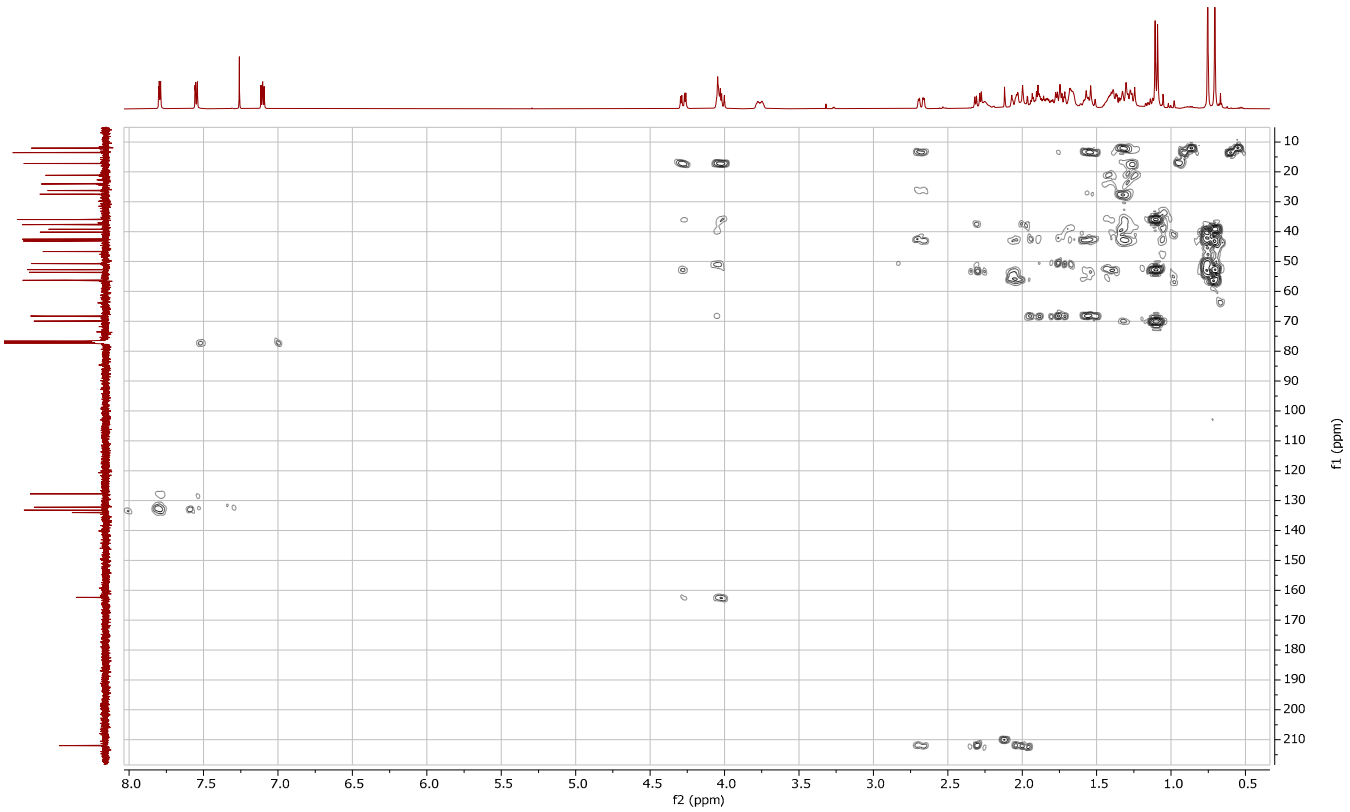


Figure S43. 2D ^{1}H-^{13}C HMBC spectrum of 2α,3α-Dihydroxy-6-oxo-23,24-dinor-5α-cholan-22-yl-thiophene-2-carboxylate (**35**)

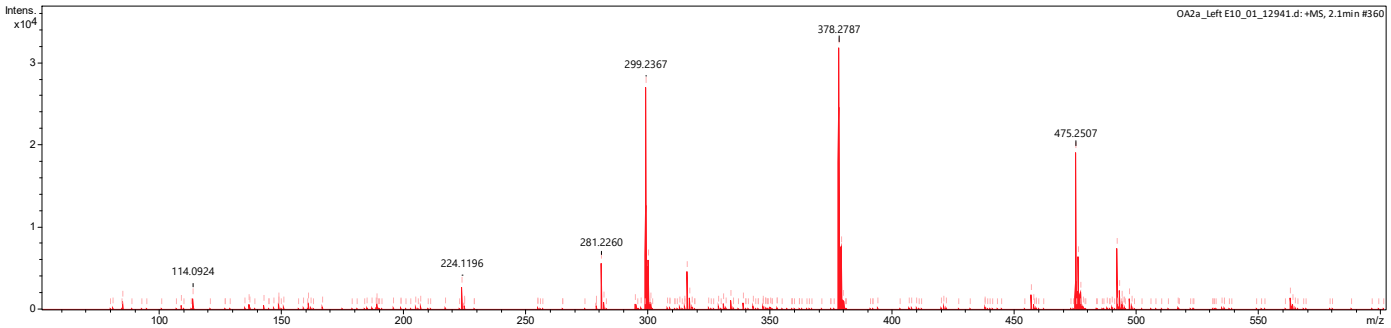


Figure S44. HRMS spectrum of 2α,3α-Dihydroxy-6-oxo-23,24-dinor-5α-cholan-22-yl-thiophene-2-carboxylate (**35**)

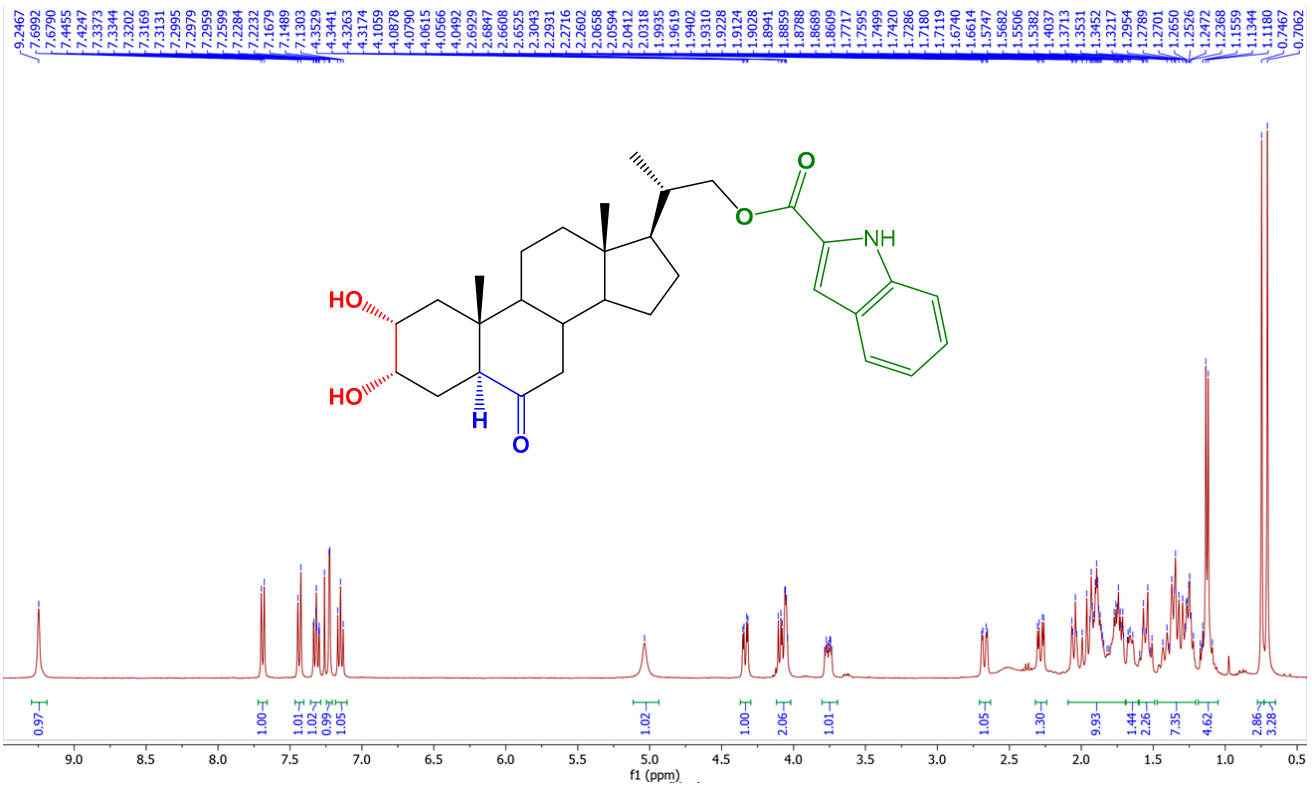


Figure S45. ^{1}H NMR spectrum of 2*α*,3*α*-Dihydroxy-6-oxo-23,24-dinor-5*α*-cholan-22-yl-1*H*-indole-2-carboxylate (**36**)

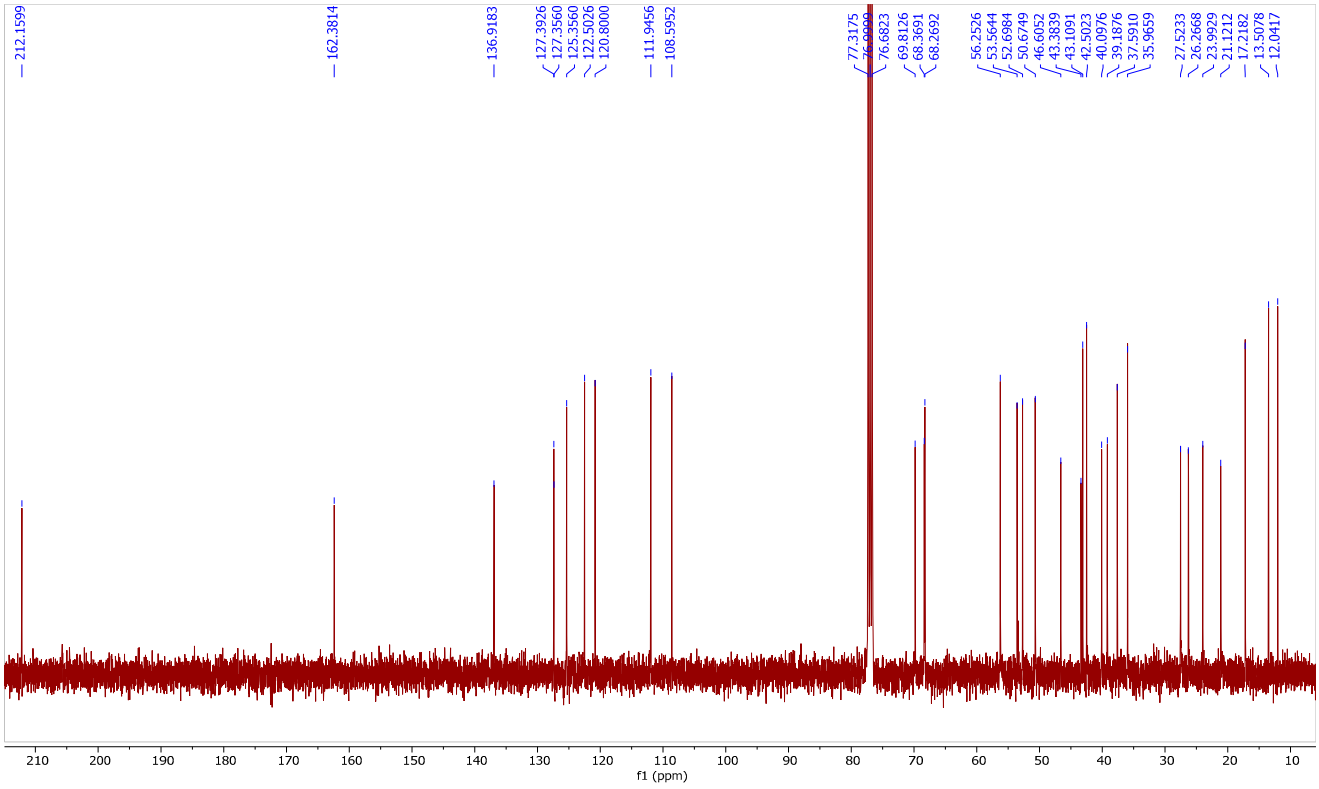


Figure S46. ^{13}C{^{1}H} NMR spectrum of 2*α*,3*α*-Dihydroxy-6-oxo-23,24-dinor-5*α*-cholan-22-yl-1*H*-indole-2-carboxylate (**36**)

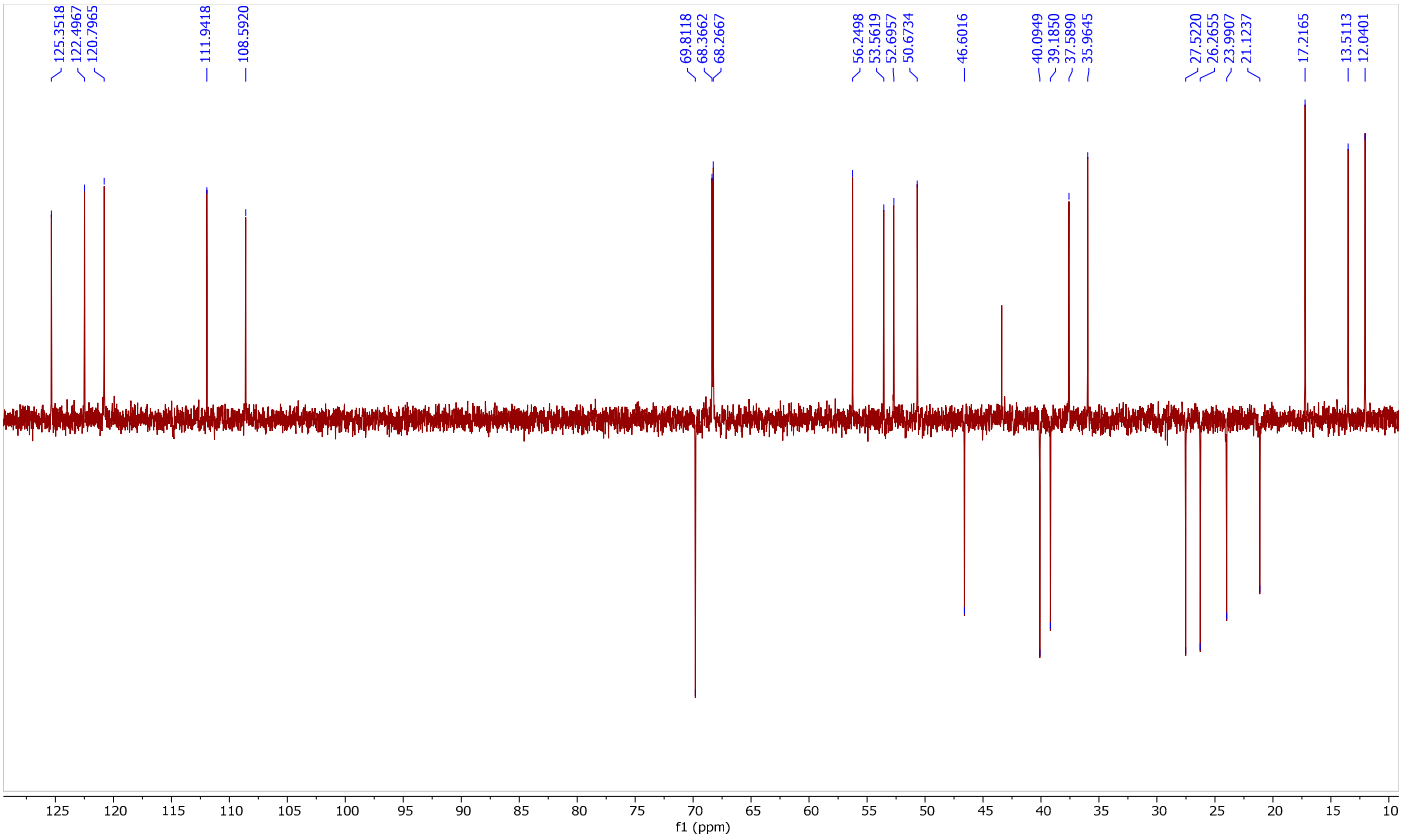


Figure S47. $^{13}C\{^{1}H\}$ DEPT-135 NMR spectrum of 2*α*,3*α*-Dihydroxy-6-oxo-23,24-dinor-5*α*-cholan-22-yl-1*H*-indole-2-carboxylate (**36**)

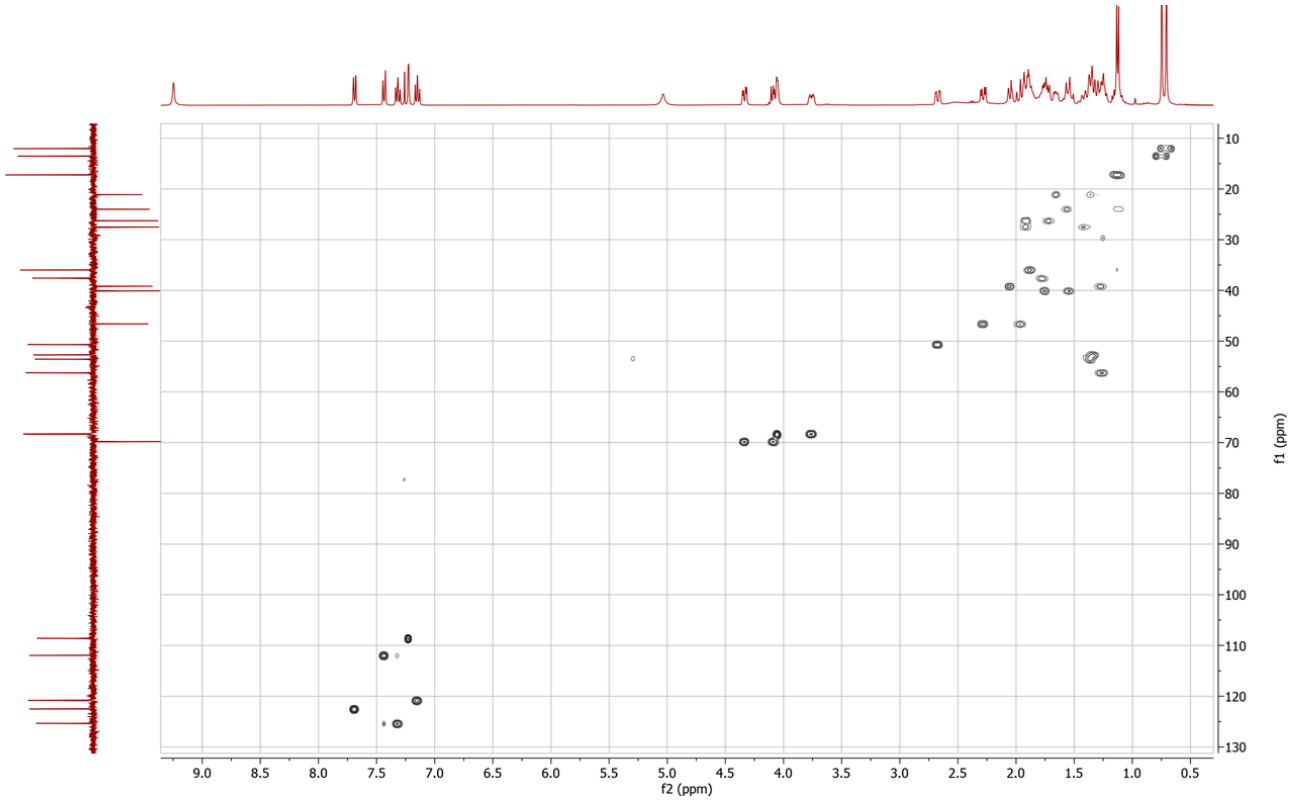


Figure S48. 2D ^{1}H-^{13}C HSQC spectrum of 2*α*,3*α*-Dihydroxy-6-oxo-23,24-dinor-5*α*-cholan-22-yl-1*H*-indole-2-carboxylate (**36**)

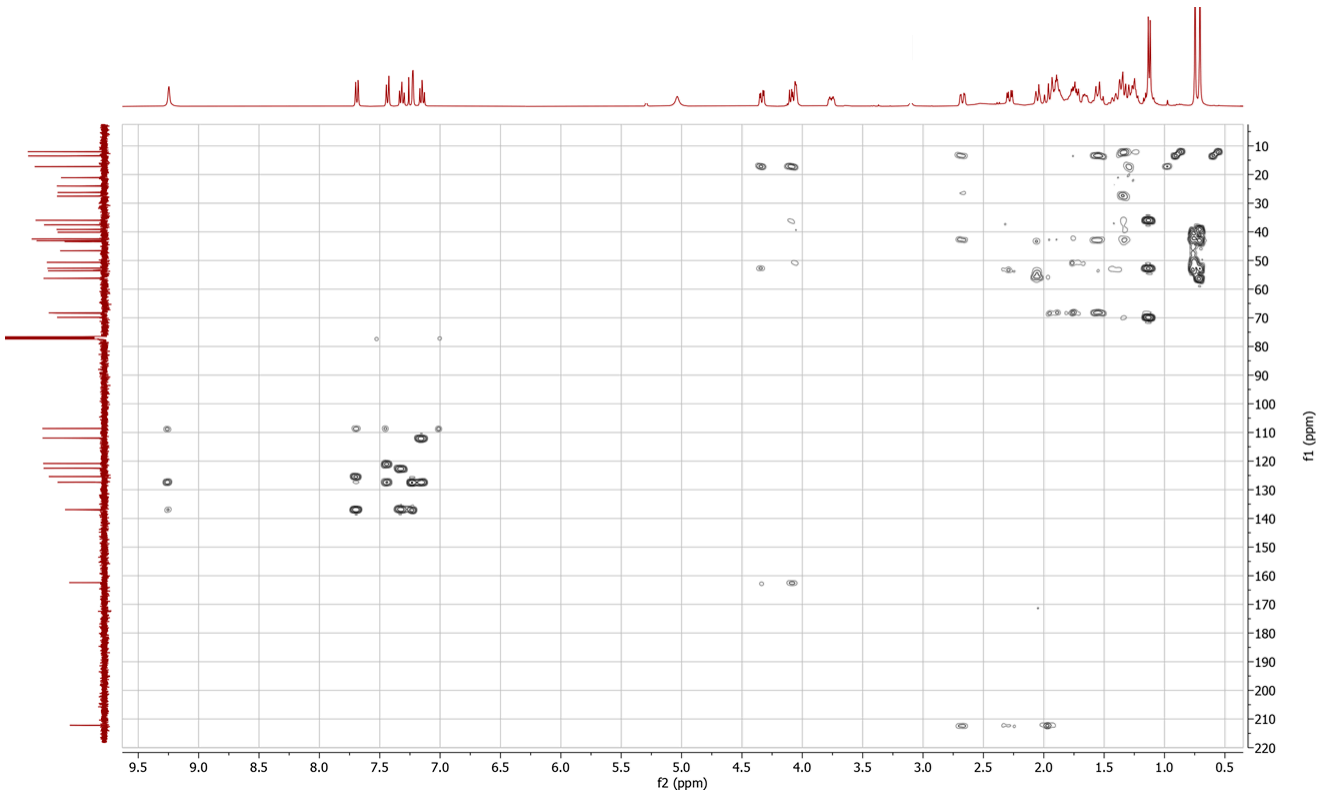


Figure S49. 2D ^{1}H-^{13}C HMBC spectrum of 2*α*,3*α*-Dihydroxy-6-oxo-23,24-dinor-5*α*-cholan-22-yl-1*H*-indole-2-carboxylate (**36**)

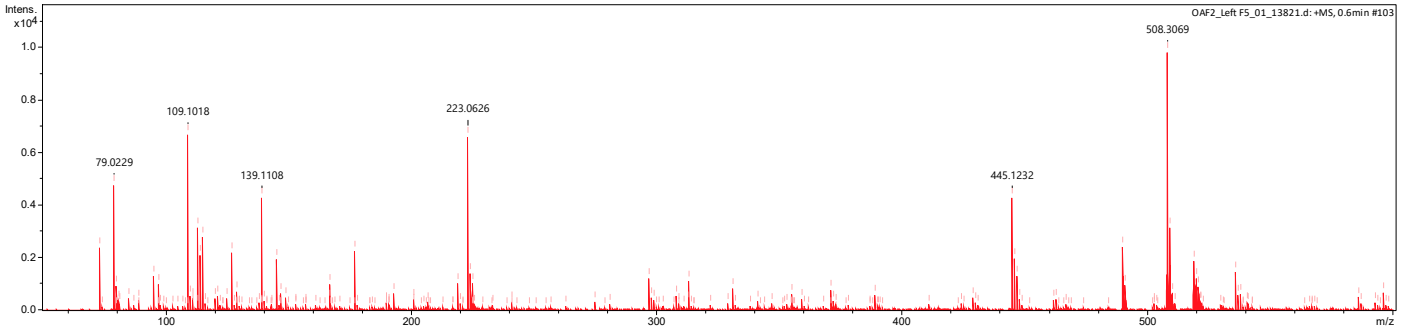


Figure S50. HRMS spectrum of 2*α*,3*α*-Dihydroxy-6-oxo-23,24-dinor-5*α*-cholan-22-yl-1*H*-indole-2-carboxylate (**36**)

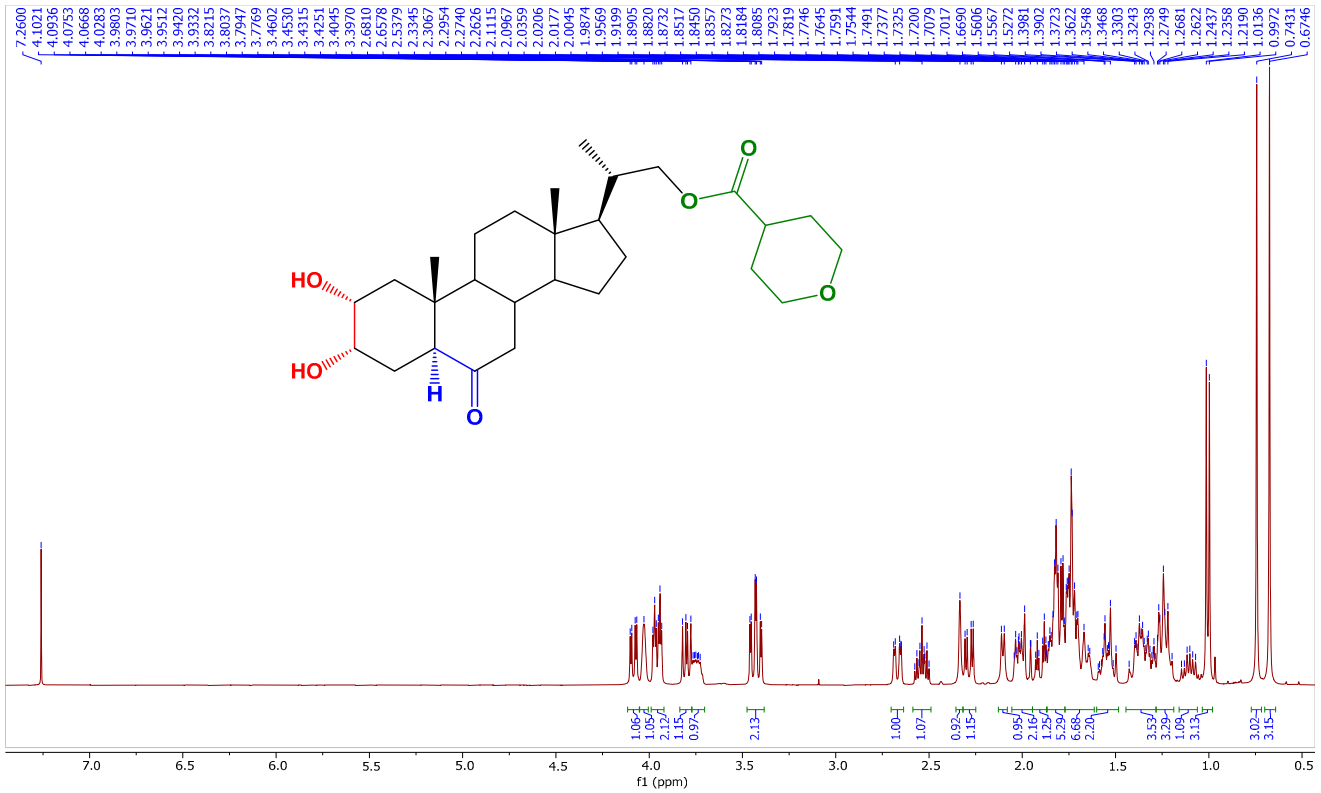


Figure S51. ^{1}H NMR spectrum of 2*α*,3*α*-Dihydroxy-6-oxo-23,24-dinor-5*α*-cholan-22-yl-2*H*-pyran-4-carbocarboxylate (**37**)

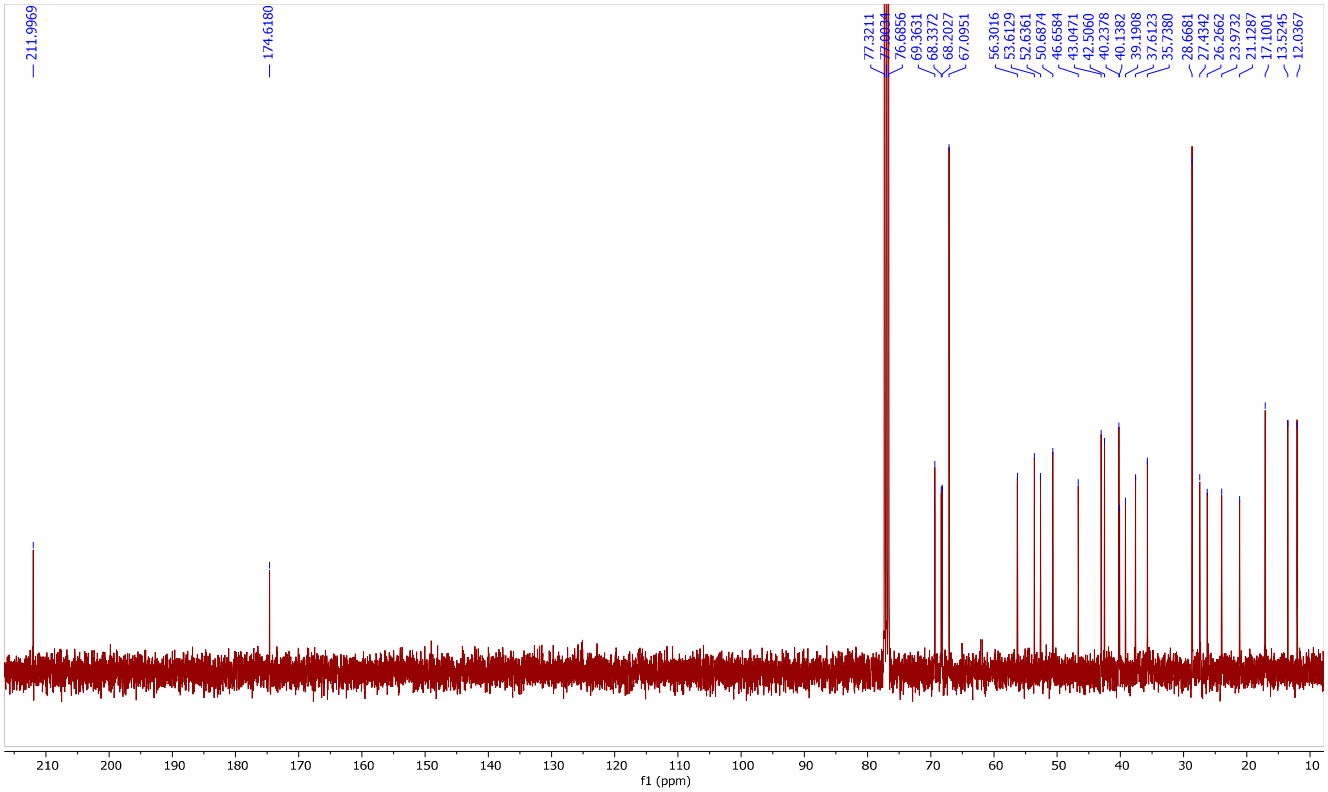


Figure S52. ^{13}C{^{1}H} NMR spectrum of 2*α*,3*α*-Dihydroxy-6-oxo-23,24-dinor-5*α*-cholan-22-yl-2*H*-pyran-4-carbocarboxylate (**37**)

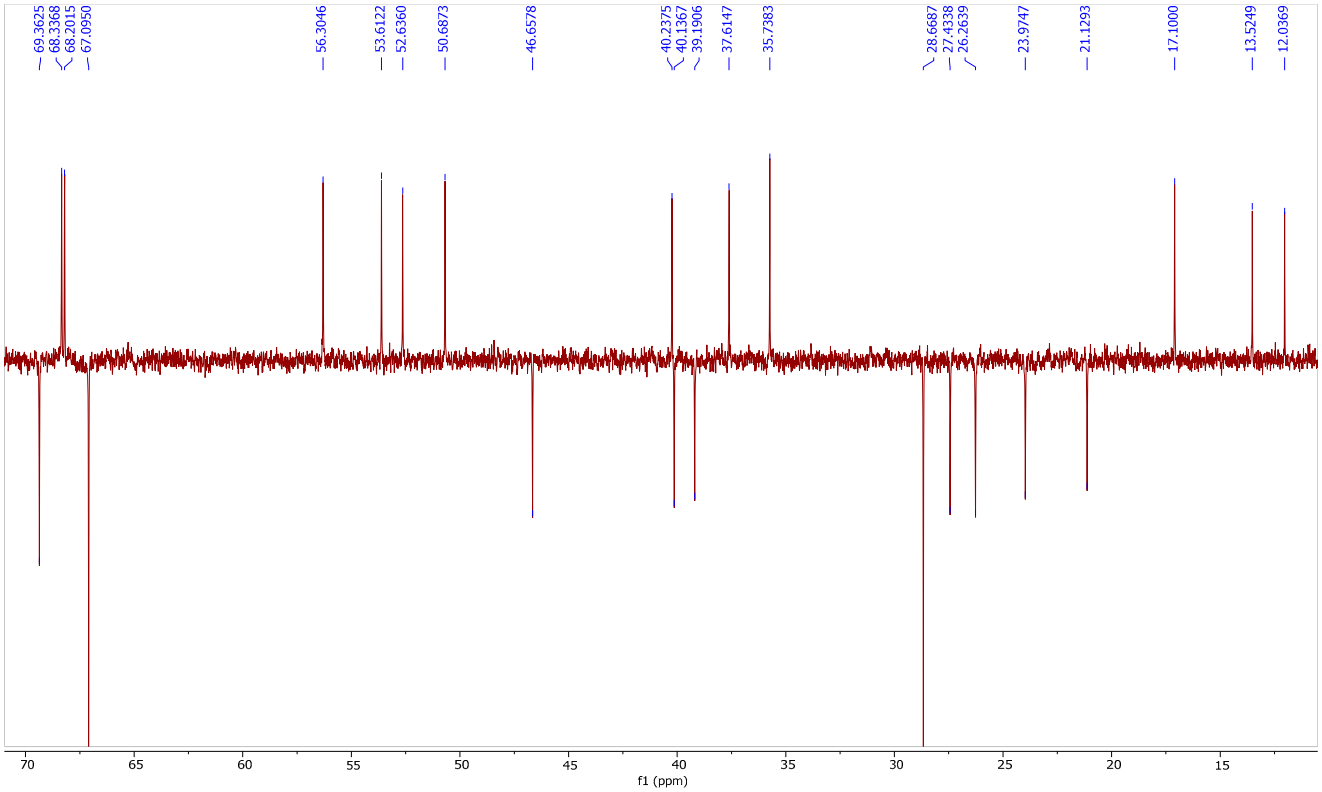


Figure S53. $^{13}C\{^{1}H\}$ DEPT-135 NMR spectrum of 2*α*,3*α*-Dihydroxy-6-oxo-23,24-dinor-5*α*-cholan-22-yl-2*H*-pyran-4-carbocarboxylate (**37**)

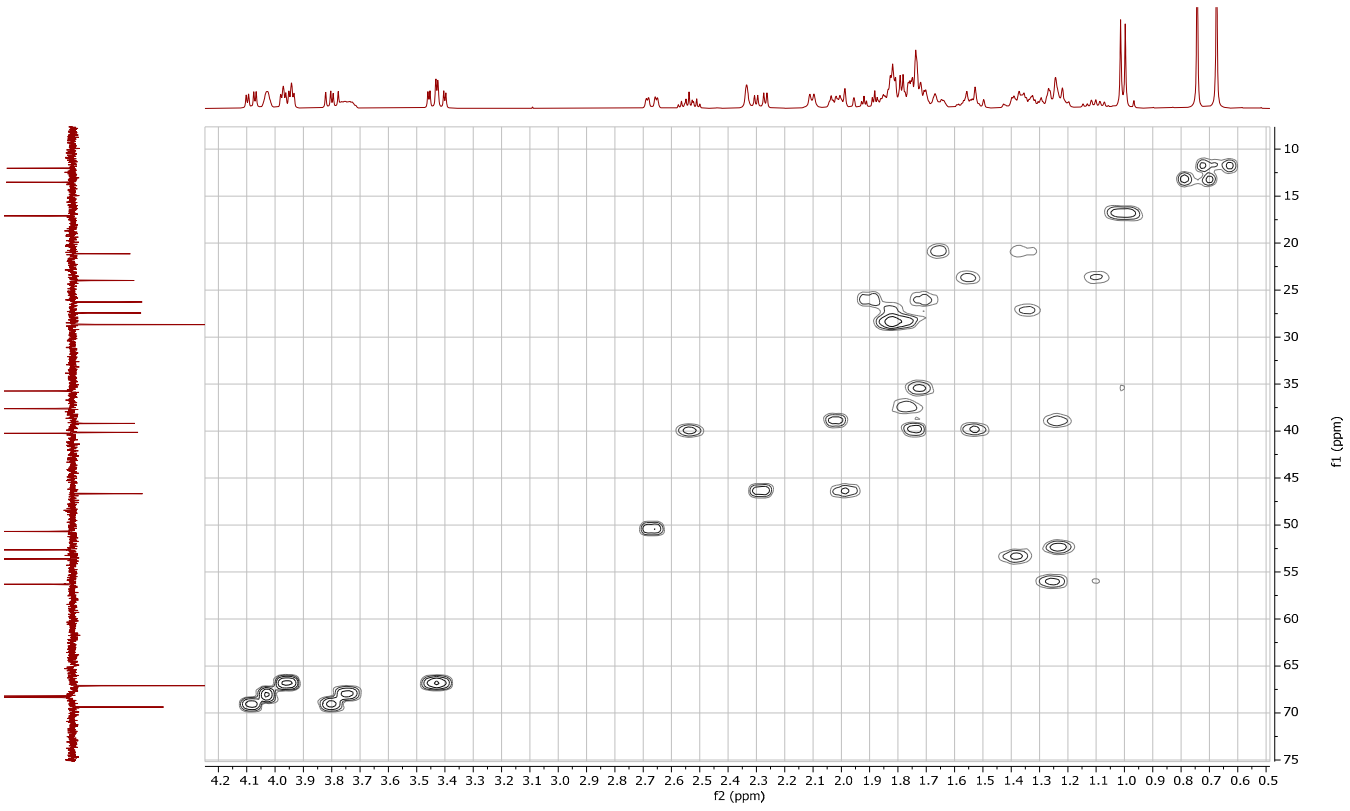


Figure S54. 2D ^{1}H-^{13}C HSQC spectrum of 2*α*,3*α*-Dihydroxy-6-oxo-23,24-dinor-5*α*-cholan-22-yl-2*H*-pyran-4-carbocarboxylate (**37**)

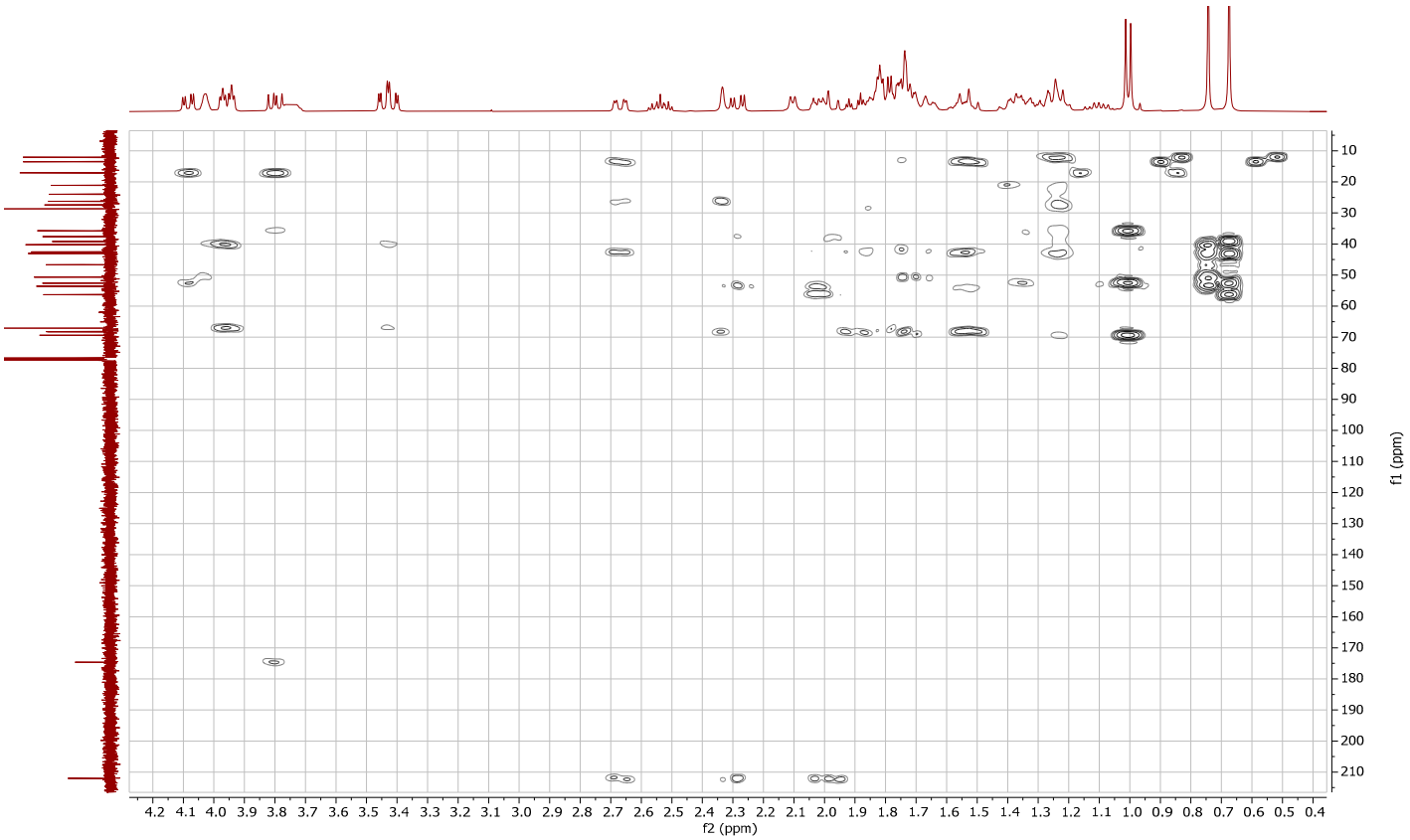


Figure S55. 2D ^{1}H-^{13}C HMBC spectrum of 2*α*,3*α*-Dihydroxy-6-oxo-23,24-dinor-5*α*-cholan-22-yl-2*H*-pyran-4-carbocarboxylate (**37**)

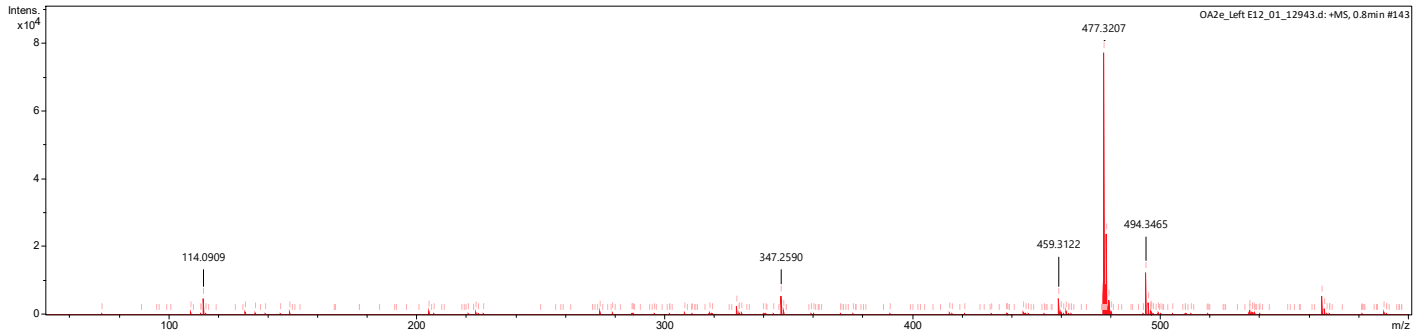


Figure S56. HRMS spectrum of 2*α*,3*α*-Dihydroxy-6-oxo-23,24-dinor-5*α*-cholan-22-yl-2*H*-pyran-4-carbocarboxylate (**37**)

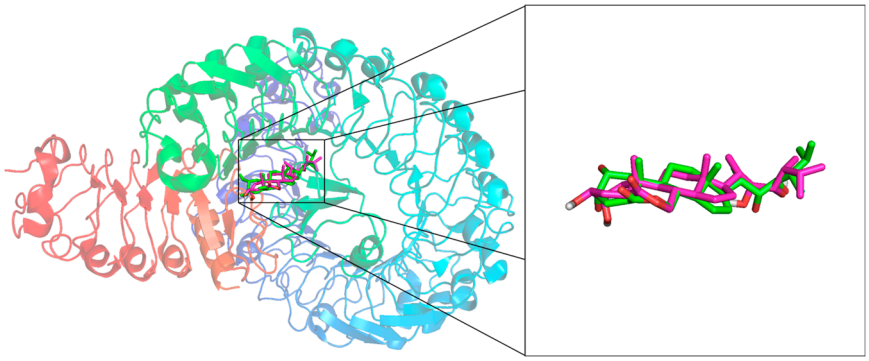


Figure S57. Redocking of brassinolide into the active site of the BRI1–BAK1. BRI1–BAK1 in cartoon mode and ligands in stick mode. Ligand color code: Green, C atoms of crystallyzed ligand BLB808; Magent: C atoms of ligand docked by using Autodock vina; Red: oxygen atoms.

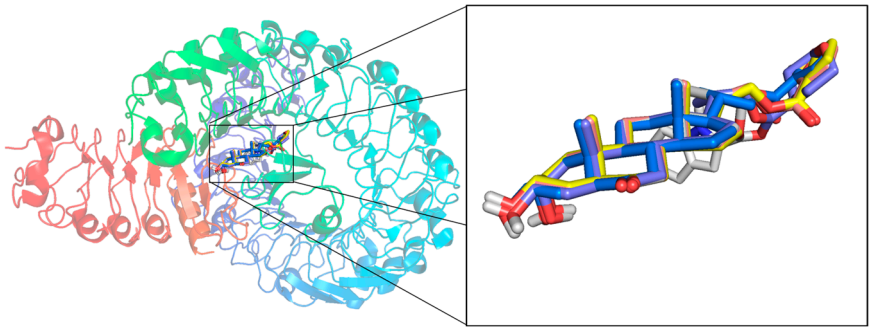


Figure S58. Results of molecular docking for new BRs analogs. BRI1–BAK1 in cartoon mode and ligands in stick mode. Ligand color code for carbon atoms: Blue: compound **33**; Yellow: compoundo **34**; Orange: compound **35**; White: compound **36**; Violet: compound **37**. Oxygen atoms: Red.

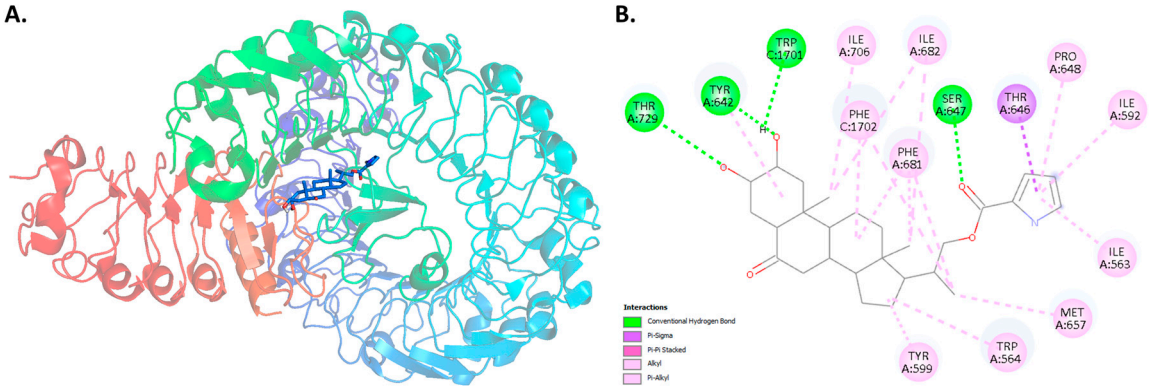


Figure S59. Results of molecular docking of compound **33** in the active site of BRI1–BAK1. A. 3D visualization and B. 2D representations of the most important interactions.

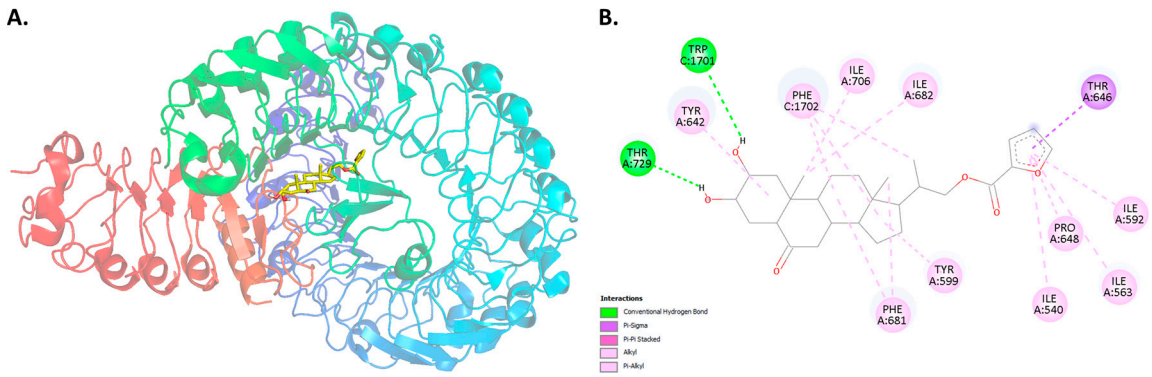


Figure S60. Results of molecular docking of compound **34** in the active site of BRI1–BAK1. A. 3D visualization and B. 2D representations of the most important interactions.

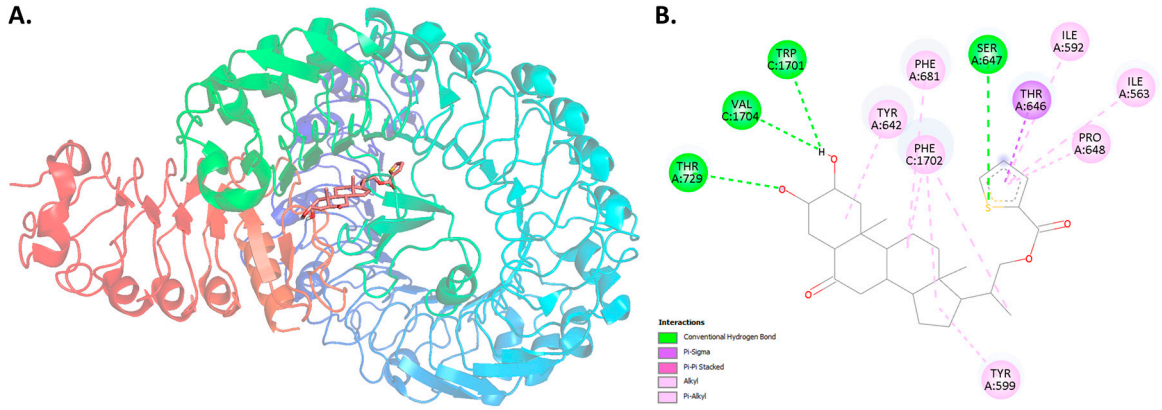


Figure S61. Results of molecular docking of compound **35** in the active site of BRI1–BAK1. A. 3D visualization and B. 2D representations of the most important interactions.

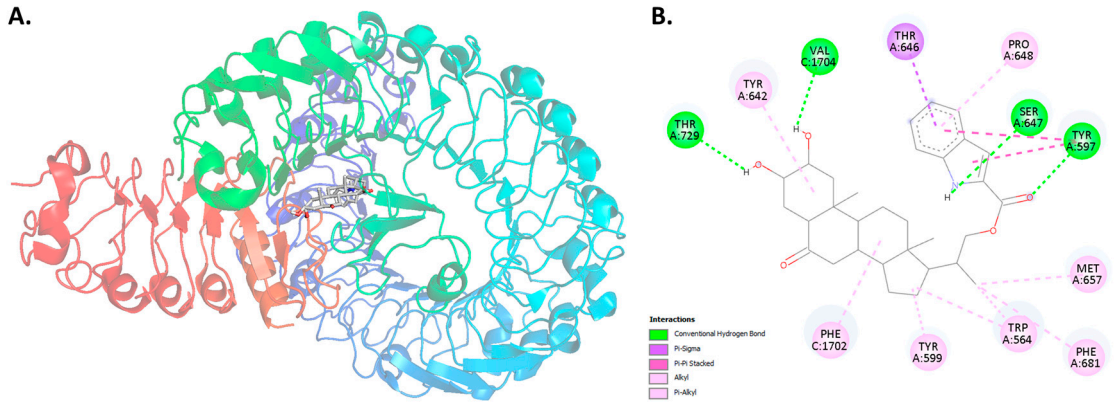


Figure S62. Results of molecular docking of compound **36** in the active site of BRI1–BAK1. A. 3D visualization and B. 2D representations of the most important interactions.

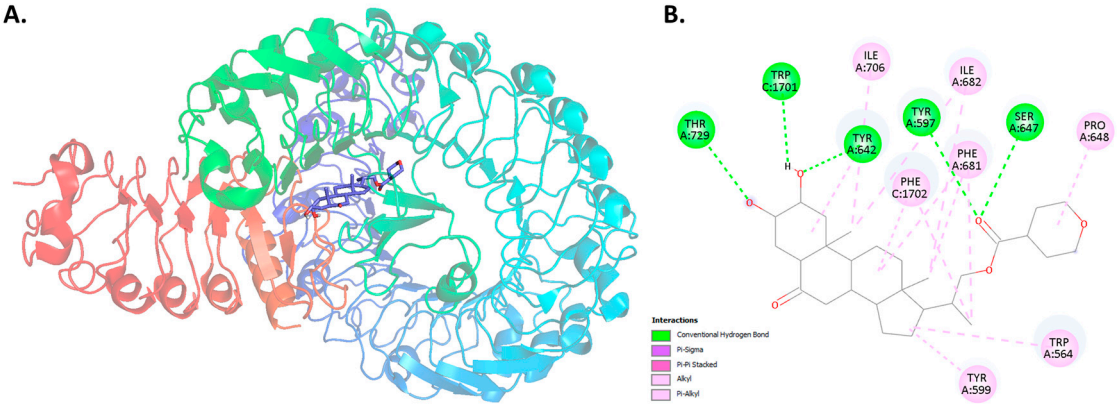


Figure S63. Results of molecular docking of compound **37** in the active site of BRI1–BAK1. A. 3D visualization and B. 2D representations of the most important interactions.

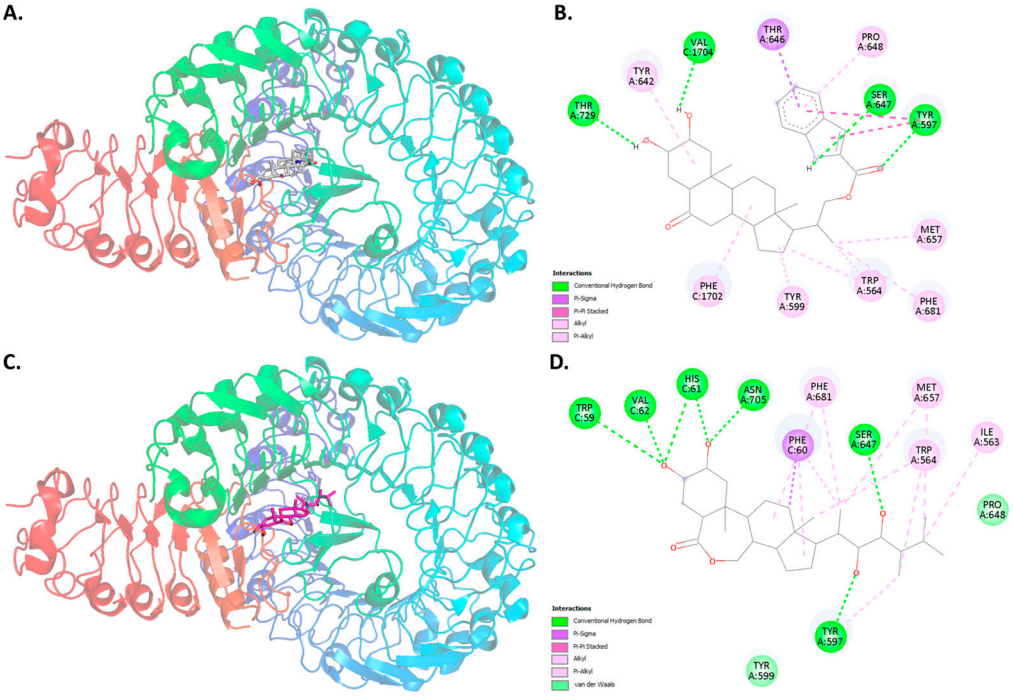


Figure S64. Results of molecular docking for compound **36** and brassinolide within the active site of BRI1–BAK1. A. 3D visualization of compound **36**; B. 2D representation of interactions of **36** with residues in BRI1–BAK1; C. 3D visualization of brassinolide docked to the active site; D. 2D representation of interactions of brassinolide with residues in BRI1–BAK1.

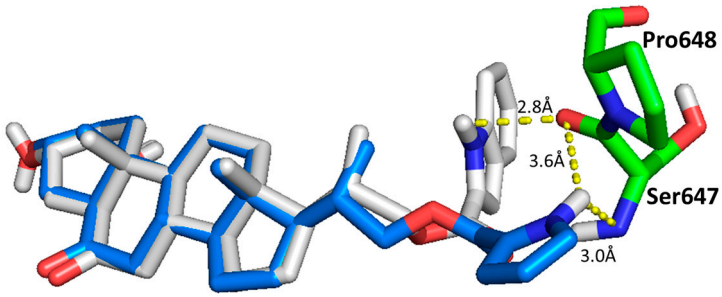


Figure S65: Molecular docking results for **33** and **36** in the active site of BRI1–BAK1, showing the aminoacids and distance for potential hydrogen bonding. Color code: Blue: C atoms of **33**; White: C atoms compound **33**; Green: C atomos of BRI1–BAK1.

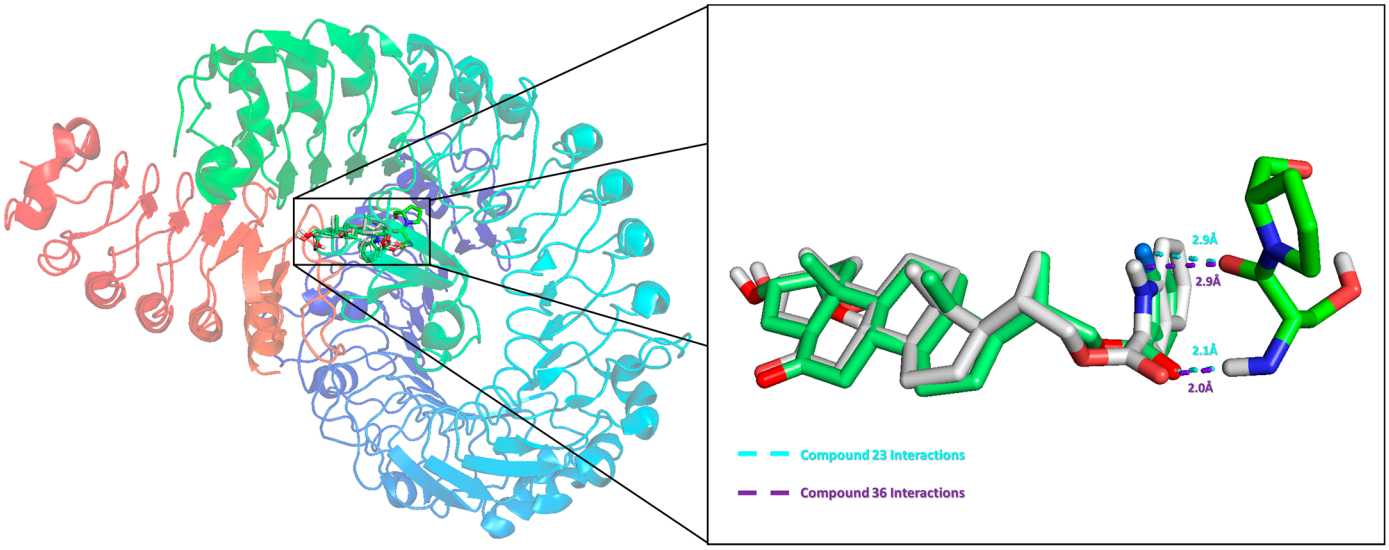


Figure S66. Results of molecular docking of compound **36** and compound **23** in the active site of BRI1–BAK1 showing the aminoacids and distance for potential hydrogen bonding. **Color code:** White: C atoms of **36**; Lime: C atoms compound **23**; Navy: F atom of **23**. Green: C atoms of BRI1–BAK1.

Table S1. Binding energies and interactions obtained for BRs analogs (**33-37**) and brassinolide

Compound	Binding energy (kcal/mol)	Interactions
Brassinolide	-12.9	**Hydrogen bond:**His61(3.2 Å, C), Val62(2.9 Å, C), Trp59(2.6 Å, C), Ser647(2.3 Å, A), Tyr597(2.3 Å ,A). **Hydrophobic:** Phe681(4.0 Å, A), Phe60(3.0 Å, C), Met657(3.3 Å, A), Trp564(3.7 Å, A), Ile563(4.2 Å, A), Leu615(3.8 Å, A), Tyr597(4.0 Å, A). **Stacking:** Phe60(3.8 Å, C)
33	-12.6	**Hydrogen bond:** Thr729(2.8 Å, A), Trp1701(3.0 Å, C). **Hydrophobic:** Tyr642(3.9 Å, A), Tyr599(3.7 Å, A), Trp564(3.7 Å, A), Met567(3.6 Å, A), Ile563(5.5 Å, A), Ile592(3.6 Å, A), Pro648(3.8 Å, A), Phe681(3.1 Å, A), Ile682(4.1 Å, A), Ile706(4.1 Å, A), Phe1702(3.5 Å, C). **Stacking:** Thr646(5.0 Å, A)
34	-12.7	**Hydrogen bond:** Thr729(2.1 Å, A), Tyr642(3.4 Å, A), Ser647(3.5 Å, A), Trp1701(3.0 Å, C). **Hydrophobic:** Tyr642(3.4 Å, A), Phe681(3.4 Å, A), Ile682 (4.3 Å, A), Ile706(4.1 Å, A), Ile592(4.0 Å, A), Tyr599(4.0 Å, A), Ile540(3.6 Å, A), Ile563(3.5 Å, A), Pro648(3.9 Å, A), Phe1702(3.5 Å, C) **Stacking:** Thr646(4.5 Å, A)
35	-12.7	**Hydrogen bond:** Thr729(3.5 Å, A), Val1704(3.0 Å, C), Trp1701(3.0 Å, C), Ser647(3.3 Å, A). **Hydrophobic:** Tyr642(3.9 Å, A), Phe681(3.6 Å, A), Tyr599(4.0 Å, A), Trp564(3.5 Å, A), Pro648(3.7 Å, A), Ile563(3.5 Å, A), Ile592(4.4 Å, A), Phe1702(4.1 Å, C) **Stacking:** Thr646(4.8 Å, A)
36	-13.7	**Hydrogen bond:** Thr729(3.5 Å, A), Val1704(3.0 Å, C), Ser647(2.8 Å, A), Tyr597(3.2 Å, A). **Hydrophobic:** Tyr642(3.9 Å, A), Tyr599(4.0 Å, A), Trp564(3.5 Å, A), Pro648(5.4 Å, A), Phe681(3.6 Å, A), Met657(3.7 Å, A), Phe1702(4.1 Å, C) **Stacking:** Tyr597(3.5 Å, A) y Thr646(5.0 Å, A).
37	-12.9	**Hydrogen bond:** Thr729(3.1 Å, A), Trp1701(3.0 Å, C), Tyr642(3.1 Å, A), Tyr597(2.7 Å, A), Ser647 (2.1 Å, A). **Hydrophobic:** Tyr599(3.9 Å, A), Trp564(5.9 Å, A), Pro648(3.8 Å, A), Phe681(3.3 Å, A), Ile682(4.2 Å, A), Ile706(4.0 Å, A), Phe1702(3.8 Å, C)

Distance and letter in parenthesis indicate the shortest distance between the aminoacid and ligand, while the letter corresponds to the monomer of BRI1-BAK1.Detalils of the ligand fragment and aminoacid interaction, see Figures S59-S63